

SECOND-ORDER STEADY DRIFT OF A FLOATING
TRIANGULAR PLATFORM: THEORY AND EXPERIMENT

CENTRE FOR NEWFOUNDLAND STUDIES

**TOTAL OF 10 PAGES ONLY
MAY BE XEROXED**

(Without Author's Permission)

PATRICIA M. DUNPHY, B.Eng., P.Eng.



SECOND-ORDER STEADY DRIFT
OF A
FLOATING TRIANGULAR PLATFORM:
THEORY AND EXPERIMENT

BY

© PATRICIA M. DUNPHY, B.Eng., P.Eng.

A thesis submitted to the School of Graduate
Studies in partial fulfillment of the
requirements for the degree of
Master of Engineering

Faculty of Engineering and Applied Science
Memorial University of Newfoundland

October 1989

St. John's

Newfoundland



National Library
of Canada

Bibliothèque nationale
du Canada

Canadian Theses Service

Service des thèses canadiennes

Ottawa, Canada
K1A 0N4

The author has granted an irrevocable non-exclusive licence allowing the National Library of Canada to reproduce, loan, distribute or sell copies of his/her thesis by any means and in any form or format, making this thesis available to interested persons.

The author retains ownership of the copyright in his/her thesis. Neither the thesis nor substantial extracts from it may be printed or otherwise reproduced without his/her permission.

L'auteur a accordé une licence irrévocable et non exclusive permettant à la Bibliothèque nationale du Canada de reproduire, prêter, distribuer ou vendre des copies de sa thèse de quelque manière et sous quelque forme que ce soit pour mettre des exemplaires de cette thèse à la disposition des personnes intéressées.

L'auteur conserve la propriété du droit d'auteur qui protège sa thèse. Ni la thèse ni des extraits substantiels de celle-ci ne doivent être imprimés ou autrement reproduits sans son autorisation.

ISBN 0-315-59242-7

ABSTRACT

As ocean industries have grown to demand larger offshore vessels achieving ever increasing levels of performance, the need for a better understanding of the phenomena which govern motions and loading of these structures has been recognized. These motions and forces are a result of complex environmental conditions including ice, wind, current and waves. A significant part of the environmental loading is due to waves.

In general wave loading on a structure is a complex non-linear process of which the first- and second-order (in wave amplitude) components are of main interest. The steady second-order component of drift force may cause large excursions of the structure and therefore must be seriously considered in the design considerations of mooring and dynamic positioning systems.

In this thesis second-order mean drift forces on a triangular floating structure in regular waves are calculated utilizing far field potential theory. These computed forces are compared to those measured during testing of a 1:200 scale model of a moored triangular body. This is done in an attempt to decide whether mooring forces can be reasonably estimated for such a structure.

It was concluded that the mean drift forces can be reasonably well predicted using the method presented. Therefore this method can be used as an aid in the design process.

ACKNOWLEDGEMENTS

First of all I would like to express sincere gratitude to Mr.H.L.Snyder, P.Eng. and Mr.T.Kierans, P.Eng. for giving me the opportunity to become involved with the Deltaport Project at the Graduate level. It is a privilege to have worked with these two distinguished engineers.

I would also like to thank Mr.N.E.Jeffrey, P.Eng. and Dr.J.S.Pawlowski, P.Eng. for the opportunity to conduct research at the National Research Council's Institute for Marine Dynamics in St. John's. The experience gleaned during my stay in this world-class facility is invaluable.

The project was suggested as suitable for an M.Eng. degree by one of my supervisors, Dr.M.J.Hinchey. I wish to thank him and my other supervisors, Dr.Pawlowski and Mr.Snyder, for their assistance and guidance. The suggestions of Dr.J.Murray, P.Eng. of IMD and the assistance of co-worker Mr.R.Yetman, P.Eng. are also greatly appreciated.

Although too numerous to mention individually, I wish to thank everyone at MUN and IMD who helped me to decipher and analyse data, debug programs, implement in-house software and answer my never-ending questions about the AES wordprocessor.

Lastly, there is my husband, Garry, who kept life interesting and laughable and encouraged me to the finish.

I would like to acknowledge funding and assistance provided by Deltaport Limited, the National Research Council, various Provincial and Federal Government Departments, Unistrut Limited, Fenco Newfoundland Limited, and Memorial University of Newfoundland.

TABLE OF CONTENTS

	Page
ABSTRACT	ii
ACKNOWLEDGEMENTS	iv
LIST OF TABLES	viii
LIST OF FIGURES	iv
NOMENCLATURE	xii
CHAPTER I INTRODUCTION	1
CHAPTER II LITERATURE REVIEW	3
CHAPTER III THEORY	9
3.1 Governing Equations	9
3.2 Modelling Theory	13
3.3 Slender Structures: Morison's Equation	22
3.4 Large Structures: Linear Diffraction Theory	25
CHAPTER IV THE STUDY OF DRIFT FORCES	29
4.1 Experimental Study	29
4.1.1 Purpose of Model Tests	29
4.1.2 The Model	30
4.1.3 Test Facility	34
4.1.4 Test Set-Up	36
4.1.5 Data Acquisition	39
4.1.6 Data Analysis	39
4.2 Numerical Evaluation of Steady Drift Forces Using Linear Diffraction Theory	54
4.2.1 A Model for Steady Drift Forces	54
4.2.2 Numerical Application	62
4.2.3 Computational Results	68
CHAPTER V COMPARISON OF EXPERIMENTAL AND NUMERICAL RESULTS	84
CHAPTER VI CONCLUSIONS	90
REFERENCES	94

	Page
APPENDIX A FIGURES	99
APPENDIX B CALCULATIONS OF PARTICULARS OF THE MODEL	152
APPENDIX C POWER SPECTRA OF WAVE AMPLITUDE AND MOORING FORCE	168
APPENDIX D PROGRAM LISTINGS: DPORT2.FOR AND OUTPORT2.FOR	237
APPENDIX E PROGRAM LISTING: SHAPE.FOR	265
APPENDIX F INPUT PANEL DATA	270
APPENDIX G RESULTS OF PROGRAM OUTPORT2.FOR	275
APPENDIX H MAIN SUBROUTINES IN PROGRAM DPORT2.FOR	292

LIST OF TABLES

	Page
Table 1 Test Wave Frequencies and Wave Heights	42
Table 2 Input Data and Test Results: Uncovered Model	44
Table 3 Input Data and Test Results: Covered Model	45
Table 4 Model Test Incident Wave Frequencies	47
Table 5 Particulars of the Model	65

LIST OF FIGURES

(For convenience all figures are contained in Appendix A and reproduced when directly referred to in the main text.)

	Page	
FIGURE 1	Coordinate System	11
FIGURE 2	Regions of Validity of Force Prediction Methods for a Fixed Pile.	12
FIGURE 3	Wave Force Regimes	20
FIGURE 4	Vortex Shedding Patterns Around a Vertical Cylinder in Waves as Functions of K-C	23
FIGURE 5	Measured Forces in Regular Waves	31
FIGURE 6	Measured Forces in Beating Waves	32
FIGURE 7a	Model Space Frame and Buoyancy Tubes	33
FIGURE 7b	1:200 Scale Model Used in Testing	33
FIGURE 8	Model Dimensions	35
FIGURE 9	IMD Towing Tank Facility	37
FIGURE 10	Test Set-Up	38
FIGURE 11	Plot of Experimental Results: Uncovered Model; Drift Force .vs. Frequency	48
FIGURE 12	Plot of Experimental Results: Covered Model; Drift Force .vs. Frequency	49
FIGURE 13	Plot of Experimental Results: Uncovered Model; Nondimensional Drift Force .vs. Nondimensional Frequency	50
FIGURE 14	Plot of Experimental Results: Covered Model; Nondimensional Drift Force .vs. Nondimensional Frequency	51
FIGURE 15	Comparison of Covered and Uncovered Model Test Results	53

	Page
FIGURE 16 Model Panels used in Numerical Analysis	64
FIGURE 17 Plot of Computed Results: All Motions; Head Seas	69
FIGURE 18 Plot of Computed Results: First-Order Motions:	
18a Surge Amplitude Operator	116
18b Surge Phase	117
18c Heave Amplitude Operator	118
18d Heave Phase	119
18e Pitch Angle Parameter	120
18f Pitch Phase	121
FIGURE 19 Plot of Computed Results:	
19a Surge Added Mass Coefficient	122
19b Surge Damping Coefficient	123
19c Heave Added Mass Coefficient	124
19d Heave Damping Coefficient	125
19e Pitch Added Mass Coefficient	126
19f Pitch Damping Coefficient	127
19g Yaw Added Mass Coefficient	128
19h Yaw Damping Coefficient	129
FIGURE 20 Pinkster's Results for Head Seas and Quartering Seas	71
FIGURE 21 Hearn's Results for a Semi-submersible	72
FIGURE 22 Calculated First-Order Surge Force	74
FIGURE 23 Calculated Froude-Krylov Force - Surge	75
FIGURE 24 Calculated Scattering Force - Surge	76
FIGURE 25a 2-D Numerical Results: Added Mass	78
FIGURE 25b 2-D Numerical Results: Damping	79

	Page	
FIGURE 26	Plot of Computed Steady Drift Forces for Restricted Motions:	
26a	Surge Motion Only	137
26b	Heave Motion Only	138
26c	Pitch Motion Only	139
26d	Surge and Heave Only	140
26e	Surge and Pitch Only	141
26f	Heave and Pitch Only	142
FIGURE 27	Plot of Computed Steady Drift Forces: Fixed Body	82
FIGURE 28	Plot of Computed Steady Drift Forces: Surge Only:	
28a	Mooring #2 Stiffness Input to Program	144
28b	Mooring #3 Stiffness Input to Program	145
FIGURE 29	Plot of Computed Steady Drift Forces: Quartering Seas;	
29a	Free Floating Body	146
29b	Fixed Body	147
FIGURE 30	Plot of Comparison of Steady Drift Forces: Computed Free-Floating Structure .vs. Experimental Uncovered Model	85
FIGURE 31	Plot of Comparison of Steady Drift Forces: Computed Free Floating Structure .vs. Experimental Covered Model	86
FIGURE 32	Plot of Comparison of Steady Drift Forces: Computed Fixed Structure .vs. Experimental Uncovered Model	88
FIGURE 33	Plot of Comparison of Steady Drift Forces: Computed Fixed Structure .vs. Experimental Covered Model	89

NOMENCLATURE

A	nondimensional table of offsets describing the geometry of the structure nondimensionalized with characteristic length
A_D	= $\frac{1}{2}\rho D$
A_I	= $\frac{\rho \pi D^2}{4}$
A_{jk}	added mass coefficient
A_{wp}	water plane area
B_{jk}	Damping coefficients
C	restoring coefficients
C_A	added mass coefficient
C_d	drag coefficient
C_d'	drag coefficient for oscillating body in still water
C_m	inertia coefficient
D	body characteristic length
d	depth of water
dS	differential of surface area
F	total force on body
\tilde{F}	nondimensional force
F_d	horizontal drift force
$F_{d,x}$	drift force in x-direction
$F_{d,y}$	drift force in y-direction
F_g	force due to gravity
F_j	generalized force
f_{ex}	external forces acting on the body
f	frequency

f_{02}, f_{03}	natural frequency of moorings 2 and 3 respectively
g	acceleration due to gravity
$G(\vec{x}, \vec{\xi})$	Green's function
H	wave height
Im	imaginary part of complex term
K	spring constant
kg	kilogram mass
kG	kilogram force
$K-C$	Keulegan-Carpenter number
k_R	structure relative roughness coefficient
k	ω^2/g , wave number
L	linear momentum
M	mass of body
M_{jk}	body mass matrix (6 x 6)
M_V	virtual mass of body
m, p	subscripts representing model and prototype, respectively
\vec{n}	unit normal vector (into the fluid)
n_j	$= (\vec{n})_j$, for $j=1,2,3$ $(\vec{r} \times \vec{n})_{j-3}$, for $j=4,5,6$
P	pressure
$Q(\xi)$	source density function
Q_j	source densities, $j=1, \dots, 7$
R	reflection coefficient (ratio of reflected wave height to incident wave height)
Re	real part of complex term
Rn	Reynolds number
r	radius of cylindrical control surface

r_{xx}	} radii of gyration	
r_{yy}		
r_{zz}		
S	surface of control volume	
S_b	mean wetted body surface area	
$S_b(t)$	instantaneous wetted body surface area	
S_f	free surface area	
S_h	sea bed surface area	
S_∞	fixed control surface	
S_L	wave elevation spectral density	
T	wave period	
T_r	relative period; wave period as observed from the floating vessel	
$T(\theta)e^{i\tau(\theta)}$	Kotchin function	
t	time	
$\begin{matrix} u \\ v \\ w \end{matrix}$ }	} velocity components in x,y,z directions	
u_0		amplitude of horizontal water particle velocity
$\vec{U}, \dot{\vec{U}}$		rigid body velocities and accelerations
U_n	velocity of the surface normal to itself	
\vec{U}	$= u\vec{i} + w\vec{j} + z\vec{k}$, fluid velocity vector	
\dot{u}	acceleration of fluid	
u_r	relative velocity	
u_R	radial component of fluid velocity	
u_θ	tangential component of fluid velocity	
u_{ro}	amplitude of relative velocity	

X	response of wave-structure system used in dimensional analysis
$\left. \begin{matrix} x \\ y \\ z \end{matrix} \right\}$	coordinates, z positive up
\vec{x}	$= x\vec{i} + y\vec{j} + z\vec{k}$, position vector
$\dot{\vec{x}}, \ddot{\vec{x}}$	velocity and acceleration of body
\vec{x}_{CG}	vector defining center of gravity
z_b	z coordinate of center of bouyancy
z_c	z coordinate of center of gravity
α	wave elevation
β	incident angle of wave system, measured from positive x axis to the direction of wave propagation.
ζ_a	wave amplitude of incident wave
δ	diameter of fluid particle orbits
η	wave amplitude
$\eta^*(t)$	time-dependent first-order linear and angular motions
$\vec{\eta}$	complex amplitude of body motion
θ	angle
λ	wave length
μ	dynamic viscosity of fluid
ν	kinematic viscosity of fluid
$\vec{\xi}$	$= (\xi, \eta, \zeta)$, position vector of a point
π	3.14159
ρ	density of fluid
ϕ	represents a functional relationship
Φ	velocity potential

Φ_I	incident wave potential
Φ_S	scattered wave potential
ω	circular frequency
$\tilde{\omega}$	nondimensional frequency
ω_0	natural circular frequency
ω_{02}, ω_{03}	natural frequency, mooring 2 and 3 respectively
$\delta\omega$	frequency bandwidth
∇	$\frac{\partial}{\partial x}\vec{i} + \frac{\partial}{\partial y}\vec{j} + \frac{\partial}{\partial z}\vec{k}$
Λ	displaced volume of fluid
$\langle \rangle$	time average over one period

CHAPTER I

INTRODUCTION

A floating vessel with zero forward speed acted upon by ocean waves will experience forces which produce vessel motions in six degrees of freedom. These forces are generally the result of a complex, non-linear process of which the first- and second-order components are of main interest. The first-order forces are proportional to wave amplitude and oscillate at a frequency equal to the wave frequency. The mean and low frequency components of the second-order forces are commonly referred to as "wave drift forces". These second-order forces are proportional to the square of the wave amplitude, and are generally small compared to first-order forces. The mean, or "steady", component is recognized (Standing et al 1981) as a second-order consequence of the first-order waves interacting with the structure. This force results in a mean horizontal excursion of the moored vessel. The slow-oscillating second-order component is due to non-linear interactions with the wave field. As the name indicates, these forces cause the vessel to oscillate slowly about the mean position. These second-order forces are often the cause of low frequency, large amplitude

motions of moored vessels, and are, therefore, of great importance in the design considerations of mooring and dynamic positioning systems.

It is the purpose of this work to compare computational and experimental estimations of mean drift forces on a large floating triangular structure in regular waves. Experiments were conducted at the National Research Council's Institute for Marine Dynamics in St. John's. Mooring force data collected by IMD were used to evaluate the validity of the computational estimations, and therefore of their influences in the design process. Such a structure is being considered for operation as a support base in the Hibernia region. It is known as the Deltaport. Experiments were carried out on the 1:200 scale model at IMD. However, they were not designed for the research purposes of interest here. Although it is felt that sufficient data was obtained for the purpose of the present study, more test information would have been an asset.

Chapter II of this report reviews the historical progress of work in the field of wave force prediction. Theory governing wave-structure interaction is presented in Chapter III. Experimental results and numerical evaluations of steady drift forces are discussed in Chapter IV. Chapter V compares computations with experiments. Conclusions from this comparison are drawn in Chapter VI.

CHAPTER II

LITERATURE REVIEW

One of the earliest studies of drift forces on floating bodies in waves was the experimental study by Suyehiro (1924). He measured the steady drift force experienced by a ship model in beam seas. He believed the drift force was a result of the model rolling motion causing the waves to be reflected. In 1938 Watanabe derived an expression for lateral drift force acting on a ship subject to beam waves based on the product of the first-order roll motion and the Froude-Krylov component of the roll moment. This expression indicated that the force was a second-order phenomenon. Havelock (1940,1942) later made use of Watanabe's theory to develop formulae to predict the mean drift force acting on a ship heaving and pitching in regular head waves.

Dean (1948) concluded that if there is no reflection from a restrained submerged circular cylinder the incident wave only changes by a shift in phase. Ursell (1950) developed a procedure to resolve forces on a

submerged cylinder based on Dean's findings. Ogilvie (1963) developed expressions for and calculated the first- and second-order forces on a submerged cylinder based on Ursell's procedure. A body subject to forced oscillations in an otherwise calm fluid was analysed by Kotchin (1937, translation 1951) while considering the problem of wave radiation. He developed expressions for the steady forces through the use of body surface integrals which are now known as Kotchin functions.

After examining Watanabe's and Havelock's progress the "far field" approach was taken by Maruo (1960) to develop expressions for steady second-order forces on a fixed body in regular waves. In this approach the wave field far from the structure is used to evaluate the loads on the structure. He included both radiation and diffraction effects. Newman (1967) extended this theory and used it with slender body and strip theory to calculate mean forces on ships. Mei and Black (1969) calculated the mean drift force on a moored barge of infinite breadth utilizing the waves travelling outward from the body. Kim and Chou (1970) developed an expression for the two dimensional case of a ship in oblique waves by extending Maruo's expression. They applied their theory using the strip method.

Hsu and Blenkarn (1970) and Remery and Hermans (1971) showed that the low frequency components of drift force in irregular waves could excite large amplitude, low frequency horizontal motions. Remery and Hermans established that these low frequency components are associated with group effects. Faltinsen and Michelsen (1974) worked with the theory presented by Maruo and Newman and utilized three-dimensional source singularities on body surface panels to obtain their results. Experimental and theoretical results for the mean horizontal force showed good agreement for the case of a rectangular barge in regular waves. Faltinsen and Loken (1978) developed a procedure to calculate slow drift oscillations of a ship in irregular beam seas using a boundary integral technique combined with Newman's method. Molin (1979) also modified Maruo's expression for the horizontal drift force by changing the surface of integration. His theoretical results compared well with experiments.

An added resistance formula was developed by Gerritma and Beukelman (1972) by assuming that the energy in waves progressing outward from the vessel is equal to the work done by incoming waves. Results for a ship travelling in head waves showed good agreement between theory and experiment. A significant conclusion from their

work was the dependency of drift force on the square of the wave amplitude. The energy-work theory was also employed by Salvesen (1974,1978) and Lin and Reed (1976). Kaplan and Sargent (1976) used it to research the drift forces on a semi-submersed barge in regular oblique seas.

Pinkster et al (1976,1977,1979) initiated the near field approach to study first- and second-order wave forces on bodies floating in waves. Their work included methods based on direct integration of pressure and included the force components presented by Boese (1970). Pinkster and Hooft (1978) and Pinkster (1979) extended the method of direct pressure integration to include the low frequency components of the second-order wave forces set up by regular wave groups. Karppinen (1979) developed a method to estimate mean second-order wave forces and moments based on an assumption that the structure can be subdivided into noninteractive slender elements. The mean forces on the elements were summed to get total mean forces on the structure.

Pinkster (1981) and Standing et al (1981) presented insight into theory and experiment for predicting mean and slowly-varying second order forces. Kaplan (1983) utilized an approximate 3-D method to predict the steady drift force on a floating ship model. He applied Maruo's far field theory for drift forces but used a modified

Kotchin function. He professed that the forces could be resolved numerically in relatively short CPU time. Marthinsen (1983) studied the effect of short crested seas on second-order slowly varying drift forces and motions. He developed a method to predict these forces, which is shown to agree very well with Newman's method. Isaacson (1984) presented a useful review of nonlinear wave effects on offshore structures. Murray (1984) discussed the effects of wave grouping on slow drift oscillations of floating moored structures. Rahman (1987) presented a method to predict second-order wave diffraction caused by large offshore structures. He has extended Lighthill's (1979) deep water theory to shallow water waves. Chakrabarti (1987) has also reviewed this subject.

In summary, there are two basic approaches that can be used to analyse drift forces on a floating structure: the "near field" method and the "far field" method. The near field approach involves direct integration of pressure over the wetted surface of the body and can be used to predict mean and low-frequency second-order forces. The far field method can be used to predict mean second-order forces on the basis of conservation of momentum and energy. The potential far from the structure is used to describe fluid motions. In general the near field method is more cumbersome to

utilize. Therefore many researchers have attempted to develop simple methods for prediction of the low-frequency second-order forces to use in conjunction with the far field approach of predicting the mean second-order forces.

The present work is a study of the mean second-order forces on a floating triangular platform utilizing the far field method.

The following section outlines the theory which governs wave-structure interactions.

CHAPTER III

THEORY

3.1 Governing Equations

The equations describing the flow of fluid around a marine structure are the Navier-Stokes equations and the conservation of mass (continuity) equation, supplemented with appropriate boundary conditions. For a constant density Newtonian fluid they are, in primitive variable form:

$$\frac{\partial u}{\partial t} + u \frac{\partial u}{\partial x} + v \frac{\partial u}{\partial y} + w \frac{\partial u}{\partial z} = - \frac{1}{\rho} \frac{\partial P}{\partial x} + \nu \nabla^2 u \quad (3.1a)$$

$$\frac{\partial v}{\partial t} + u \frac{\partial v}{\partial x} + v \frac{\partial v}{\partial y} + w \frac{\partial v}{\partial z} = - \frac{1}{\rho} \frac{\partial P}{\partial y} + \nu \nabla^2 v \quad (3.1b)$$

$$\frac{\partial w}{\partial t} + u \frac{\partial w}{\partial x} + v \frac{\partial w}{\partial y} + w \frac{\partial w}{\partial z} = - \frac{1}{\rho} \frac{\partial P}{\partial z} + \nu \nabla^2 w + \frac{1}{\rho} F_g \quad (3.1c)$$

$$\frac{\partial u}{\partial x} + \frac{\partial v}{\partial y} + \frac{\partial w}{\partial z} = 0 \quad (3.1d)$$

where u, v , and w are velocity components in the x, y , and z directions respectively, t is time, ρ is density of fluid, ν is kinematic viscosity of fluid, F_g is force due to gravity, P is pressure and ∇ indicates the gradient such

that:

$$\nabla = \frac{\partial}{\partial x} \vec{i} + \frac{\partial}{\partial y} \vec{j} + \frac{\partial}{\partial z} \vec{k} \quad (3.2)$$

A right hand cartesian coordinate system (x,y,z) is fixed with respect to the mean position of the body with z positive upwards through the center of gravity and the origin in the plane of the undisturbed free surface. (see Figure 1*)

The governing equations are comprised of these four partial differential equations along with pertinent boundary conditions. In practice it has not been possible to obtain exact solutions for flows about complex geometric bodies.

Many theories have been developed to predict the motion of and hydrodynamic loading on floating bodies. It has been determined that the theory to be utilized in any particular case depends on the ratio of body characteristic length to wavelength, D/λ . It is generally accepted that two flow regimes can be distinguished as presented by Standing (1981) and shown in Figure 2:

(i) wave diffraction around large structures:

for $D/\lambda > 0.2$ the influence of viscosity is negligible and potential flow theory applies:

$$\vec{u} = \nabla\phi \quad (3.3)$$

* For convenience all figures are contained in Appendix A and reproduced when directly referred to in the main text.

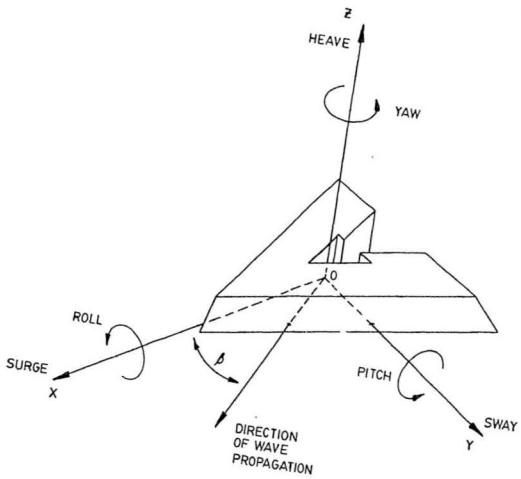


Figure 1
Coordinate System

where \vec{U} is the velocity vector and ϕ is the velocity potential.

(ii) flow separation around slender structures:

for $D/\lambda < 0.2$ viscous stresses are important and vorticity is not neglected.

These two regimes are also acceptable for floating structures.

The following section develops the scaling equations corresponding to each of these flow regimes.

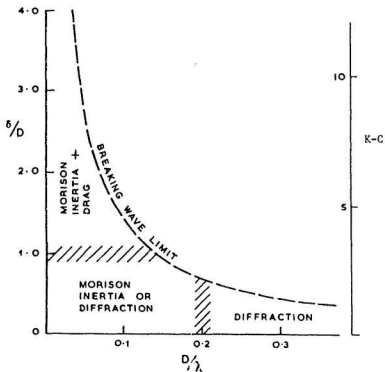


Figure 2
Regions of Validity of Force Prediction Methods
for a Fixed Pile (Standing 1981)

3.2 Modelling Theory

Dimensionless functional equations can provide the laws whereby phenomena such as those presently being discussed may be successfully modelled. These equations are important in the design of model tests and in the interpretation of the results.

One approach of analysing the basic functional equations of a system was developed by Rayleigh (Sharp 1981) and is known as the indicial approach. In this method the basic functional equations are rewritten in terms of the dimensions involved. The exponents of the dimension^s are equated to ensure that the equation is dimensionally homogeneous. Buckingham utilized this method and developed the π theorem which relates the number of parameters in a correct functional equation to the number of variables necessary to specify the phenomenon and the number of dimensions involved. He concluded that, in general, if m variables describe the system with n dimensions, there will be $(m-1)$ exponents to be determined from n simultaneous equations and $(m-n)$ dimensionless parameters will correctly describe the system. He refers to the dimensionless parameters as π -terms.

The functional relationship is written:

$$\phi(b_1, b_2, \dots, b_n) = 0 \quad (3.4)$$

where ϕ represents a functional relationship, $b_1 \dots b_n$ are the variables describing the system in which b_1, b_2, \dots, b_k ($k \leq n$) are dimensionally independent physical quantities. In the present case these quantities are length, l , mass, m , and time, t . (ie. $k=3$)

Now the functional relationship may be written for the general case:

$$b_1^{a_1} b_2^{a_2} \dots b_k^{a_k} \phi(\beta_{k+1}, \beta_{k+2}, \dots, \beta_n) = 0 \quad (3.5)$$

where ϕ is nondimensional and:

$$\beta_{k+i} = b_1^{a_1^i} b_2^{a_2^i} \dots b_k^{a_k^i}, \quad i = 1, 2, \dots, n-k \quad (3.6)$$

where β_{k+i} are nondimensional.

For the case of a body floating in waves with no forward speed the variables which correctly describe the system can be written in functional form as:

$$\phi(X, \rho, \mu, g, d, H, T, M, \bar{x}_{cg}, r, D, A, k_R) = 0 \quad (3.7)$$

where:

- X represents a response of the wave-structure system in terms of force [N], motion [m], or velocity [m/s]
- ρ, μ are physical properties of water; density [kg/m³] and dynamic viscosity [kg/ms], respectively

g, d are environmental properties affecting wave propagation; acceleration due to gravity [m/s^2] and water depth [m] respectively
 H, T are wave parameters; wave height [m] and period [s] respectively (wavelength, λ [m] or frequency, ω [rads/s], or f [Hz] could replace T)
 $M, \bar{x}_{CG}, r, D, A, k_R$ parameters of the structure; mass [kg], center of gravity [m], radii of gyration [m], characteristic length [m], nondimensional table of offsets, and relative roughness, respectively.

Taking $\rho, g,$ and D as dimensionally independent parameters and resolving the functional equation for X , equation 3.7 can be rewritten:

$$\Phi_X(\rho, \mu, g, d, H, T, M, \bar{x}_{CG}, r, D, A, k_R) = X \quad (3.8)$$

Now π -terms are formed by combining all other terms, separately, with these three relevant variables which cannot form a π -term on their own, but contain all three dimensions involved in the problem. Now one can write:

$$\rho^{\alpha_1} g^{\alpha_2} d^{\alpha_3} (X - \Phi_X(\frac{v}{\sqrt{gD}}, \frac{d}{D}, \frac{H}{D}, T\sqrt{g/D}, \frac{M}{\rho D^3}, \frac{\bar{x}_{CG}}{D}, \frac{r}{D}, A, k_R)) = 0 \quad (3.9)$$

or,

$$\hat{\lambda} = \hat{\phi}_X \left(\frac{v}{\sqrt{gD}}, \frac{d}{D}, \frac{H}{D}, T\sqrt{g/D}, \frac{M}{\rho D^3}, \frac{\bar{x}_{cg}}{D}, \frac{r}{D}, \lambda, k_R \right) \quad (3.10)$$

where $\hat{\phi}_X$ is nondimensional and $\hat{\lambda}$ represents X normalized with respect to ρ , g , and D , depending on the definition of X as a force, velocity or motion. If X is taken* as a force F, then $\hat{\lambda}$ can be written:

$$\hat{\lambda} = \frac{F}{\rho g D^3} \quad (3.11)$$

The first term on the right hand side, $\frac{v}{\sqrt{gD}}$, represents Reynolds number $\frac{uD}{v}$, where u is a characteristic wave speed. Let $X=u$ in equations 3.9 and 3.10 such that nondimensional $\hat{\lambda}$ is the Froude number:

$$\hat{\lambda} = \frac{u}{\sqrt{gD}} = \hat{\phi}_u \left(\frac{v}{\sqrt{gD}}, \frac{d}{D}, \frac{H}{D}, T\sqrt{g/D}, \frac{M}{\rho D^3}, \frac{\bar{x}_{cg}}{D}, \frac{r}{D}, \lambda, k_R \right) \quad (3.12)$$

Compounding dimensionless terms one can write the Reynolds number:

$$\frac{v}{\sqrt{gD}} \cdot \left(\frac{v}{\sqrt{gD}} \right)^{-2} \cdot \frac{u}{\sqrt{gD}} = \frac{uD}{v} \quad (3.13)$$

Substituting this into equation 3.12:

$$\frac{uD}{v} = \frac{\sqrt{gD}}{v} \hat{\phi}_u \left(\frac{v}{\sqrt{gD}}, \frac{d}{D}, \frac{H}{D}, T\sqrt{g/D}, \frac{M}{\rho D^3}, \frac{\bar{x}_{cg}}{D}, \frac{r}{D}, \lambda, k_R \right) \quad (3.14)$$

Therefore the Reynolds number, $Rn = \frac{uD}{v}$, can be substituted for $\frac{v}{\sqrt{gD}}$ in equation 3.10. This also shows that the Froude number, $\frac{u}{\sqrt{gD}}$, cannot in general be modelled between

the scale model and prototype unless viscous scale effects can be neglected.

In a similar way the parameter $T\sqrt{g/D}$ represents the Keulegan-Carpenter number, $K-C = \frac{UT}{D}$, since:

$$T\sqrt{g/D} \cdot \frac{u}{\sqrt{gD}} = \frac{UT}{D} \quad (3.15)$$

Now equation 3.10 can be written in terms of well known parameters:

$$\tilde{\chi} = \tilde{\phi}_X \left(\frac{uD}{v}, \frac{d}{D}, \frac{H}{D}, \frac{UT}{D}, \frac{M}{\rho D^3}, \frac{\bar{X}}{D}, \frac{cg}{D}, \frac{r}{D}, A, k_R \right) \quad (3.16)$$

$\downarrow \qquad \downarrow$
 $Rn \qquad K-C$

This is the most convenient representation when both wave and viscous effects, such as flow separation, are of primary importance.

Now if viscous scale effects are negligible and, therefore the dependence on Rn can be neglected, it is common to replace $T\sqrt{g/D}$ in equation 3.16 by nondimensional frequency, $\tilde{\omega}$:

$$2\pi T\sqrt{g/D} (T\sqrt{g/D})^{-2} = \omega\sqrt{D/g} = \tilde{\omega} \quad (3.17)$$

If λ had been used in the basic functional equation 3.7 in place of T , the resulting π -term would be λ/D . Equation 3.10 can be written for Froudian similarity:

$$\hat{\chi} = \hat{\phi}_X \left(\frac{d}{D}, \frac{H}{D}, \omega \sqrt{D/g}, \frac{M}{\rho D^3}, \frac{\bar{x}_{cg}}{D}, \frac{r}{D}, \Lambda, k_R \right) \quad (3.18)$$

Now considering first- and second-order quantities X with respect to the wave height, H :

$$\hat{\chi} = \hat{\chi}^{(1)} + \hat{\chi}^{(2)} = \left(\frac{H}{D} \right) \hat{\phi}_X^{(1)} + \left(\frac{H}{D} \right)^2 \hat{\phi}_X^{(2)} \quad (3.19)$$

Therefore it follows that:

$$\hat{\chi}^{(1)} \frac{D}{H} = \hat{\phi}_X^{(1)} \left(Rn, \frac{d}{D}, \frac{H}{D}, K-C, \frac{M}{\rho D^3}, \frac{\bar{x}_{cg}}{D}, \frac{r}{D}, \Lambda, k_R \right) \quad (3.20)$$

$$\hat{\chi}^{(2)} \left(\frac{D}{H} \right)^2 = \hat{\phi}_X^{(2)} \left(Rn, \frac{d}{D}, \frac{H}{D}, K-C, \frac{M}{\rho D^3}, \frac{\bar{x}_{cg}}{D}, \frac{r}{D}, \Lambda, k_R \right) \quad (3.21)$$

for Reynolds modelling, or;

$$\hat{\chi}^{(1)} \frac{D}{H} = \hat{\phi}_X^{(1)} \left(\frac{d}{D}, \frac{H}{D}, \hat{\omega}, \frac{M}{\rho D^3}, \frac{\bar{x}_{cg}}{D}, \frac{r}{D}, \Lambda, k_R \right) \quad (3.22)$$

$$\hat{\chi}^{(2)} \left(\frac{D}{H} \right)^2 = \hat{\phi}_X^{(2)} \left(\frac{d}{D}, \frac{H}{D}, \hat{\omega}, \frac{M}{\rho D^3}, \frac{\bar{x}_{cg}}{D}, \frac{r}{D}, \Lambda, k_R \right) \quad (3.23)$$

for Froudian scaling.

Therefore one can write nondimensional force as:

$$\hat{F} = \hat{\chi} = \frac{F}{\rho g D^3} \quad (3.24)$$

consisting of first- and second-order components:

$$\hat{F} = \hat{F}^{(1)} + \hat{F}^{(2)} \quad (3.25)$$

The first-order component is written:

$$\hat{F}^{(1)} = \hat{\chi}^{(1)} \frac{D}{H} = \frac{F^{(1)}}{\rho g D^2 H} \quad (3.26)$$

indicating that the first-order force is proportional to the waveheight. The second-order component is written:

$$\hat{F}^{(2)} = \hat{\chi}^{(2)} \left(\frac{D}{H} \right)^2 = \frac{F^{(2)}}{\rho g D H^2} \quad (3.27)$$

indicating that the second-order forces are proportional to the square of the waveheight.

Miller and M^CGregor (1978) recommended that, despite which modelling technique is employed, model tests should not be carried out in a flow regime that is different than that of the prototype, as indicated in Figure 3 (Miller and M^CGregor 1978). This is often impossible to achieve. It is useful to look at the Reynolds number and Keulegan-Carpenter number in more detail.

The usual form of the Reynold's number is:

$$Rn = \frac{u_0 D}{\nu} \quad (3.28)$$

where u_0 is the amplitude of u , the horizontal water particle velocity

The Keulegan-Carpenter number is generally of the form:

$$K-C = \frac{u_0 T}{D} \quad (3.29)$$

The horizontal water particle velocity, at an elevation s above the seabed, is given by:

$$u = \frac{\pi H}{T} \frac{\cosh ks}{\sinh kd} \cos \theta \quad (3.30)$$

where $s=\alpha+d$, α is wave amplitude, k is the wave number, T is the wave period and $\theta=(kx-\omega t)$.

Now the amplitude of this velocity, at $\alpha=0$, is:

$$u_0 = \pi H \frac{\cosh kd}{\sinh kd} \quad (3.31)$$

Assuming deep water, the wave number is:

$$k = \frac{2\pi}{\lambda} = \frac{\omega^2}{g} = 4\frac{\pi^2}{T^2g} \quad (3.36)$$

and the wavelength is:

$$\lambda = \frac{g}{2\pi f^2} \quad (3.37)$$

Rn and K-C can be more accurately evaluated for the dynamic response of offshore platforms by utilizing relative velocity terms:

$$K-C = \frac{u_{r0} T_r}{D} \quad (3.38)$$

$$Rn = \frac{u_{r0} D}{v} \quad (3.39)$$

where u_{r0} is amplitude of relative velocity, $u_r = (u - \dot{x})$, and T_r is relative period of encounter.

It is necessary to choose which scaling laws should be used for any particular case. In general when viscous forces are dominant due to structural detail Reynolds scaling is utilized, which is represented by equation 3.16. In this case the second flow regime described in section 3.1 exists. When gravity forces are dominant, as in the present case where the body appears to act as a fully solid structure, Froudian scaling best describes the system. This is represented by equation 3.18 and the first flow regime of section 3.1 is presumed to exist.

These scaling equations are important in the design of model tests and in the interpretation of the results of the tests. They are utilized in section 4.1.6 for analyzing the data generated in present work.

The following section presents theory used for predicting forces on slender bodies in waves.

3.3 Slender Structures

The oscillatory flow about a slender structure is depicted by the second regime of section 3.1 in which drag is significant. In this case there is little disturbance to the incident wave, but a vortex wake forms behind the body as the flow separates from its surface. Figure 4 (Chakrabarti 1987) illustrates the shedding of vortices around a vertical circular cylinder in waves for various $K-C$ values. In practice this type of wave-structure interaction is dealt with by neglecting free surface effects, accounting for viscous effects semi-empirically and adopting Morison's equation. This equation has been developed to estimate hydrodynamic loads and motions in this case and is reported in many sources (Morison et al 1950, Sarpkaya and Isaacson 1981, and Lovaas 1983).

The Morison Equation is a formula which was developed by Morison, Johnson, O'Brien and Schaaf (1950) to predict the hydrodynamic force acting on a section of pile

and is comprised of two components: an inertial force and a drag force. It is assumed that the body is small relative to the wave length so that the incident flow is uniform near the body and diffraction effects are negligible. For the common case of a vertical circular section of diameter D and sufficiently small length dL :

$$\frac{dF}{dL} = 0.5 \rho D C_d u |u| + 0.25 \rho n D^2 C_m \frac{du}{dt} \quad (3.40)$$

where F is hydrodynamic force and u is velocity of fluid.

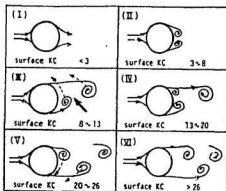


Figure 4
Vortex Shedding Patterns Around a Vertical Cylinder
in Waves as Functions of $K-C$ (Chakrabarti 1987)

The first term on the right hand side represents the force required to overcome the drag due to vortex separation and skin friction effects. C_d is the drag coefficient.

The second or potential flow term involves momentum (scattering) effects. C_m is the inertia coefficient. Data for C_m and C_d have been determined experimentally for a variety of bodies (Sarpkaya and Isaacson 1981). These show that C_m and C_d are functions of the Keulegan-Carpenter number, the Reynold's number and the body surface roughness.

Note that the drag force is a nonlinear function of the flow velocity while the inertia term is linear. For the latter, the total horizontal acceleration is:

$$\frac{du}{dt} = \frac{\partial u}{\partial t} + u \frac{\partial u}{\partial x} + v \frac{\partial u}{\partial y} + w \frac{\partial u}{\partial z} \quad (3.41)$$

Equation (3.40) has been modified to describe a floating rigid structure in waves. Two independent flow fields are superimposed: the field due to wave motion alone:

$$F = C_m A_I \dot{u} + C_d A_d |u|u \quad (3.42)$$

and the field due to structure motion alone:

$$F = -C_A A_I \ddot{x} - C_d A_d |\dot{x}| \dot{x} \quad (3.43)$$

where \dot{x} and \ddot{x} are velocity and acceleration of the structure, C_A is the added mass coefficient and C_d is the

drag coefficient. The resulting form is known as the independent flow fields model (Chakrabarti 1987):

$$F = C_m A_I \dot{u} - C_A A_I \ddot{x} + C_{cl} A_d |u|u - C_d A_d |\dot{x}| \dot{x} \quad (3.44)$$

With the following relations:

$$C_m = 1 + C_A \quad (3.45)$$

$$A_I = \frac{\rho \pi D^2}{4} \quad (3.46)$$

$$A_d = \frac{1}{2} \rho D \quad (3.47)$$

$$C_d = C_d' \quad (3.48)$$

When forces are written in terms of relative motion, single coefficients are assumed to apply and the force can be written:

$$F = C_m A_I (\dot{u} - \ddot{x}) + A_I \ddot{x} + C_d A_d |u - \dot{x}| (u - \dot{x}) \quad (3.49)$$

$$F = \frac{1}{2} \rho D^2 C_m (\dot{u} - \ddot{x}) + \frac{1}{2} \rho \pi D^2 \ddot{x} + \frac{1}{2} \rho D C_d |u - \dot{x}| (u - \dot{x}) \quad (3.50)$$

The final section of this chapter describes the potential flow theory for predicting wave forces on large bodies.

3.4 Large Structures

When a structure is large compared to the wavelength the first flow regime is assumed in which the incident wave undergoes significant scattering in the region of the body and free surface effects cannot be neglected. The motions and forces on the structure are affected by this phenomenon and must be calculated

accordingly. Linear diffraction theory is well developed (Faltinsen and Michelsen 1974, Morrison et al 1950, Garrison 1975) and widely used to predict motions and hydrodynamic loading on offshore structures.

This theory assumes ideal or potential fluid flow (i.e. acyclic, irrotational flow). See Milne-Thomson 1968. It describes the scattering of small-amplitude waves by large objects in the ocean and predicts the wave loads associated with both the local accelerating flow field and the wave scattering process.

The governing equations are:

(i) continuity (in fluid domain):

$$\nabla^2 \Phi = \frac{\partial^2 \Phi}{\partial x^2} + \frac{\partial^2 \Phi}{\partial y^2} + \frac{\partial^2 \Phi}{\partial z^2} = 0 \quad (3.51)$$

(ii) impermeability:

$$\frac{\partial \Phi}{\partial n} = U_n \quad \text{on solid submerged boundaries} \quad (3.52)$$

$$\frac{\partial \Phi}{\partial z} = 0 \quad \text{on bottom surface} \quad (3.53)$$

(iii) free surface conditions (z=0):

$$\frac{\partial \Phi}{\partial z} = \frac{\partial \eta}{\partial t} \quad \text{kinematic condition} \quad (3.54)$$

$$\frac{\partial \Phi}{\partial t} + g\eta = 0 \quad \text{dynamic condition} \quad (3.55)$$

which together give:

$$\frac{\partial^2 \Phi}{\partial t^2} + g \frac{\partial \Phi}{\partial z} = 0 \quad (3.56)$$

(iv) radiation condition

Together with the appropriate initial conditions for the time domain problem are the radiation conditions for the steady frequency domain problem. In this latter case the radiation condition demands that the waves scattered by the structure represent a wave field propagating away from the structure. In the panel method utilized in this study the radiation condition is implicitly satisfied by the use of an appropriate Green's function.

In the fluid domain, pressure, P , is defined by the linearized Bernoulli equation:

$$P = -\rho g z - \rho \frac{\partial \Phi}{\partial t} \quad (3.57)$$

Now the force on the body may be expressed in terms of the pressure on the body surface:

$$F_j = \int_{S_b} P \, dS = \int_{S_b} (\rho g z + \rho \frac{\partial \Phi}{\partial t}) n_j \, dS \quad (3.58)$$

$$j=1, \dots, 6$$

where n_j is the generalized normal, positive into the fluid, S_b is the mean wetted body surface area and F_j is the generalized force:

$$n_j = \begin{cases} (\vec{n})_j, & j=1,2,3 \\ (\vec{x} \times \vec{n})_{j-3}, & j=4,5,6 \end{cases} \quad (3.59)$$

$$F_j = \int_{S_b} \rho g z n_j \, dS + \int_{S_b} \rho \frac{\partial \Phi}{\partial t} n_j \, dS \quad (3.60)$$

The problem at hand is to solve for the velocity potential, Φ , which, because the problem is linear, can be represented by the superposition of the "incident" and "scattered" wave potentials:

$$\Phi = \Phi_I + \Phi_S \quad (3.61)$$

Equation (3.50) becomes:

$$\begin{aligned} F_j &= \left(\rho \int_{S_b} g z n_j dS + \rho \int_{S_b} \frac{\partial}{\partial t} \Phi_I n_j dS \right) + \rho \int_{S_b} \frac{\partial}{\partial t} \Phi_S n_j dS \quad (3.62) \\ &= \text{Froude-Krylov} \quad + \quad \text{scattering} \quad j=1 \dots 6 \end{aligned}$$

The scattering force consists of radiation and diffraction components.

The potential may be represented by a continuous distribution of complex sources on the surface of the body. This method is discussed in more depth in section 4.2.

The next chapter presents a study of drift forces on a triangular shaped floating structure in regular waves. An experimental study is first given, and this is followed by a numerical simulation.

CHAPTER IV

THE STUDY OF DRIFT FORCES

4.1 Experimental Study

4.1.1 Purpose of Model Tests

In general wave loading on a structure is a complex non-linear process of which the first- and second-order components are of primary interest. The first-order wave force oscillates at the wave frequency and has zero mean. This is responsible for the vessel motions with wave frequencies. The mean and low-frequency components of the second-order force are known collectively as "wave drift forces". The mean second-order force, or "steady drift" component, is recognized as a second-order consequence of first-order waves interacting with the structure. The slowly oscillating second-order force component is due to wave group effects which are non-linear interactions in the wave field. Although the second-order forces are usually substantially smaller than first-order forces, they may excite large resonant response motions if damping is low. This response can cause severe loads in mooring systems

and, therefore, must be seriously considered in the design of mooring and dynamic positioning systems.

A structure floating in regular waves will be subject to first-order forces and second-order steady drift as shown in Figure 5. A structure floating in irregular or beating waves will be additionally acted upon by second-order slow drift oscillatory forces as shown in Figure 6.

The model tests described herein were initially intended to estimate mooring forces only, in a series of regular waves, to assist in the design analysis of the offshore structure. Models of at least 1:25 scale are recommended for accurate predictions of prototype motions and forces. The results of the 1:200 scale model tests conducted here were expected to be useful in the design of the 1:25 scale model. The tests were exploratory in nature and motions were not measured. Only tension in the mooring line was measured, and the incident wave was recorded.

4.1.2 The Model

A 1:200 scale model of a proposed delta-shaped offshore service and supply base was constructed of tetrahedron space-frames and buoyancy tubes, as shown in Figures 7a and 7b. Model dimensions are shown in Figure

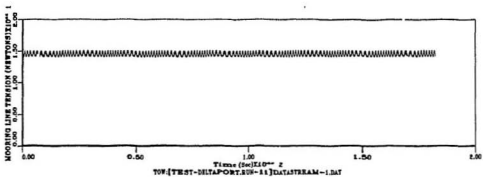
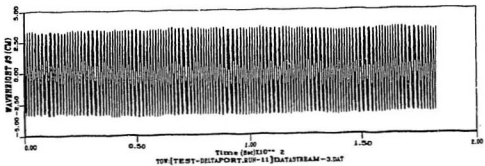


Figure 5
Measured Forces in Regular Waves

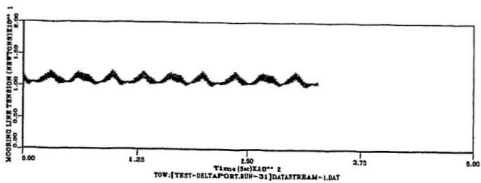
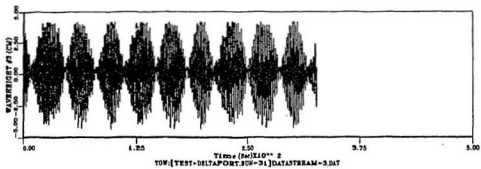


Figure 6
Measured Forces in Beating Waves

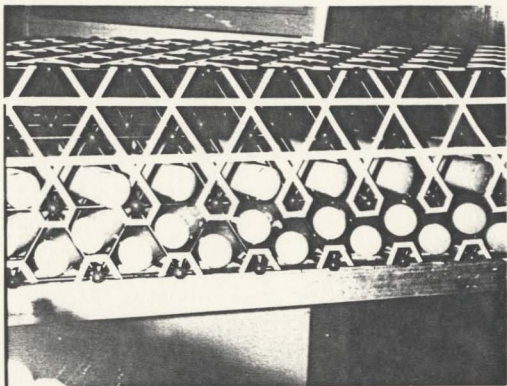


Figure 7a: Model Space Frame and Buoyancy Tubes

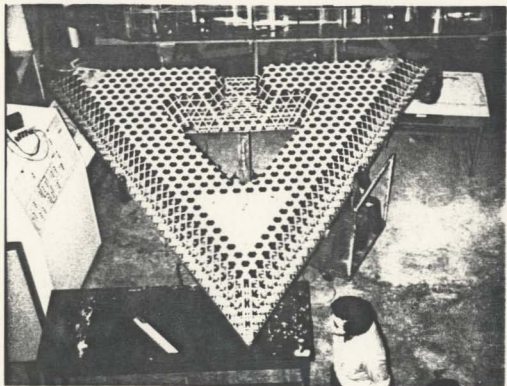


Figure 7b: 1:200 Scale Model Used in Testing

8. The main particulars of the model are calculated in Appendix B and are summarized below:

Mass	150 kg
Volume	0.30 m ³
Mooring stiffness	#2 4.6 kG/m = 45.1 N/m #3 9.2 kG/m = 90.3 N/m
Natural surge frequency	$\omega_{o_2} = 0.4477$ rps $f_{o_2} = 0.0713$ Hz $\omega_{o_3} = 0.6335$ rps $f_{o_3} = 0.1008$ Hz
Center of gravity	(0,0,0.0381m)
Center of buoyancy	(0,0,-0.0235m)
Radii of gyration	rxx = 0.91m ryy = 0.88m rzz = 1.26m
Virtual Mass	225 kg

Note that the virtual mass, $M_V = (1+C_A)M = C_m M$, is frequency dependent since the added mass coefficient is frequency dependent. $C_A = 0.5$ is used for the calculations in Appendix A.

4.1.3 Test Facility

Tests were carried out at the National Research Council's Institute for Marine Dynamics in St. John's. The towing tank is 200m long and 12m wide with a water depth of 7m. The towing carriage spans the full width of the tank and has a maximum speed of 10.0 m/s, with

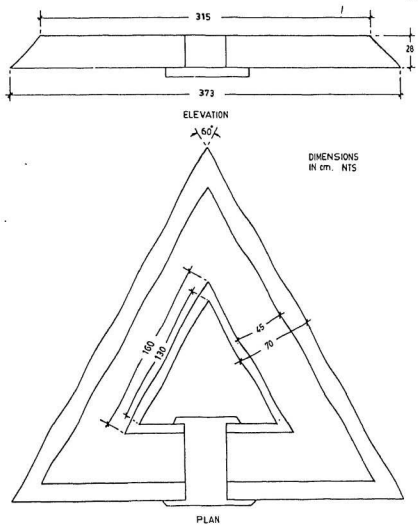


Figure 8
Model Dimensions

possible acceleration ranging from 0.2 to 1.2 m/s². The wavemaker is a hydraulically driven dual flap type which provides for the modelling of regular and irregular seas. A conventional parabolic beach is located at the opposite end of the tank to prevent waves from reflecting back down the tank (see Figure 9).

4.1.4 Test Set-Up

The model was held in place at the carriage by a model mooring system consisting of linear springs, nylon line, and a counter weight, as shown in Figure 10. Mooring line tension was read with a hoop strain gauge. Tests were carried out in regular waves ranging in frequency from 0.4 to 1.4 Hertz. Two different mooring line stiffnesses were used, $K_1=4.60$ kg/m and $K_2=9.20$ kg/m. (Mooring system #1 was not used in these tests). Since the model was constructed of densely distributed elements the permeability of the structure to waves was of interest. In order to determine the extent of this the model's outer surface was covered by a plastic sheet for a test sequence in order to make the model appear solid to the wave field. The two model configurations are referred to as the covered and uncovered models throughout this text.

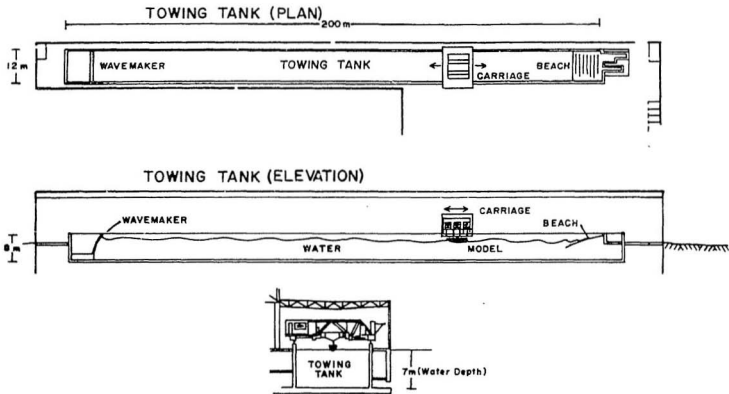


Figure 9
IMD Towing Tank Facility

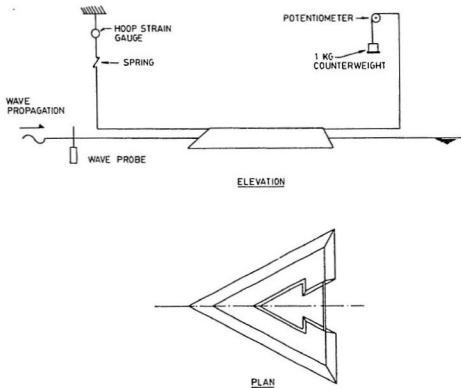


Figure 10
Test Set-Up

4.1.5 Data Acquisition

Wave data were measured by a wave probe on the carriage. Mooring line tension data were measured by the strain gauge. The data acquisition system at IMD uses a DEC microVAX II computer running on the VAX/VMS operating system. Analog data was digitized using a NEFF 620 A/D converter-multiplexer interfaced to the microVAX Q-bus. Fortran-77 acquisition software controlled the sampling of data, which was then stored on a hard disk.

4.1.6 Data Analysis

Model tests were carried out in regular head waves ranging in frequency from 0.4 to 1.4 Hz, corresponding to λ/D equal to 3.02 and 0.25 respectively for $D=3.23$ m. The analysis was carried out for the covered and uncovered models. In some test cases the incident wave lacked consistency, so the time series were truncated to include only a uniform portion for analysis. The mean mooring line tension for each test was determined using NRC's time series analysis (TSA) software. Power spectral density plots for both wave amplitude and mooring force were generated for all tests and are given in Appendix C. As can be seen, not all of the waves were of a pure sinusoidal nature. In fact, most of them showed group effects to some degree. Wave amplitudes, η , were

determined by a statistical analysis of the peaks and troughs of each time series. The wave amplitude power spectrum can be represented by (Abkowitz et al 1965):

$$\eta_n = (S_{\zeta n} \delta\omega_n)^{1/2} \quad (4.1)$$

where S_{ζ} is the wave elevation spectral density, n the number of representative frequencies in the power spectra and $\delta\omega$ is the frequency bandwidth.

For the case of regular waves, the mooring line tension time series indicates two components of force; a high frequency first-order component which oscillates at the wave frequency and a second-order steady drift component.

When wave group effects are apparent, the mooring line tension time series shows three force components; the two mentioned above along with a second-order slowly oscillating force. The frequency of this force is equivalent to the frequency difference of the wave components contributing to the group effects.

The steady horizontal drift force in the x -direction, $F_{d,x}$, is being analysed herein. It may be written for regular waves:

$$F_{d,x} = \frac{1}{2} \rho g \eta^2 D R^2 \quad (4.2)$$

where R is the reflection coefficient, the ratio of the reflected wave height to the incident wave height, in two dimensional flow. R^2 becomes a nondimensional drift force in three (or two) dimensional flow.

When two wave frequencies are present, according to Remery and Hermans (1971), this equation for steady drift force becomes:

$$F_{d,x} = \frac{1}{2} \rho g (\eta_1^2 + \eta_2^2) D R^2 \quad (4.3)$$

where η_1 and η_2 are the amplitudes of the waves corresponding to frequencies 1 and 2.

Now we can rewrite equation 4.2:

$$R^2 = \frac{F_{d,x}}{\frac{1}{2} \rho g \eta^2 D} \quad (4.4)$$

A similar form of this equation was previously derived in section 3.2 on modelling laws (see equation 3.27). With proper modelling this term, which is the nondimensional drift force, should be equal for model and prototype structures if previously discussed modelling laws are obeyed.

In order to keep consistent with literature on this subject, we substitute the following relation into equation 4.4:

$$D = \Lambda^{1/3} \quad (4.5)$$

where Λ is the displaced volume of fluid. Thus, equation 4.4 becomes:

$$R^2 = \frac{F_{d,x}}{\frac{1}{2} \rho g \eta^2 \Lambda^{1/3}} \quad (4.6)$$

Similarly, equation 4.3 can be rewritten:

$$R^2 = \frac{F_{d,x}}{\frac{1}{2} \rho g (\eta_1^2 + \eta_2^2) \Lambda^{1/3}} \quad (4.7)$$

In either case this term is known as the nondimensional steady drift force, and is plotted against nondimensional frequency:

$$\tilde{w} = \omega(\Lambda^{1/3}/g)^{1/2} \quad (4.8)$$

Table 1 shows test frequencies for model and prototype, with corresponding nondimensional frequency and wave lengths. The wave lengths at lower frequencies are not common in real sea states and are considerably longer than the body.

TABLE 1
Test Wave Frequencies and Wave Lengths

f_m (Hz) ^m	f_p (Hz) ^p	$f_{\text{non-dim.}}$	λ_m (m)	λ_p (m) ^p
0.4	0.028	0.578	9.76	1952
0.5	0.035	0.731	6.25	1248
0.6	0.042	0.878	4.34	868
0.7	0.049	1.02	3.19	638
0.8	0.057	1.17	2.44	488
0.9	0.064	1.32	1.26	252
1.0	0.071	1.46	1.56	312
1.1	0.078	1.61	1.29	258
1.2	0.085	1.75	1.08	260
1.3	0.092	1.90	0.92	184
1.4	0.099	2.05	0.80	160

Results of the model tests are recorded in Tables 2 and 3 for the uncovered and covered model, respectively. The drift forces are noted negative due to the direction of the incoming wave with respect to the x-axis. Plots of the measured steady drift force against frequency are given in Figures 11 and 12. An interactive

graphics program was used to fit elastic splines through the data points.

In Tables 2 and 3 the wave number and wavelength estimates are based on deep water theory. The mean drift force recorded in the time series is reduced by the 10N counterweight used in experiments. This is based on an assumption that the spring elongation is due to surge motion only. Reynolds number and Keulegan-Carpenter number are calculated according to equations 3.33 and 3.35, respectively. Since the model is fabricated of small tubular members of two different sizes in a near-solid matrix, Reynolds numbers and Keulegan-Carpenter numbers are calculated for cases of three characteristic dimensions of the body (see figures 7 and 8):

- (i) the linear space frame component diameter, 0.007m
- (ii) the buoyancy tube diameter, 0.04m
- (iii) the width of one side leg of the triangular structure, based on a near-solid hull assumption, 0.625m

Test results, judged from power spectra, were grouped in four categories; (i) regular waves, (ii) waves with some group characteristics (vague groups) (iii) fully developed (distinct) groups and (iv) discarded results due to many wave frequencies. In general, the

Table 3
Input Data and Test Results: Covered Model

DELTAPORT TEST RESULTS											d=7m	
REGULAR WAVES											v=1.56x10 ⁻⁴ m ² /s	
COVERED MODEL												
		f	k	λ	F _d	η	Rn			K-C		
TEST NUMBER	MOORING SPRING NUMBER	FREQ.	WAVE NUMBER	WAVE LENGTH	MEAN DRIFT FORCE	WAVE AMPL.	REYNOLDS NUMBER			KEULEGAN-CARPENTER NO.		
		(Hz)	(rad/m)	(m)	(N)	(m)	D=0.007	D=0.04	D=0.625	D=0.007	D=0.04	D=0.625
	input	input	$k=2\pi/\lambda$	$\lambda = \frac{g}{2\pi f^2}$	meas'd-10N wt.		$Rn = \frac{2\pi f \eta D \cosh kd}{v \sinh kd}$			$K-C = \frac{2\pi \eta \cosh kd}{D \sinh kd}$		
60	2	0.4	0.644	9.76	-0.59	0.0374	421.9	2410.8	37658.8	33.6	5.88	0.376
61	3	0.4	0.644	9.76	-0.69	0.0356	401.9	2296.7	35846.4	32.0	5.60	0.358
62	3	0.6	1.450	4.34	-5.72	0.0601	1015.8	5804.7	90773.9	53.9	9.43	0.604
63	2	0.6	1.450	4.34	-5.53	0.0591	1000.1	5714.8	89263.5	53.1	9.29	0.594
64	2	0.8	2.580	2.44	-7.75	0.0372	837.9	4788.1	74914.9	33.3	5.84	0.374
65	3	0.8	2.580	2.44	-8.97	0.0443	999.6	5712.2	89213.2	39.8	6.96	0.445
66	3	1.0	4.020	1.56	-12.15	0.0338	951.5	5437.4	85084.8	30.3	5.30	0.340
67	2	1.0	4.020	1.56	-14.52	0.0500	1409.1	8052.1	125865.2	44.9	7.85	0.503
68	2	1.2	5.800	1.08	-6.83	0.0285	964.2	5509.9	86091.8	25.6	4.48	0.287
69	3	1.2	5.800	1.08	-7.70	0.0302	1020.4	5830.8	91227.1	27.1	4.74	0.304
70	3	1.4	7.890	0.80								
71	2	1.4	7.890	0.80								

lower frequency waves were most regular, while the group phenomena increased with increasing frequency. Table 4 indicates the status of each test and the significant frequencies and frequency differences. In the case of beating waves (ie. two or more waves of small frequency differences contributing to the incident wave) the frequency difference can be of great importance. If this frequency of the slow drift oscillations coincides with the natural frequency of the mooring system, resonance may occur. In model tests this can be controlled by varying the stiffness of the mooring. From observing Table 4 one can see that many of the frequency differences are near the calculated natural frequency of the moored structure. Therefore these test results are questionable, and they are indicated as such on the plots. At higher frequencies some of the test results were discarded due to the number of wave frequencies present in the test.

Drift force plots, Figures 11 and 12, indicate that drift forces were near zero for low frequencies. For the covered model the drift forces were considerably higher than those of the uncovered model as frequency increased. No significant difference due to mooring systems is obvious.

The nondimensionalized plots of Figures 13 and 14, with higher frequency results discarded (see Table 4), should be a better interpretation of test results.

TABLE 4
Model Test Incident Wave Frequencies

RUN NUMBER	MAIN FREQ (Hz)	OTHER FREQ (Hz)	DELTA FREQ.	STATUS
4	0.4			i) regular
5	0.4			i) regular
6	0.5			i) regular
7	0.5			i) regular
8	0.6			i) regular
9	0.6			i) regular
10	0.7	0.6	0.1	iii) distinct
11	0.7			i) regular
12	0.8			i) regular
13	0.8			i) regular
14	0.9	1.0	0.1	iii) distinct
15	0.9			i) regular
16	1.0	0.9, 1.1	0.1	iii) distinct
17	1.0	0.9, 1.1	0.1	iii) distinct
18	1.1	0.9, 1.0, 1.2, 1.3	0.1, 0.2	iii) distinct
19	1.1	1.2	0.1	iii) distinct
20	1.2	1.1, 1.3	0.1	iii) distinct
21	1.2	1.05, 1.35	0.15	iii) distinct
22	1.3	many	?	discarded
23	1.3	many	?	discarded
24	1.4	many	?	discarded
25	1.4	many	?	discarded
60	0.4			ii) vague
61	0.4			i) regular
62	0.6			ii) vague
63	0.6			ii) vague
64	0.8	0.6	0.2	ii) vague
65	0.8			ii) vague
66	1.0	0.8, 1.2	0.2	iii) distinct
67	1.0	0.8, 1.2	0.2	iii) distinct
68	1.2	many	?	discarded
69	1.2	many	?	discarded
70	1.4	many	?	discarded
71	1.4	many	?	discarded

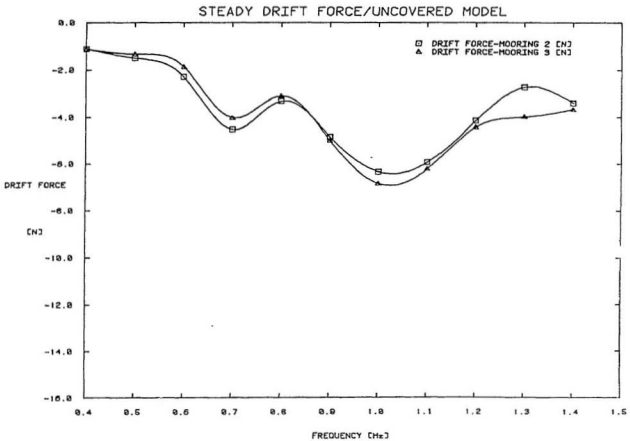


Figure 11
 Plot of Experimental Results: Uncovered Model;
 Drift Force .vs. Frequency

STEADY DRIFT FORCE/COVERED MODEL

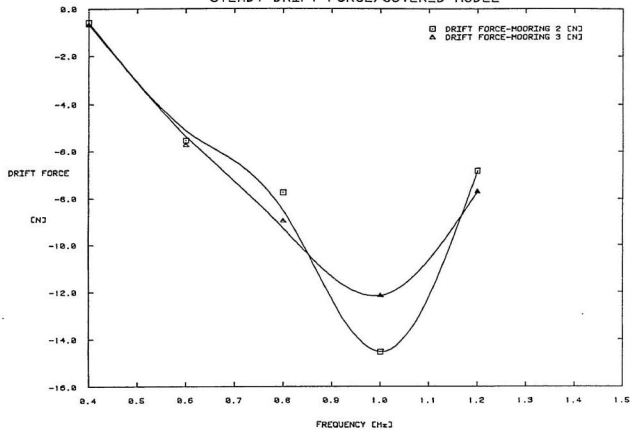


Figure 12
Plot of Experimental Results: Covered Model;
Drift Force .vs. Frequency

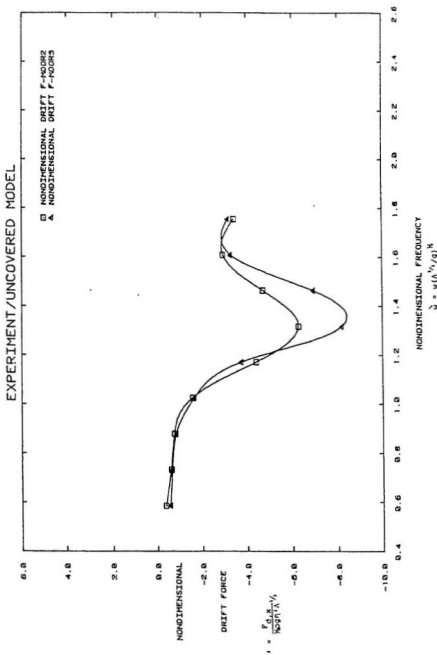


Figure 13
 Plot of Experimental Results: Uncovered Model:
 Nondimensional Drift Force .vs. Nondimensional Frequency

EXPERIMENT/COVERED MODEL

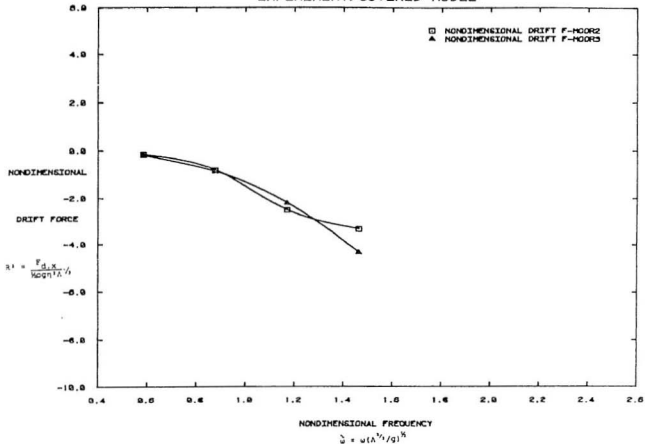


Figure 14
 Plot of Experimental Results: Covered Model;
 Nondimensional Drift Force .vs. Nondimensional Frequency

$\Lambda_m = 0.15m^2$ was used in the nondimensionalization. Figure 15 displays the nondimensional forces for both models for comparison. The differences relative to the variations displayed in forces observed for individual cases appear to be not significant. More covered model data would be necessary to pick up significant differences, if any. It is apparent from the analysis that in the uncovered model case the structural members blocked the flow paths such that the model acted as a near solid structure in the wave field. From the present work it is concluded that both models react similarly in regular waves. Of course, the higher frequency results are questionable due to group effects.

Due to the geometry of the model, any wave reflection via the sides of the model off the wave tank walls would be directed behind the model. Therefore contamination of results due to wave reflection is not considered a problem.

In the following section a numerical scheme corresponding to the tests previously described is developed and implemented.

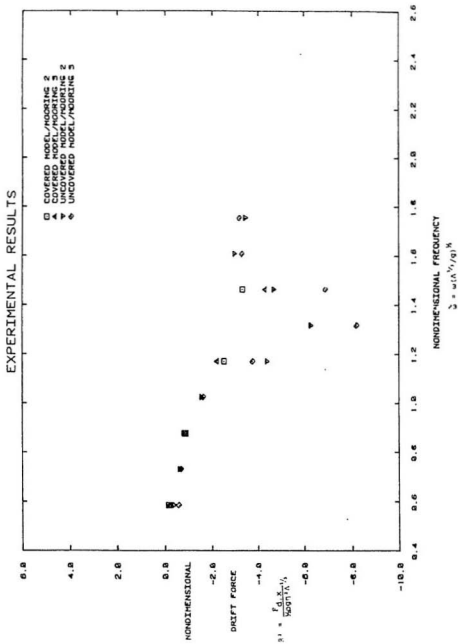


Figure 15
 Comparison of Covered and Uncovered Model Test Results

4.2 Numerical Evaluation of Steady Drift Forces Using Linear Diffraction Theory

4.2.1 A Model for Steady Drift Forces

The two main components of the model, linears and buoyancy cells, are small compared to the wavelength and fall into the slender structure category. Typically Morison's equation would be used in such a case, but that theory does not allow for the interactions due to the proximity of the structural elements of the model. Thus, the most obvious alternative was to use the well developed linear diffraction theory, assuming a solid hull construction for calculation purposes. It is also possible to assume that due to the dense distribution of the structural elements the blockage effects significantly the permeability of the structure in waves, thus bringing it close to the diffraction model. A numerical scheme developed by Faltinsen and Michelsen (1974) and presented by Tse (1984) is used.

The numerical model presented is based on linear diffraction theory using the 3-D source distribution method. The software Tse presents calculates the first-order wave forces, response motions, second-order steady horizontal drift forces and vertical drift moment for a floating body in regular waves. The steady drift

forces, which are of main interest here, are evaluated by the far field (wave momentum) approach (Standing et al 1981, Murray 1984). This method utilizes potential flow theory and conservation of momentum and energy. Changes in momentum in the fluid surrounding the body are equated to the steady force acting on the vessel in regular waves.

The equations of motion of the body may be written in the following form:

$$M_{jk} \dot{U}_k = \int_{S_b(t)} \left(\rho \frac{\partial \Phi}{\partial t} + \frac{\rho}{2} \frac{\partial \Phi}{\partial x_1} \frac{\partial \Phi}{\partial x_1} + \rho g z \right) n_j dS + (f_{ex})_j \quad (4.9)$$

$$j, k = 1, \dots, 6$$

where \dot{U} is the acceleration of the structure, $S_b(t)$ is the instantaneous wetted surface of the body. The integral term on the right hand side represents the forces due to the integration of pressure distribution over the instantaneous wetted surface. $(f_{ex})_j$ are external forces which are assumed to be known.

When one assumes that the external forces balance the sum of all second or higher-order hydrodynamic forces, equation 4.9 can be reduced to:

$$\int_{S_b} \rho \frac{\partial \Phi}{\partial t} n_j dS - C_{jk} \dot{\eta}_k^*(t) = M_{jk} \dot{U}_k \quad (4.10)$$

$$j, k = 1, \dots, 6$$

where,

$$\dot{U}_k = \frac{d^2}{dt^2} (\eta_k^*(t)) \quad (4.11)$$

$\eta_k^*(t)$ are the time-dependent first-order linear ($k=1,2,3$) and angular ($k=4,5,6$) rigid body motions. C_{jk} are the restoring coefficients. Since the body is symmetric with respect to the x-z plane the restoring coefficients can be written (Tse 1984, Faltinsen and Michelsen 1974):

$$C_{3,3} = \rho g A_{wp} \quad (4.12)$$

$$C_{3,5} = C_{5,3} = -\rho g \int_{A_{wp}} x \, dS \quad (4.13)$$

$$C_{4,4} = \rho g \Lambda (z_D - z_C) + \rho g \int_{A_{wp}} y^2 \, dS \quad (4.14)$$

$$C_{5,5} = \rho g \Lambda (z_D - z_C) + \rho g \int_{A_{wp}} x^2 \, dS \quad (4.15)$$

where A_{wp} is the water plane area, Λ is the displaced volume of fluid, z_D and z_C are the z-coordinates of the center of buoyancy and center of gravity of the body.

For steady harmonic excitations and motions it is more convenient to represent the potential, Φ , and motion, η_j^* , by the real part of the complex function such that:

$$\eta_j^*(t) = \text{Re}[\vec{\eta}_j e^{-i\omega t}] \quad (4.16)$$

$$\Phi(\vec{x}, t) = \text{Re}[\Phi(\vec{x}) e^{-i\omega t}] \quad (4.17a)$$

Now $\Phi(\vec{x})$ can be broken down into three parts for this linear case:

$$\Phi = \Phi_0 + \Phi_j + (-i\omega \vec{\eta}_j) \Phi_j \quad (4.17b)$$

$j, k=1, \dots, 6$

Now, $\Phi_0 = \Phi_I$, the incident wave potential, can be obtained from small amplitude wave theory:

$$\Phi_0 = \zeta_a \frac{\cosh k(z+h)}{\cosh kh} e^{i(kx \cos \beta + ky \sin \beta)} \quad (4.18)$$

where ζ_a is the amplitude of the incident wave, β is the incident angle of the incident wave, and Φ_0 is known as the solution of the wave diffraction problem. Φ_j , $j=1..6$ are the solutions to the radiation problem.

Using the following definitions (Faltinsen and Michelsen 1974):

added mass coefficients;

$$A_{jk} = -\rho \operatorname{Re} \left[\int_{S_b} \Phi_j n_k \, dS \right] \quad (4.19)$$

damping coefficients;

$$B_{jk} = -\rho \omega \operatorname{Im} \left[\int_{S_b} \Phi_j n_k \, dS \right] \quad (4.20)$$

generalized exciting force;

$$F_j = (-i\omega)\rho \int_{S_b} (\Phi_0 + \Phi_j) \vec{n}_j \, dS \quad (4.21)$$

the equation of motion can be written:

$$(-\omega^2 \{A_{jk} + M_{jk}\} - i\omega B_{jk} + C_{jk}) \vec{n}_k = F_j \quad (4.22)$$

$$j, k=1, \dots, 6$$

The velocity potential associated with the flow about a body, Φ_j , $j=1, \dots, 7$, for the infinite fluid case, can be described by either a complex source or doublet distribution over the body surface through the application of Green's Theorem. For the region bounded by the body surface, the free surface and the sea bed, the velocity potential, based on a distribution of complex sources, can be written:

$$\Phi_j(\vec{x}) = \int_{S_b} Q_j(\vec{E}) G(\vec{x}, \vec{E}) dS(\vec{E}) \quad (4.23) \quad j=1, \dots, 7$$

where $Q_j(\vec{E})$ is the source density function and $G(\vec{x}, \vec{E})$ is the Green's function which satisfies the free surface and radiation conditions. The Green's function and its derivative are evaluated by either the series form or the integral form (see Tse 1984), depending on Bessel function criteria. The integral form is used when the maximum value of the Bessel function of the first kind is greater than 1000, otherwise the series form is used. Tse states some cases where these criteria do not work well in the evaluation of the Green's function.

Q_j , $j=1, \dots, 7$ is solved by a surface discretization panel method (Tse 1984, Faltinsen and Michelsen 1974). and A_{jk} , B_{jk} , F_j are computed from equations 4.19, 4.20, and 4.21. Φ_j is obtained from equation 4.23. The complex amplitudes of body motions, $\vec{\eta}_k$, are then calculated from equation 4.22.

The steady horizontal drift forces can be expressed as:

$$(F_d)_j = \left\langle \int_{S_b} P n_j dS \right\rangle \quad j=1, 2 \quad (4.24)$$

where $\langle \rangle$ denotes the time average over one period. $(F_d)_j$ is the drift force in the x and y directions. P is the hydrodynamic pressure. n_j denotes the unit normal positive into the fluid.

The direct evaluation of expression 4.24

involves the second-order effect due to the instantaneous wetted surface $S_b(t)$ and is known as the near field approach. It can be used to predict mean forces as well as low frequency components, but is cumbersome and extensive in terms of CPU time. The second-order mean forces can also be calculated by implementing conservation of momentum over some cylindrical control surface requiring little computational effort beyond that required for the first-order solution.

Conservation of momentum over a control volume of the fluid domain which is bounded by the body surface $S_b(t)$, the free surface S_f , the sea bed S_h , and a chosen fixed control surface at infinity S_∞ , can be written:

$$\frac{dL_j}{dt} = -\rho \int_S \left(\left(\frac{P}{\rho} + g x_3 \right) n_j + u_j (u_n - U_n) \right) dS \quad (4.25)$$

$j, k=1, 2, 3$

where; $S = S_b(t) + S_\infty + S_f + S_h$ (4.26)

and L_j ($j=1, 2, 3$) is the linear momentum in x, y, z directions, u_j is the fluid velocity vector, u_n is the normal velocity component of fluid particles on S , U_n is the normal velocity component of the surface S .

If contributions in the horizontal plane only are considered this equation reduces to:

$$\frac{dL_j}{dt} = -\int_S (P n_j + \rho u_j (u_n - U_n)) dS \quad (4.27)$$

$$j=1, 2$$

Applying the corresponding boundary conditions on S :

on S_f : $P=0, u_n=U_n$

on S_n : $\vec{n} = (0, 0, n_3)$, $u_n = U_n = 0$

on $S_D(t)$: $u_n = U_n$

on S_∞ : $U_n = 0$

the equation becomes:

$$\int_{S_D(t)} P n_j dS = - \int_{S_\infty} (P n_j + \rho u_j u_n) dS - \frac{dL_j}{dt} \quad (4.28)$$

j=1,2

Taking the time average over one period and choosing the control volume to have a vertical cylindrical surface of large radius, r , extending from the free surface down to the sea bed, the horizontal mean drift forces can be written using polar coordinates:

$$(F_d)_x = - \left\langle \int_{S_\infty} (P \cos \theta + \rho u_r (u_r \cos \theta - u_\theta \sin \theta)) r d\theta dz \right\rangle \quad (4.29)$$

$$(F_d)_y = - \left\langle \int_{S_\infty} (P \sin \theta + \rho u_r (u_r \sin \theta + u_\theta \cos \theta)) r d\theta dz \right\rangle \quad (4.30)$$

where u_r and u_θ are the radial and tangential velocity components and $x = r \cos \theta$, and $y = r \sin \theta$.

Using expanded versions of equations 4.17 and 4.23 as given in Tse (1984) (see also Faltinsen and Michelsen 1974) the far field expression for the first-order potential is:

$$\begin{aligned} \phi \sim & \frac{g_a}{g_w} \frac{\cosh k(z+h)}{\cosh kh} e^{i(kx \cos \beta + k y \sin \beta - \omega t)} \\ & + T(\theta) e^{i\tau(\theta)} \cosh[k(z+h)] \sqrt{1/r} e^{j(kr - \omega t)} \end{aligned} \quad (4.31)$$

where $T(\theta)$ and $\tau(\theta)$ are real functions of θ and $T(\theta) e^{i\tau(\theta)}$ is in the form of a Kotchin function:

$$T(\theta) e^{i\tau(\theta)} = \frac{2\pi(v^2-k^2)}{k^2h-v^2h+v} \sqrt{2/\pi k} e^{-i\frac{1}{2}\pi} \cdot \int_{S_b(t)} (Q(\vec{E})) \cosh[k(\zeta+h)] e^{-i(k\xi \cos\theta + k\eta \sin\theta)} ds \quad (4.32)$$

where $Q(\vec{E})$ is the total source density.

$$Q(\vec{E}) = Q_j + (-i\omega\vec{\eta}_j) Q_j \quad (4.33)$$

$$j=1, \dots, 6$$

Substituting relations:

$$u_r = \operatorname{Re} \left[\frac{\partial \Phi}{\partial r} e^{-i\omega t} \right] \quad (4.34)$$

$$u_\theta = \operatorname{Re} \left[\frac{1}{r} \frac{\partial \Phi}{\partial \theta} e^{-i\omega t} \right] \quad (4.35)$$

and retaining terms up to second-order in Φ , the mean horizontal forces can be written:

$$\begin{aligned} (F_d)_x = & - \frac{\rho}{2} \frac{\omega \zeta_a}{\sinh(kh)} \sqrt{\frac{2\pi}{k}} \left(\frac{1}{2} \sinh(2kh) + \frac{kh}{2} \right) \cdot 2T(\beta) \cdot \cos(\tau(\beta) + \frac{\pi}{4}) \cdot \cos \beta \\ & - \frac{\rho k}{2} \left(\frac{1}{2} \sinh(2kh) + \frac{kh}{2} \right) \cdot \int_0^{2\pi} T^2(\theta) \cdot \cos \theta d\theta \end{aligned} \quad (4.36)$$

$$\begin{aligned} (F_d)_y = & - \frac{\rho}{2} \frac{\omega \zeta_a}{\sinh(kh)} \sqrt{\frac{2\pi}{k}} \left(\frac{1}{2} \sinh(2kh) + \frac{kh}{2} \right) \cdot 2T(\beta) \cdot \cos(\tau(\beta) + \frac{\pi}{4}) \cdot \sin \beta \\ & - \frac{\rho k}{2} \left(\frac{1}{2} \sinh(2kh) + \frac{kh}{2} \right) \cdot \int_0^{2\pi} T^2(\theta) \cdot \sin \theta d\theta \end{aligned} \quad (4.37)$$

It is documented (John 1949, 1950) that there are particular 'irregular' wave frequencies at which the numerical scheme presented breaks down. These frequencies are dependent on body shape, and in the present case are

not easy to predict. They are generally associated with wave lengths in the order of, or less than, the characteristic dimension of the body, but not always. Murphy (1978) found that for a circular cylinder irregular frequencies existed at wavelengths considerably longer than the characteristic dimension of the body.

4.2.2 Numerical Application

Tse's programs were designed for a body symmetrical about both the x and y axes. His programs were modified to handle a body symmetrical about the x axis only. Before proceeding it was necessary to confirm that the program, with modification, was executing properly. The new version was tested thoroughly by executing it for Tse's rectangular box in 500m of water and wave heading zero degrees, with consistent results. The program was also successfully executed for Pinkster's (1981) barge model in head waves. Thus, it was concluded that the newly modified program is working correctly in comparison with other available results. The new versions of the programs are called DPORT2.FOR and OUTPORT2.FOR and are listed in Appendix D. A list of main subroutines in DPORT2.FOR with their functions and pertinent equations is found in in Appendix H. Program DPORT2 computes first- order wave forces, response motions, steady horizontal drift forces and vertical drift moment. Program OUTPORT2

is a simple program which formats this information and creates output files. Programs DPORT2 and OUTPORT2 were executed with the triangular shaped platform input as a full scale solid hull structure. The body wetted surface was partitioned into 230 panels, as shown in Figure 16, utilizing program SHAPE.FOR in Appendix E. The panels are small relative to the wavelength. The inputs to the program, as determined by the geometry of the model, are: panel centroids, areas, and unit normal vectors (as given in Appendix F); center of gravity; water depth; a characteristic dimension of the structure; and radii of gyration (as estimated in Appendix B). In addition to the geometric inputs, various water depths and wave headings can be input. The program was run with 500m water depth, and wave periods ranging from 10.5 to 34.4 (λ/D equal to 0.266 to 2.86 for $D = 646m$) seconds, which correspond to the wave frequencies used in model tests. Inputs specific to this model are listed in Table 5.

Four computational schemes were investigated to determine which is best suited to the model tests previously described. The basic differences in the schemes was in the representation of the space in between the structural elements of the model.

CASE 1: Center of gravity, radii of gyration and displaced volume were estimated for the model

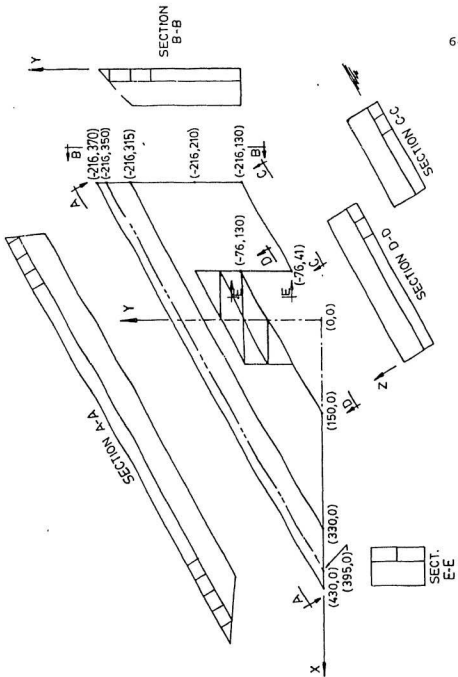


Figure 16
Model Panels Used in Numerical Analysis

TABLE 5
Particulars of the Model

	MODEL	PROTOTYPE
mass (kg)	150	1.2×10^9
volume (m ³)	0.30	2.4×10^6
submerged volume (m ³)	0.150	1.2×10^6
draft (m)	0.0595	11.9
c of g (m)	(0,0,0.0381)	(0,0,7.62)
c of b (m)	(0,0,-0.0235)	(0,0,-4.7)
nat.freq. ω_{02}	0.4477	0.0317
(rads/s) ω_{03}	0.6335	0.0448
radii of r_{xx}	0.91	182
gyration r_{yy}	0.88	176
(m) r_{zz}	1.26	252
CONSIDERING ENTRAPPED WATER PART OF MODEL		
	MODEL	PROTOTYPE
mass (kg)	350	2.8×10^9
submerged volume (m ³)	0.350	2.8×10^6
draft (m)	0.0595	11.9
c of g (m)	(0,0,0.0063)	(0,0,-1.26)
c of b (m)	(0,0,-0.0358)	(0,0,-7.16)
nat.freq. ω_{02}	0.293	0.0207
ω_{03}	0.415	0.0293
radii of r_{xx}	0.85	170
gyration r_{yy}	0.83	166
r_{zz}	1.18	236

in air. Other particulars of the model, center of buoyancy and water plane area, were calculated by the program which assumes a solid hull structure.

CASE 2: The center of gravity, radii of gyration and submerged volume were estimated for the model including entrapped water in the space between the structural components. Water plane area and center of buoyancy were calculated in the programs.

CASE 3: Water plane area, radii of gyration and center of buoyancy were estimated for the model in air. The submerged volume and center of gravity were calculated with entrapped water.

CASE 4: The radii of gyration, submerged volume, center of gravity, center of buoyancy, and water plane area were all estimated for air entrapped.

The program thus took on four versions DPORT1 through DPORT4. The results of each version were analysed for the full range of frequencies and version 2, DPORT2, was best suited to the experimental results. This version represents the structure and entrapped water acting together as a dynamic body. As is mentioned in section

4.1.6 the covered model tests did in fact have water entrapped in the structure and showed little difference in uncovered model tests. This also suggests that case 2 is the most suitable version of the program.

Initially the program was executed for the model free floating with six degrees of freedom in head seas. Results of this run are listed in Appendix G. Errors in Green's function calculations due to Bessel function restrictions were noted at several wave periods: 10.8, 11.7, 11.9, 12.7, 13.5, 16.0, 23.4. The program failed to execute at periods in the neighbourhood of 11, 12, 15, 18, and 20 secs, so no results are available in these areas. Note that drift forces are generally negative due to the orientation of the body in the waves.

The program was then executed for head seas with motions of the body restricted in seven combinations in an attempt to determine the influence of first-order motions on the body:

- (i) Surge motion only;
- (ii) Heave only;
- (iii) Pitch only;
- (iv) Surge and heave only;
- (v) Surge and pitch only;
- (vi) Heave and pitch only;

(vii) Zero motions (fixed structure).

The numerical scheme for surge only was extended to include the two mooring systems. These stiffnesses were impressed upon the numerical model by equating the stiffness in surge, $C(1,1)$, to each mooring spring stiffness separately.

The program was finally run for the free floating model in quartering seas of 240° . In this case the waves are head long into the side of the model.

4.2.3 Computational Results

Results of the numerical evaluation of drift force in the x-direction have been nondimensionalized as previously discussed in section 4.1.6 and plotted against nondimensional frequency for comparison to experimental results. $A_p = 1.2 \times 10^6 \text{ m}^3$ was used for nondimensionalization. A discussion of these numerical results follows.

Figure 17 shows the nondimensional results of the free floating model in head seas. Figures 18a to 18f, shown in Appendix A, are plots of the calculated first-order surge, heave and pitch RAO's and phases. Added mass and damping coefficients are given in Figures 19a to 19h for surge, heave, pitch and yaw and are also shown in Appendix A.

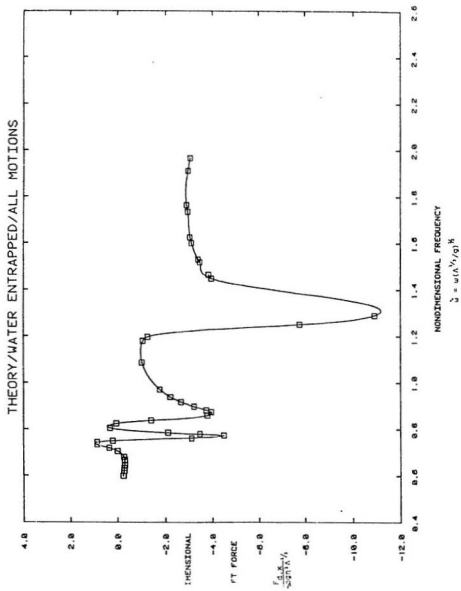
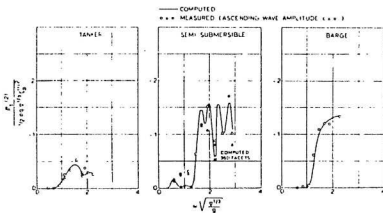


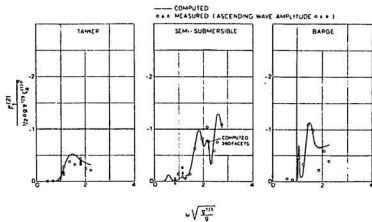
Figure 17
Plot of Computed Results:
All Motions; Head Seas

From Figure 17 it is seen that at low frequencies, $\tilde{\omega} < 0.7$, the nondimensional mean drift force is near zero. As frequency increases, drift force increases in the direction opposite to wave propagation. In this frequency range, the first-order heave motion transfer function is not quite equal to 1 while phase is near zero. Therefore the body is not exactly following the wave motion completely. As frequency increases heave motion decreases, and surge motion increases.

In the nondimensional frequency range of 0.7 to 1.0, the drift force varies considerably. The order of magnitude of these variations is close to 50% of the maximum mean second-order force calculated. Similar trends in drift force can be seen in Pinkster's (1981) results for a semisubmersible in head waves, and for a barge in bow quartering seas, as shown in Figure 20. Similarities are also shown in Hearn and Tong (1987) in the plot of mean drift forces computed by the near field method for a semisubmersible displayed in Figure 21. In the lower frequency range both semisubmersibles show oscillations of a much smaller order of magnitude when compared to the maximum force. The barge in quartering seas shows results at lower frequencies in the order of magnitude of 50% of the maximum, as in the present case. Head waves on the

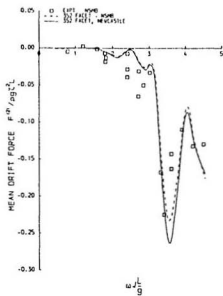


Mean longitudinal drift forces in head waves.



Mean longitudinal and transverse drift forces and yawing moment in bow quartering waves.

Figure 20
 Pinkster's Results for Head Seas and Quartering Seas



Comparison of predicted and measured zero forward speed added resistance (drift force).

Figure 21
Hearn's Results For a Semisubmersible

triangular model are comparable to quartering seas on a barge.

The plot of first-order surge force (Figure 22) displays a maximum force in the nondimensional frequency range 0.7-0.8. Inspection of corresponding Froude-Krylov (Figure 23) and scattering (Figure 24) forces indicate that the scattering force is the main contributor to this maximum surge force.

First-order motions, particularly surge, show considerable variations in this frequency range. Superimposing Figures 17 and 18a it is seen that an increase in surge motion corresponds to an increase in mean horizontal drift force. Alternately, a decrease in surge motion matches a decrease in drift force. (Note that a higher negative number indicates an increase in drift force in the direction of wave propagation). Pitch angle follows the same trend.

Also in this frequency range, surge added mass (Figure 19a) peaks at $\tilde{\omega} \approx 0.7$ and goes negative at $\tilde{\omega} \approx 0.8$ while surge damping (Figure 19b) peaks at 0.8. Added mass and damping in heave (Figures 19c and 19d) dip negative at $\tilde{\omega} \approx 0.77$ while added mass peaks at $\tilde{\omega} \approx 0.8$. Pitch damping (Figure 19f) also shows a distinct negative dip at 0.77.

Negative added mass is expected, on the basis of two dimensional calculations, in such a structure with outwardly sloping sides, but negative damping is not

FIRST-ORDER SURGE EXCITING FORCE

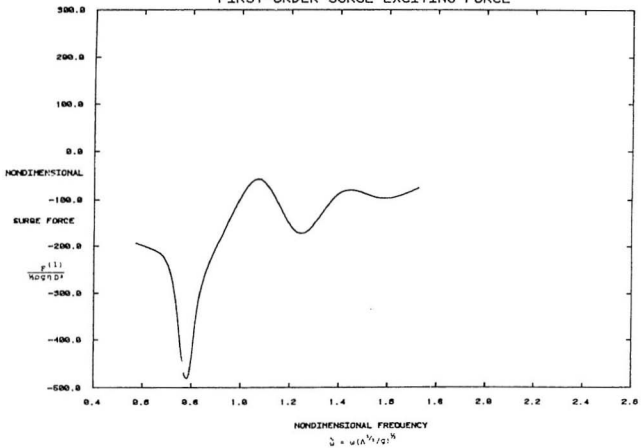


Figure 22
Calculated First-Order Surge Force

SURGE FROUDE-KRYLOV FORCE/MODEL IN HEAD WAVES

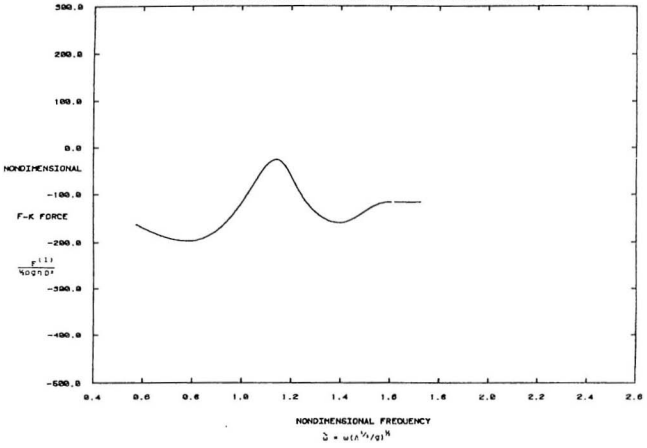


Figure 23
Calculated Froude-Krylov Force - Surge

SURGE SCATTERING FORCE/MODEL IN HEAD SEAS

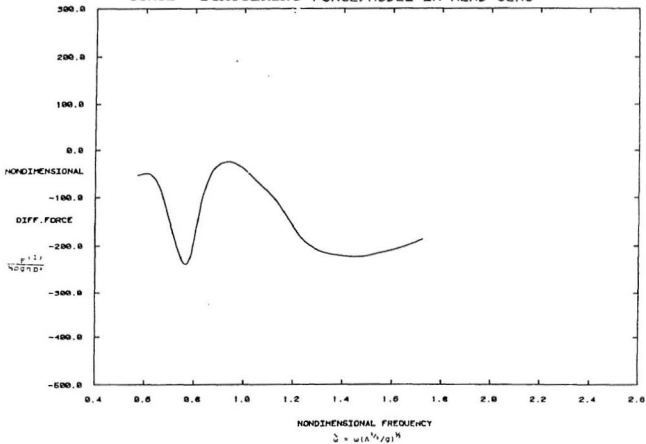


Figure 24
Calculated Scattering Force - Surge

physically justified when considering pure (uncoupled) motions. In order to investigate this, NRC's program for the solution of generalized two dimensional scattering problems was implemented to compute added mass and damping in heave for a solid cross-sectional area of one leg of the model. The model scale was used in the program and results are plotted in Figures 25a and 25b. Added mass shows a pronounced trough at $\hat{\omega} \approx 0.7$ where damping shows a distinct peak. It is noted that in general for two dimensional problems a zero crossing in added mass corresponds to a peak in damping. If this is extended to the three dimensional problem of Figures 19 it is seen by superimposing Figures 19c and 19d that the actual damping peak in heave is at $\hat{\omega} \approx 0.7$ as expected. It is then suspected that the negative damping in heave and pitch is due to accumulative errors causing an overshoot in calculations. After this frequency range, the added mass and damping tend to quickly level off again.

It is noted that at low frequencies the corresponding wavelengths based on deep water theory (ie. $(\lambda/d) \geq 2$) exceed the limits based on 500 m water depth used in computations. Therefore the program was executed for 1000 m water depth to represent deep water for all ranges of frequency. The results were not significantly different from those for 500 m.

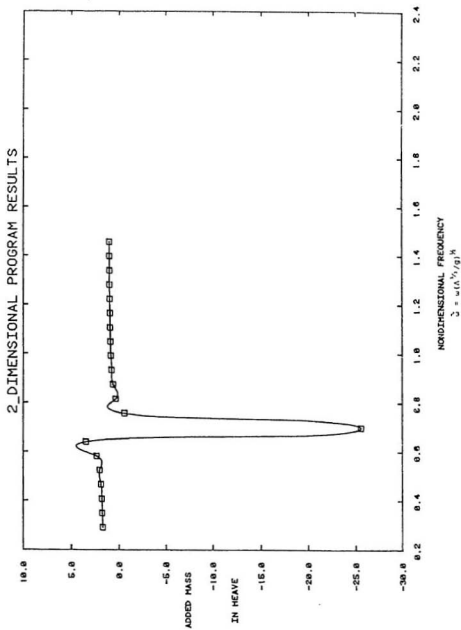


Figure 25a
2-D Numerical Results: Added Mass

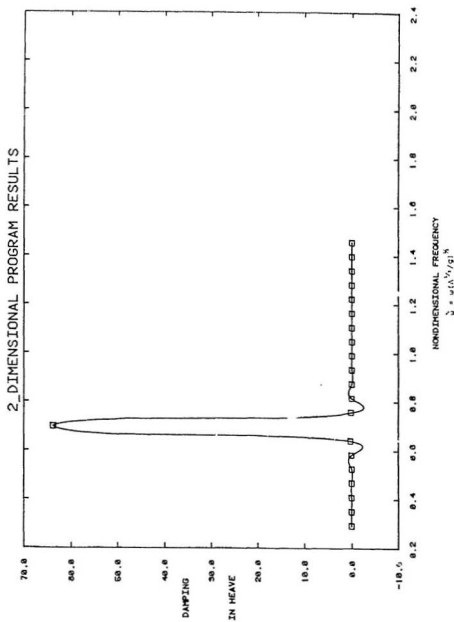


Figure 25b
2-D Numerical Results: Damping

In the nondimensional frequency range 0.8 to 1.1 the drift forces increase to a small peak close to 0.9 and level off for a narrow band of frequencies. Surge amplitude shows a minimum at 0.9, peaks sharply at 1.0, and decreases again. Heave amplitude exhibits a small dip between 0.8 and 1.0. The pitch angle increases sharply in this range. Damping increases in heave and pitch and decreases slightly in surge.

It is interesting to note that at $\tilde{\omega} < 0.9$ the corresponding wavelengths are longer than the structure, which in prototype is 646 m along the x-axis and approximately 745 m along each leg. The inside dimensions of the prototype are approximately 225 m along the x-axis and 260 m along the leg.

The maximum mean drift force occurs in the nondimensional frequency range 1.1-1.5, peaking at 1.3. This area looks conspicuous with few datapoints due to the unexplained failure of the numerical scheme. This failure might be due to irregular frequencies causing the numerical method to breakdown as discussed in section 4.2.1. The magnitude of this maximum is large compared to other computed forces. This "surge" in force corresponds closely to a distinct low point in first-order surge force and subsequent peak in heave and surge amplitudes as well as pitch angle at $\tilde{\omega} \approx 1.5$. Added mass and damping coefficients

have levelled off in this range.

At nondimensional frequency 1.4 the drift force decreases to a steady level for the higher frequencies. The heave and surge amplitudes and pitch angle tend to zero after nondimensional frequency of 1.6.

Inspection of drift force plots with model motions restricted, Figures 26a-26f (in Appendix A) shows the significance of the effect of surge motion on the mean horizontal force in the lower half of the frequency range. Heave and pitch motions appear to play a stronger role in the mid-frequency range where the force increases greatly and decreases again.

The computed drift force on the fixed body is depicted in Figure 27. As expected the forces are not as erratic, since the body is not dynamically interacting with the wave field. At the lowest frequencies the forces are somewhat higher than when the body was free to move. Near $\hat{\omega}=0.8$ the force peaks and then drops off again. At the higher frequencies the plot is virtually the same as the others in this group.

When the stiffness of the mooring systems was introduced in the program for the body free to move in surge only, the results were unaffected (see Figures 28a and 28b in Appendix A). This indicates that the moorings were too soft to restrict to body's motions in surge.

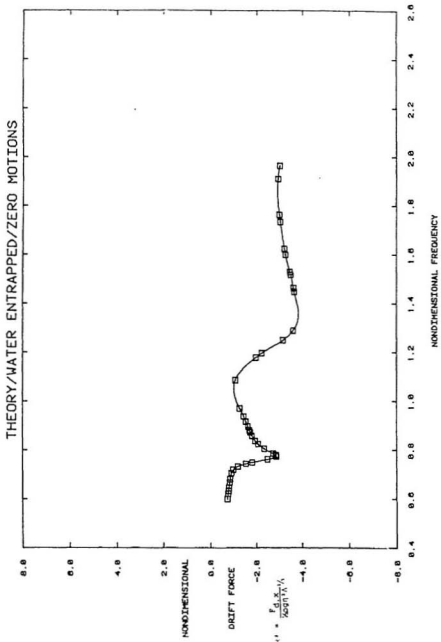


Figure 27
Plot of Computed Steady Drift Forces:
Fixed Body

Finally the numerical procedure was repeated for a free floating and fixed structure in quartering seas. Figures 29a and 29b (in Appendix A) show that the results do not vary alot from those of head seas. For the floating structure the forces are generally somewhat lower in the first half of the frequency range, but the same tendencies are obvious. Similarly, for the fixed structure, the results are not significantly different. In the lower frequency range the forces are lower, tending to zero at the lowest frequencies.

It is known that the Green's function fails for bodies with voids, such as a donut shaped structure. It was thought that the inner configuration of the structure may have caused problems in this computation. Therefore the program was executed for a similar shape with two legs but no semi-enclosed back. The results were not significantly different.

In Chapter V the theoretical results are compared to the experimental results.

CHAPTER V

COMPARISON OF EXPERIMENTAL AND NUMERICAL RESULTS

In order to determine the validity of the numerical scheme presented it is necessary to compare the theoretical results with physical reality. First, model test results are compared to the theoretical results (numerical model version 2 as described in section 4.2.2) of the free floating structure in head waves, Figures 30 and 31. In these figures it can be seen that the theoretical results closely match the model test results. Not enough experimental data were obtained to show any fluctuations in mean drift force with respect to nondimensional frequency in the lower frequency ranges as was displayed in the computed results. The experimental datapoints do correspond closely to the computed results and there is no evidence to conclude that these fluctuations do not occur. Judging from other documented cases mentioned previously and the speculated error in the damping coefficients, it is questionable if these fluctuations would be as large in reality.

Since computational and experimental results both show a pronounced maximum mean drift force of the same order of magnitude in the range of $\tilde{\omega} \approx 1.3$, it is deduced

COMPARISON OF THEORY AND EXPERIMENT

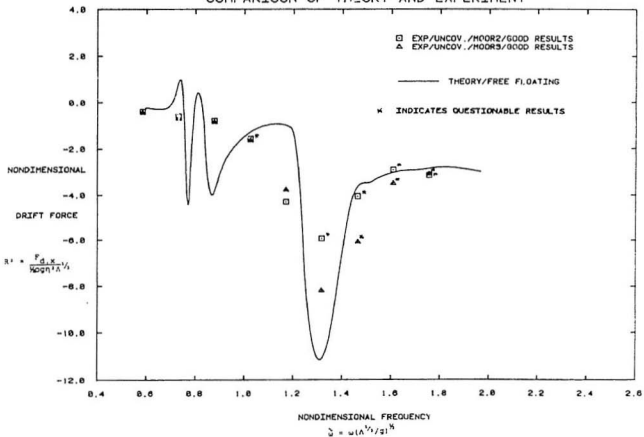


Figure 30
 Plot of Comparison of Steady Drift Forces:
 Computed Free Floating Structure .vs. Experimental
 Uncovered Model

COMPARISON OF THEORY AND EXPERIMENT

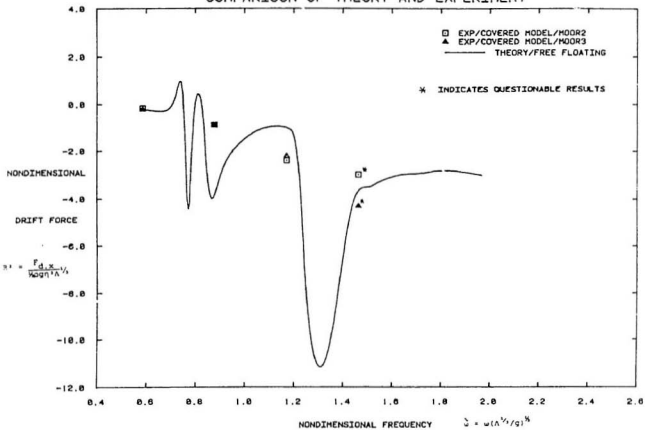


Figure 31
 Plot of Comparison of Steady Drift Forces:
 Computed Free Floating Structure .vs. Experimental
 Covered Model

that this frequency range is of major concern in the design process. The maximum mooring force is expected to occur in this range. It is noted earlier that the experimental results at high frequencies were doubtful due to group effects and the risk of resonance. This does not seem to have caused any great error in the vessels mean drift force, even though the vessel may have oscillated about this mean.

The theoretical results for a fixed structure are compared to model test results in Figures 32 and 33. The comparison of uncovered model experiments to the linear diffraction theory for the fixed model (Figure 32) indicates that model motions were, in fact, playing a role in the intermediate frequency range where this theory flattens out. At the higher and lower frequencies the theory is similar in both cases, and the experimental results compare well.

Although motions of the experimentally tested model were not measured, spring forces do indicate surge motion of the structure.

COMPARISON OF THEORY AND EXPERIMENT

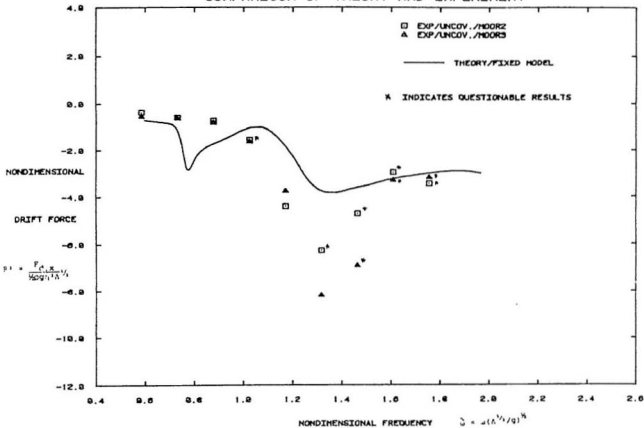


Figure 32
 Plot of Comparison of Steady Drift Forces:
 Computed Fixed Structure .vs. Experimental Uncovered
 Model

COMPARISON OF THEORY AND EXPERIMENT

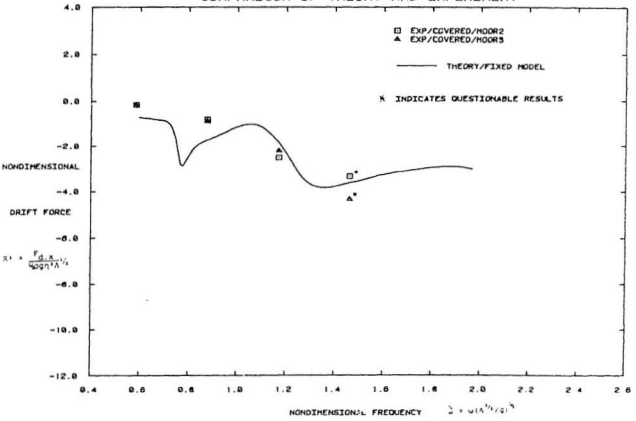


Figure 33
 Plot of Comparison of Steady Drift Forces:
 Computed Fixed Structure .vs. Experimental Covered
 Model

CHAPTER VI

CONCLUSIONS

This thesis considered, both experimentally and theoretically the mean wave-induced drift forces acting on a large moored porous-like floating structure. The following conclusions were drawn:

1. No significant difference was noted in the results for the two modelled mooring systems (which can be considered a means to measure drift forces on the otherwise free-floating structure). A softer mooring would have reduced the natural frequency of the system to better ensure that the effect of the mooring system on the first-order motions was negligible. This is necessary to avoid adverse effects due to distorted first-order motions. The fact that no significant difference is apparent indicates that no more-adverse effects were present using the stiffer mooring.
2. Covered model tests were conducted in which a plastic sheet was used to eliminate any porosity of the structure. It was found that the drift force on the covered model was basically the same as that of the uncovered model. Both were represented closely by the far field theory for a solid structure. Apparently in

model tests the structural members blocked the flow paths in the uncovered case such that the model acted as a $\frac{1}{2}$ -solid structure in the wave field. Therefore it may be concluded that viscous effects did not play a major role in the wave forces on the model. Froudian scaling, in which viscous effects are ignored, proved to be accurate verifying that diffraction effects were dominant. An investigation of first-order forces also verified this.

3. For a prototype the data suggests that the peak force due to regular 5m waves would be in the order of 10^8 N. For a 1m/s current without waves the drift force would be approximately 0.05×10^8 N. Therefore, according to this study the drift forces due to waves appear to be dominant for the structure. This is an indication of the practical significance of the present study.
4. Calculated added mass and damping coefficients are questionable, particularly in the nondimensional frequency range 0.7-0.9, probably due to accuracy of Bessel function calculations. This accuracy can be adjusted. The Green's function algorithm should be investigated for this case.
5. The far field theory using a panel method showed considerable variations in the mean drift force at low frequencies. A review of literature showed that this

had been seen earlier in data and theoretical formulations. Investigation of forces and calculated pure uncoupled motions indicated that these variations are due mainly to surge motions. The maximum drift force, which occurred at a higher frequency, was determined to be mainly a result of heave and pitch motions.

6. The mean horizontal drift forces on this particular model can be computed with reasonable accuracy using the numerical model for a free floating structure presented in which the structure includes entrapped water. The frequency range in which the maximum mooring force occurs was identified. Therefore the results presented can be utilized with confidence in the design process
7. Model motions were not measured during testing since the tests were not designed for research purposes. Observations indicated that some wave attenuation was occurring, particularly at high frequencies. It would be useful, in future work, to determine experimentally and theoretically the extent to which waves are absorbed and reflected, etc. Also the possibility of standing waves occurring in the inner triangular area of water should be investigated.

8. Although wave group effects were present in second-order slow drift oscillations of the vessel forces, they did not appear to significantly affect the steady drift offset of the model. These group effects may have caused the vessel to oscillate about the mean position which results in an additional second-order low frequency drift force. When the group frequency is near the natural frequency of the system resonance may occur. The complexity of this, both experimentally and theoretically, is well beyond the scope of the present work. In future work an attempt should be made to study this in relation to mooring design.

REFERENCES

1. ABKOWITZ, M.A., VASSILOPOULOS, L.A., SELLARS, F.H., (1966), "Recent Developments in Seakeeping Research and Its Application to Design", SNAME, Vol.74
2. BHATTACHARYYA, R. (1978), Dynamics of Marine Vehicles, John Wiley and Sons.
3. BOESE, P. (1970), "Eine Einfache Methode zur Berechnung der Widerstandserhöhung eines Schiffes in Seegang", Schiffstechnik, Ed.17.
4. CHAKRABARTI, S.K. (1987), Hydrodynamics of Offshore Structures, Computational Mechanics Publications.
5. DEAN, W.R. (1948), "On the Reflection of Surface Waves by a Submerged Cylinder", Proc. Cambridge Phil. Soc., Vol.44.
6. FALTINSEN, O.M., MICHELSEN, F.C. (1974), "Motions of Large Structures in Waves at Zero Froude Numbers", Proceedings of the International Symposium on the Dynamics of Marine Vehicles and Structures in Waves.
7. FALTINSEN, O.M., LOKEN, A.E. (1978), "Drift Forces and Slowly Varying Forces on Ships and Offshore Structures in Waves", Dynamic Analysis of Offshore Structures.
8. GARRISON, C.J. (1974,1975), "Hydrodynamics of Large Objects in the Sea, Part I - Hydrodynamic Analysis, Part II - Motion of Free Floating Bodies", Journal of Hydraulics, Vol. 8, No.1, 1974 and Vol.9, No.2, 1975.
9. GERRITSMAN, J., BEUKELMAN, W. (1972), "Analysis of the Resistance Increase in Waves of a Fast Cargo Ship", International Shipbuilding Progress, Vol.19, No.217.
10. HAVELOCK, T.H. (1940), "The Pressure of Water Waves upon a Fixed Obstacle", Proc. of the Royal Society, Series A, Vol.175.
11. HAVELOCK, T.H. (1942), "The Drifting Force on a Ship Among Waves", Philosophical Magazine, Vol.33.
12. HEARN, G.E., TONG, K.C. (1987), "Wave Drift Damping Coefficient Predictions and Their Influence on the Motions of Moored Semisubmersibles", Offshore Technology Conference (OTC), Paper No. 5455.

13. HSU, F.H., BLENKARN, K.A. (1978), "Analysis of Peak Mooring Force caused by Slow Vessel Drift Oscillation in Rando Seas", Offshore Technology Conference (OTC), Paper No.1159.
14. ISAACSON, M., de St.Q. (1985), "Recent Advances in the Computation of Nonlinear Wave Effects on Offshore Structures", Canadian Journal of Civil Engineering, Vol.12, No.3.
15. JOHN, F. (1949), "On the Motion of Floating Bodies-I", Comm. Pure Appl. Math. V 2.
16. JOHN, F. (1950), "On the Motion of Floating Bodies-II", Comm. Pure Appl. Math. V 3.
17. KAPLAN, P., SARGENT, T.P. (1976), "Motions of Offshore Structures as Influenced by Mooring and Positioning Systems", Behaviour of Offshore Structures (BOSS).
18. KAPLAN, P. (1983), "Simplified Three-Dimensional Method For Calculating Drift Forces on Ships and Semi-Submersibles in Waves", International Workshop on Ship and Platform Motions.
19. KARPPINEN, T. (1979), "An Approach to Computing the Second Order Steady Forces on Semisubmerged Structures", Helsinki University of Technology, Ship Hydrodynamics Laboratory, Report No.16.
20. KIM, C.H., CHOU, F. (1970), "Prediction of Drifting Force and Moment on an Ocean Platform Floating in Oblique Waves" Stevens Institute of Technology, Report SIT-OE-70-2.
21. KOTCHIN, N.E. (1951), "On the Wave-Making Resistance and Lift of Bodies Submerged in Water", Transactions of the Conference on the Theory of Wave Resistance, USSR, 1937, Translation: SNAME, T and R Bulletin No.1-8.
22. LIGHTHILL, J. (1979), "Waves and Hydrodynamic Loading", Behaviour of Offshore Structures (BOSS).
23. LIN, W.C., REED, A. (1976), "The Second Order Steady Force and Moment on a Ship Moving in an Oblique Seaway", Eleventh Symposium on Naval Hydrodynamics.
24. LOVAAS, J.H. (1983), "Wave and Current Loads on Offshore Structures", Offshore Göteborg '83, The Ocean Environment and its Interaction with Offshore Structures.

25. MARTHINSEN, T. (1983), "Low Frequency Motion of Moored Floating Structures", Second International Symposium on Ocean Engineering and Ship Handling.
26. MARTHINSEN, T. (1983), "The Effect of Short Crested Sea on Second Order Forces and Motions", International Workshop on Ship and Platform Motions.
27. MARTHINSEN, T. (1983), "Calculation of Slowly Varying Drift Forces", Applied Ocean Research, Vol.5, No.3.
28. MARUO, H. (1960), "The Drift of a Body Floating on Waves", Journal of Ship Research, Vol.4, No.3.
29. MEI, C.C., BLACK, J.L. (1969), "Scattering of Surface Waves", Journal of Fluid Mechanics, Vol.38.
30. MILLER, N.S., MCGREGOR, R.C. (1978), "The Problem of Scale in Model Testing for Offshore Work", Proceeding of the Seminar on Models and Their use as Design Aids in Offshore Operations, Society for Underwater Technology, London.
31. MILNE-THOMSON, L.M. (1968), Theoretical Hydrodynamics, The MacMillan Press Ltd.
32. MOLIN, B. (1979), "Computations of Drift Forces", Offshore Technology Conference (OTC), Paper No.3627.
33. MORISON, J.R., O'BRIEN, M.P., JOHNSON, J.W. and SHAAF, S.A. (1950), "The Force Excited by Surface Waves on Piles", Petroleum Transactions, AIME, 189.
34. MURPHY, J.E. (1978), "Integral Equation Failure in Wave Calculations", Journal of the Waterway, Port Coastal and Ocean Division, ASCE, Vol.104.
35. MURRAY, J.J. (1984), "The Effects of Wave Grouping on the Slow Drift Oscillations of Floating Moored Structures", PhD. Thesis, Memorial University of Newfoundland.
36. NEWMAN, J.N. (1967), "The Drift Force and Moment on Ships in Waves", Journal of Ship Research, Vol.11, No.1.
37. OGILVIE, T.F. (1963), "First- and Second-Order Forces on a Cylinder Submerged Under a Free Surface", Journal of Fluid Mechanics, Vol.16, Part 3.

38. PINKSTER, J.A. (1976), "Low Frequency Second Order Wave Forces on Vessels Moored at Sea", Eleventh Symposium on Naval Hydrodynamics.
39. PINKSTER, J.A., VAN OORTMERSSEN, G. (1977), "Computation of the First and Second Order Wave Forces on Bodies Oscillating in Regular Waves", Second International Conference on Numerical Ship Hydrodynamics.
40. PINKSTER, J.A., HOOFT, J.P. (1978), "Low Frequency Drifting Forces on Moored Structures in Waves", Fifth International Ocean Development Conference.
41. PINKSTER, J.A. (1979), "Mean and Low Frequency Wave Drifting Forces on Floating Structures", Ocean Engineering.
42. PINKSTER, J.A. (1979), "Wave Drifting Forces", Proceedings of WEGEMT.
43. PINKSTER, J.A. (1981), "Low Frequency Second Order Wave Exciting Forces on Floating Structures", Netherlands Ship Model Basin, Publication No.650.
44. RAHMAN, M. (1987), "A Design Method of Predicting Second Order Wave Diffraction Caused by Large Offshore Structures", Ocean Engineering, Vol.14, No.1.
45. REMERY, G.F.M., HERMANS, A.J. (1971), "The Slow Drift Oscillations of a Moored Object in Random Seas", Offshore Technology Conference (OTC), Paper No.1500.
46. SALVESEN, N. (1974), "Second-Order Steady-State Forces and Moments on Surface Ships in Oblique Regular Waves", International Symposium on the Dynamics of Marine Vehicles and Structures in Waves, Paper No.22.
47. SALVESEN, N. (1978), "Added Resistance of Ships in Waves", Journal of Hydronautics, Vol.12, No.1.
48. SARPKEYA, T. and ISAACSON, M. (1981), Mechanics of Wave Forces on Offshore Structures, Van Nostrand Reinhold Company.
49. SHARP, J.J. (1981), Hydraulic Modelling, Butterworths & Company (Canada) Limited, Ontario.
50. STANDING, R.G., DACUNHA, N.M.C., MATTEN, R.B. (1981), "Mean Wave Drift Forces: Theory and Experiment", National Maritime Institute, R.124.

51. STANDING, R.G., DACUNHA, N.M.C., MATTEN, R.B. (1981), "Slowly-Varying Second-Order Wave Forces: Theory and Experiment", National Maritime Institute, R.138.
52. STANDING, R.G., "Wave Loading on Offshore Structures: A Review", NMI R102, 1981
53. SUYEHIRO, K. (1924), "The Drift of Ships Caused by Rolling among Waves", Trans. INA, Vol.66.
54. TSE, Chuan-Cheung (1984), "Computation of the Motion and Drift Force for a Floating Body", Masters Thesis, Memorial University of Newfoundland.
55. URSELL, F. (1950), "Surface Waves on Deep Water in the Presence of a Submerged Circular Cylinder", Proc. Cambridge Phil. Soc., Vol.46.
56. WATANABE, Y. (1938), "Some Contribution to the Theory of Rolling", Trans. INA, Vol.175.

APPENDIX A

FIGURES

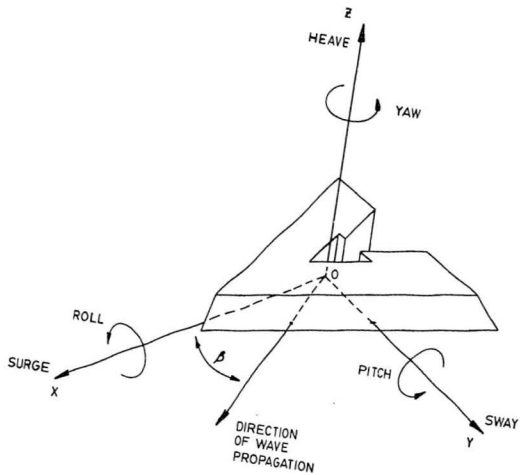


Figure 1
Coordinate System

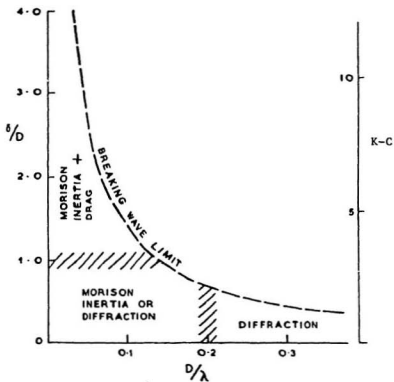


Figure 2
Regions of Validity of Force Prediction Methods
for a Fixed Pile (Standing 1981)

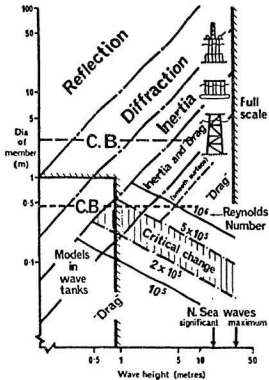


Figure 3
Wave Force Regimes (Miller and M^CGregor 1978)

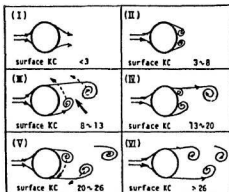


Figure 4
Vortex Shedding Patterns Around a Vertical Cylinder
in Waves as Functions of K-C (Chakrabarti 1987)

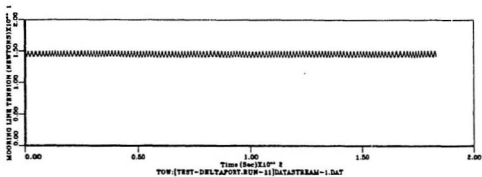
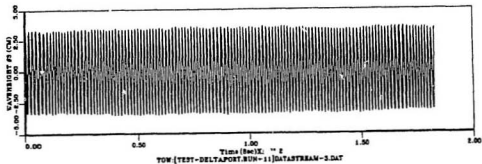


Figure 5
Measured Forces in Regular Waves

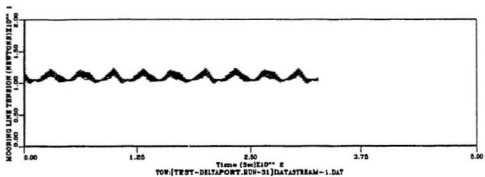
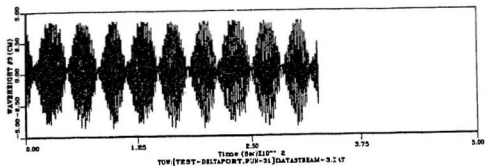


Figure 6
Measured Forces in Beating Waves

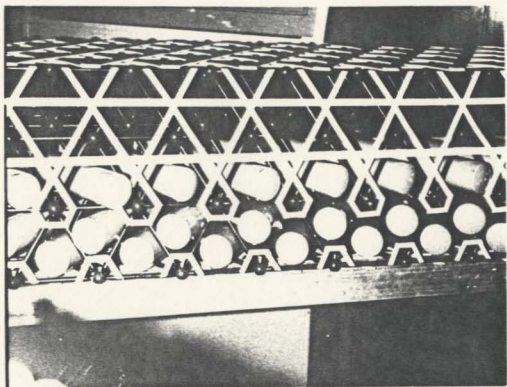


Figure 7a: Model Space Frame and Buoyancy Tubes

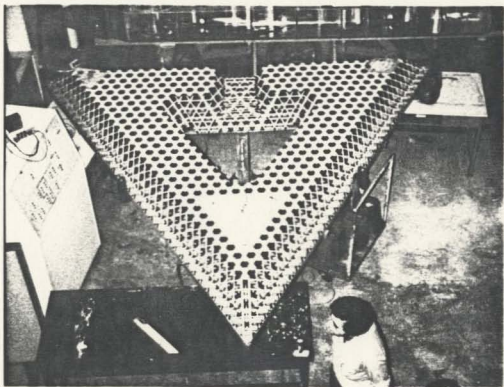
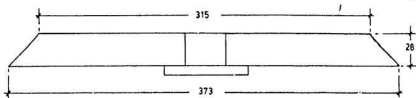
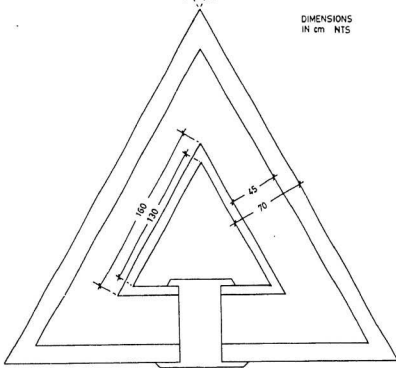


Figure 7b: 1:200 Scale Model Used in Testing



ELEVATION

60°

DIMENSIONS
IN cm NTS

PLAN

Figure 8
Model Dimensions

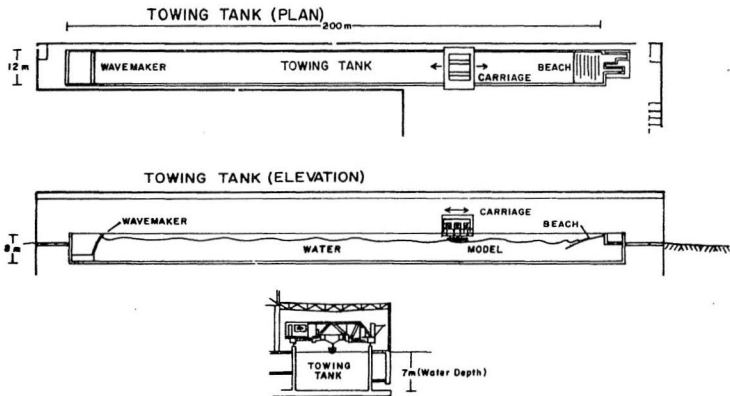


Figure 9
IMD Towing Tank Facility

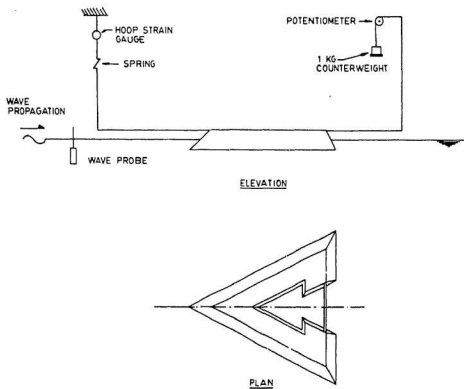


Figure 10
Test Set-Up

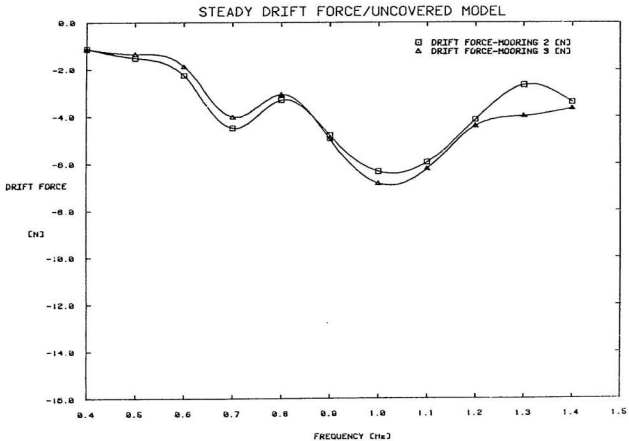


Figure 11
 Plot of Experimental Results: Uncovered Model;
 Drift Force .vs. Frequency

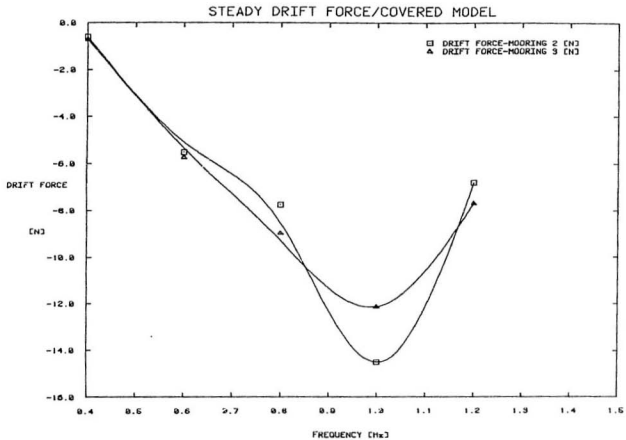


Figure 12
 Plot of Experimental Results: Covered Model;
 Drift Force .vs. Frequency

EXPERIMENT/UNCOVERED MODEL

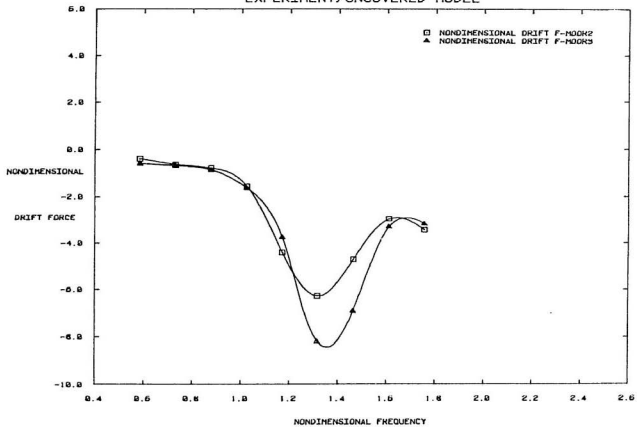


Figure 13
 Plot of Experimental Results: Uncovered Model;
 Nondimensional Drift Force .vs. Nondimensional Frequency

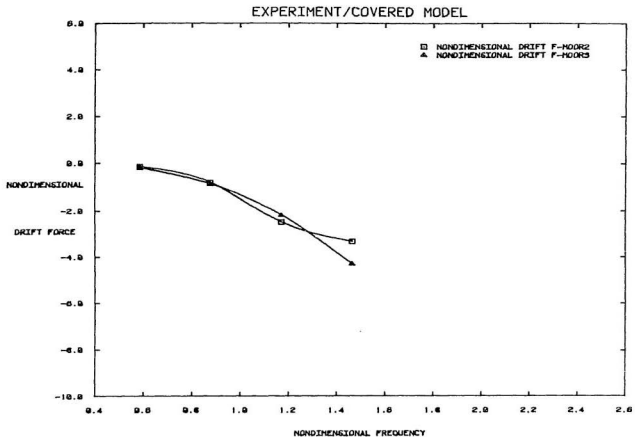


Figure 14
 Plot of Experimental Results: Covered Model;
 Nondimensional Drift Force .vs. Nondimensional Frequency

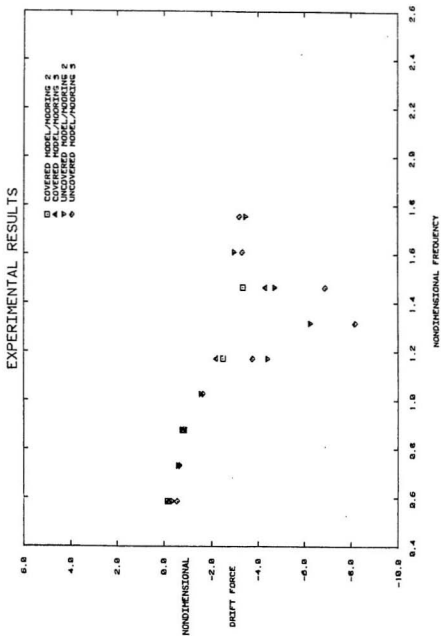


Figure 15
Comparison of Covered and Uncovered Model Test Results

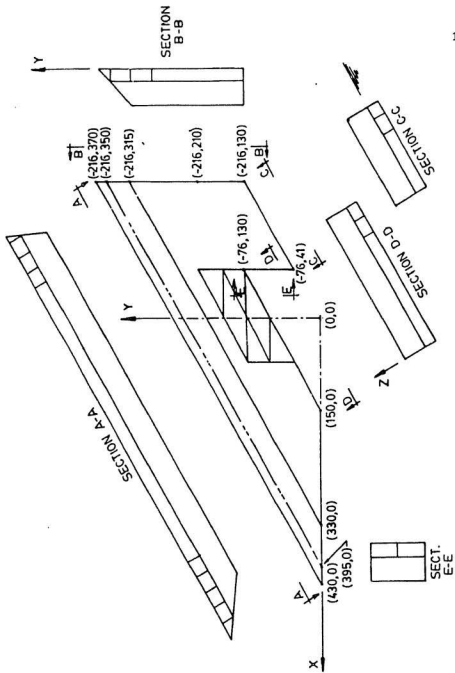


Figure 16
Model Panels Used in Numerical Analysis

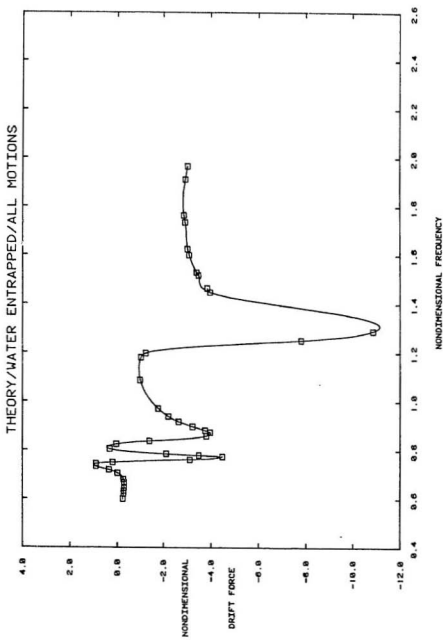


Figure 17
Plot of Computed Results:
All Motions; Head Seas

FIRST-ORDER MOTIONS/WATER ENTRAPPED/HEAD SEAS

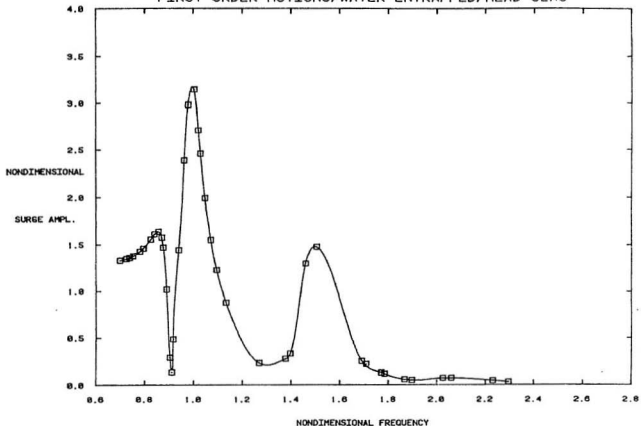


Figure 18a
Plot of Computed Results:
First-Order Motion-RAO's; Surge Amplitude Operator

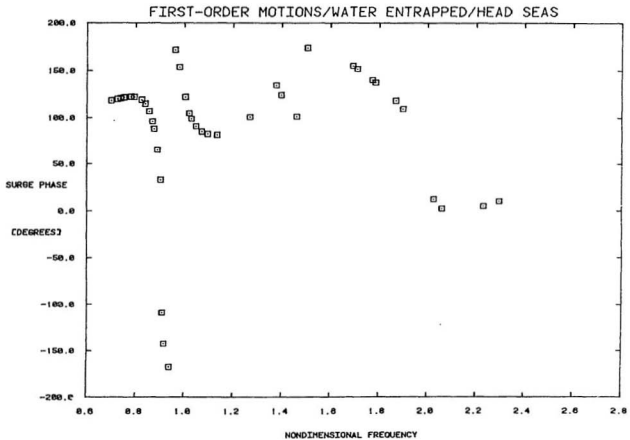


Figure 18b
 Plot of Computed Results:
 First-Order Motions; Surge Phase

FIRST-ORDER MOTIONS/WATER ENTRAPPED/HEAD SEAS

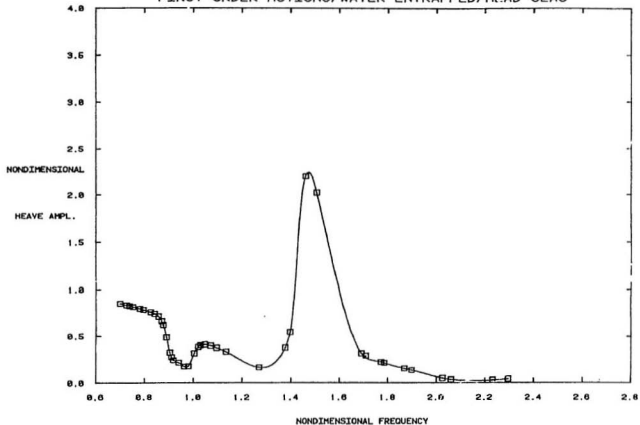


Figure 18c
Plot of Computed Results:
First-Order Motions; Heave Amplitude Operator

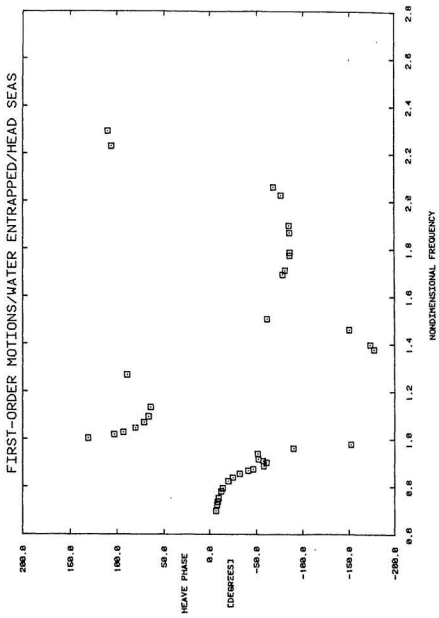


Figure 18d
 Plot of Computed Results:
 First-Order Motions; Heave Phase

FIRST-ORDER MOTIONS/WATER ENTRAPPED/HEAD SEAS

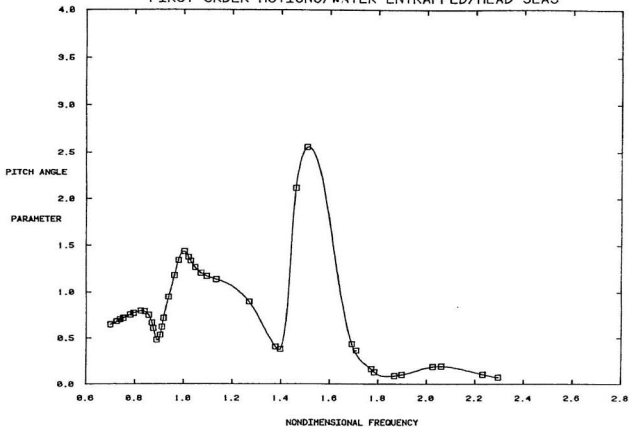


Figure 18e
Plot of Computed Results:
First-Order Motions; Pitch Angle Parameter

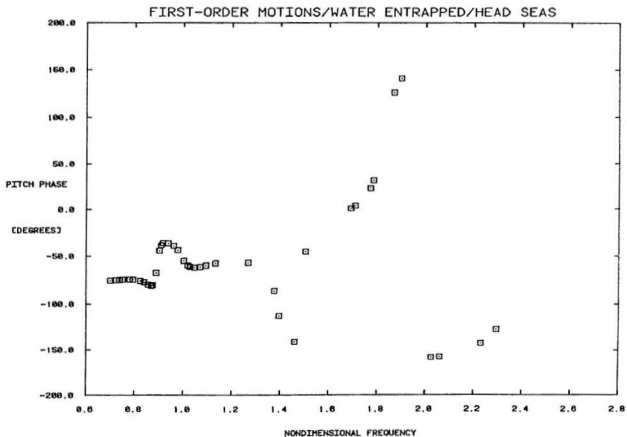


Figure 18f
 Plot of Computed Results:
 First-Order Motions; Pitch Phase

THEORY/WATER ENTRAPPED/FREE FLOATING

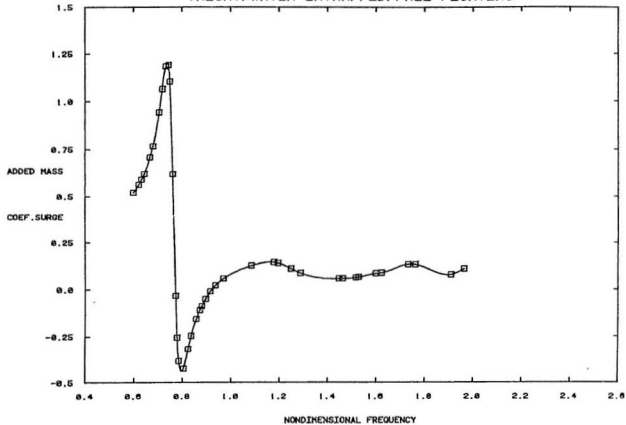


Figure 19a
Plot of Computed Surge Added Mass Coefficient

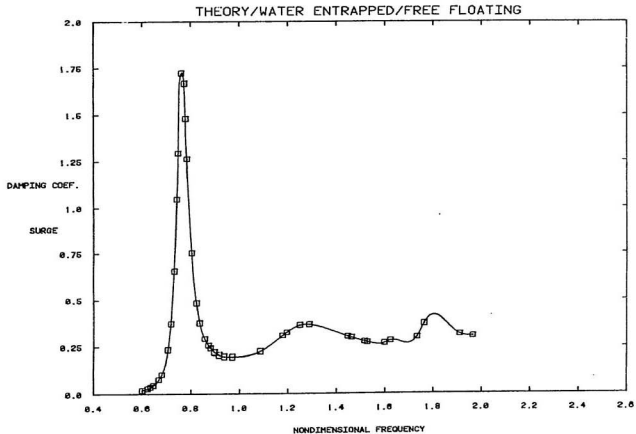


Figure 19b
Plot of Computed Surge Damping Coefficient

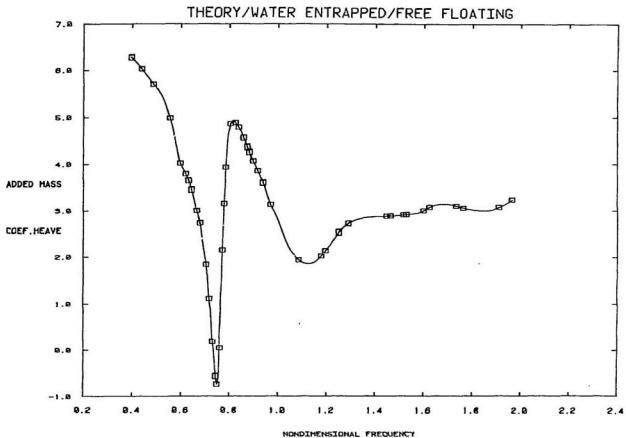


Figure 19c
Plot of Computed Heave Added Mass Coefficient

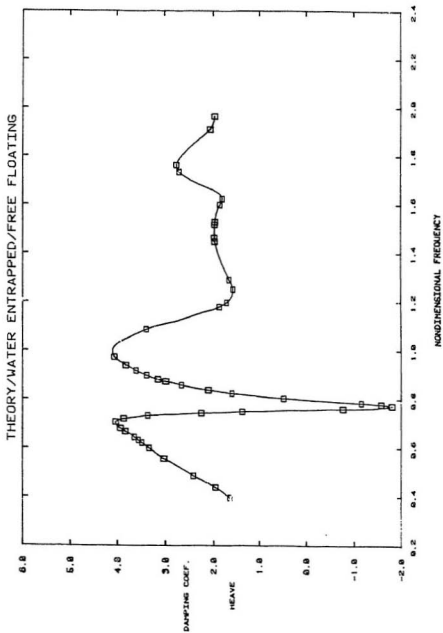


Figure 19d
Plot of computed Heave Damping Coefficient

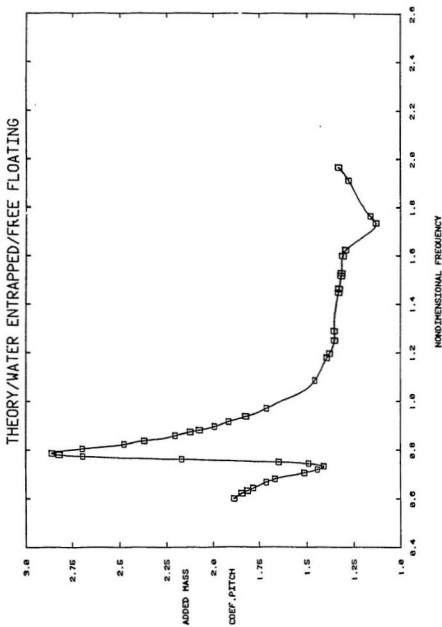


Figure 19c
Plot of Computed Pitch Added Mass Coefficient

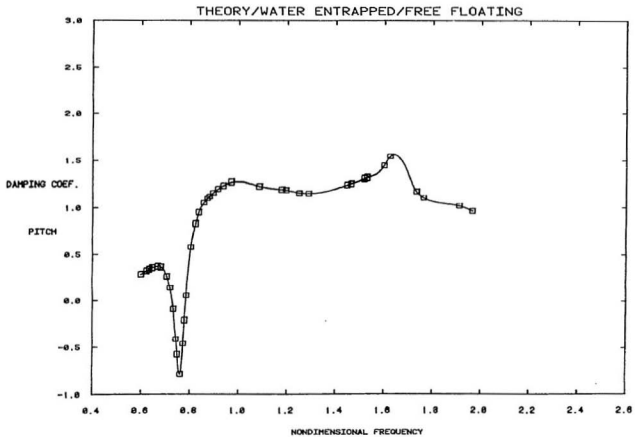


Figure 19f
Plot of Computed Pitch Damping Coefficient

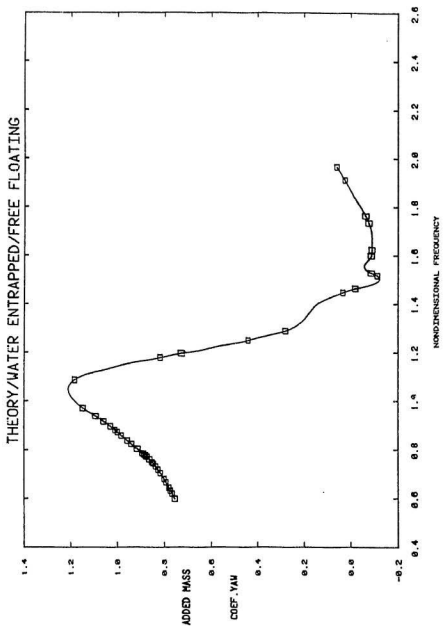


Figure 19g
 Plot of Computed Yaw Added Mass Coefficient

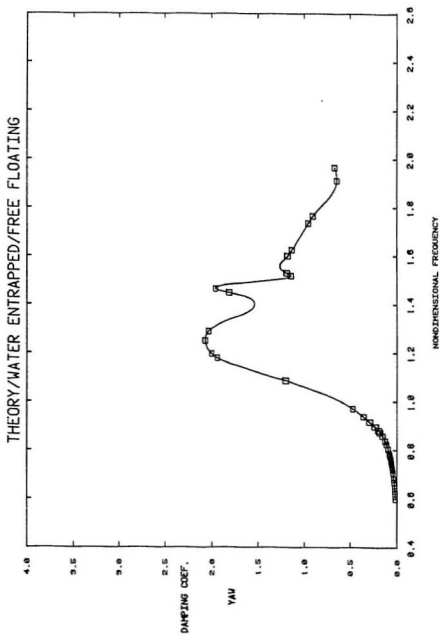
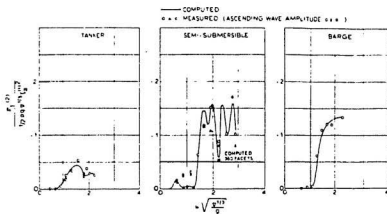
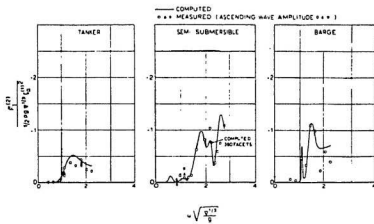


Figure 19h
Plot of Computed Yaw Damping Coefficient

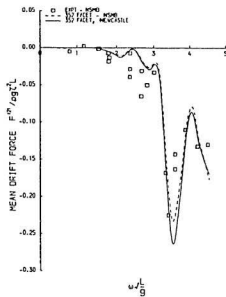


Mean longitudinal drift forces in head waves.



Mean longitudinal and transverse drift forces and yawing moment in bow quartering waves.

Figure 20
 Pinkster's Results for Head Seas and Quartering Seas



Comparison of predicted and measured zero forward speed added resistance (drift force).

Figure 21
Hearn's Results For a Semisubmersible

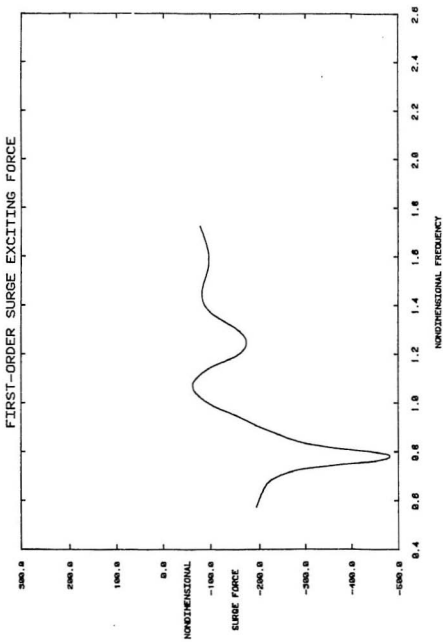


Figure 22
Calculated First-Order Surge Force

SURGE FROUDE-KRYLOV FORCE/MODEL IN HEAD WAVES

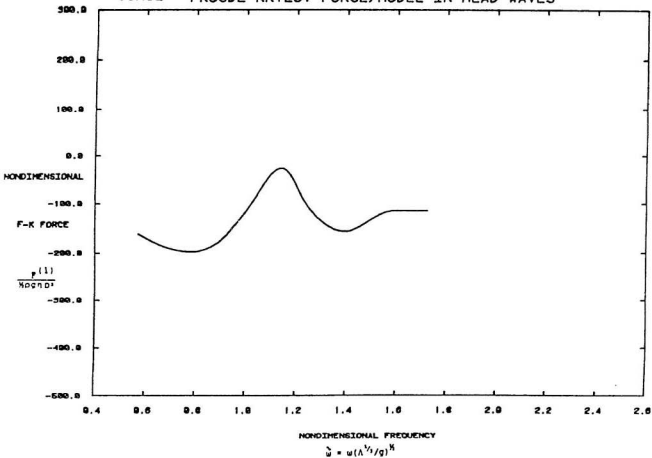


Figure 23
Calculated Froude-Krylov Force

SURGE SCATTERING FORCE/MODEL IN HEAD SEAS

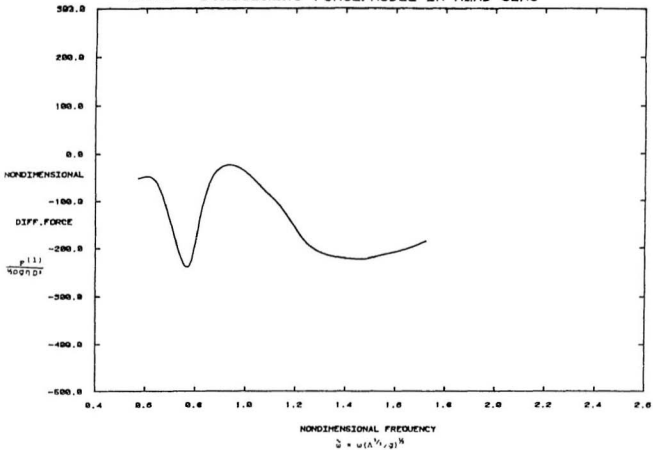


Figure 24
Calculated Scattering Force

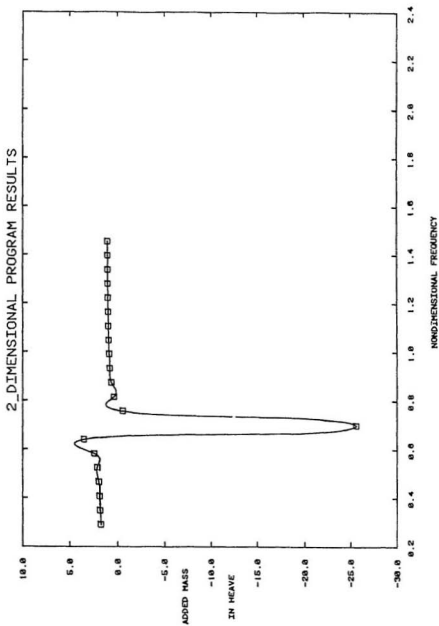


Figure 25a
2-D Numerical Results: Added Mass

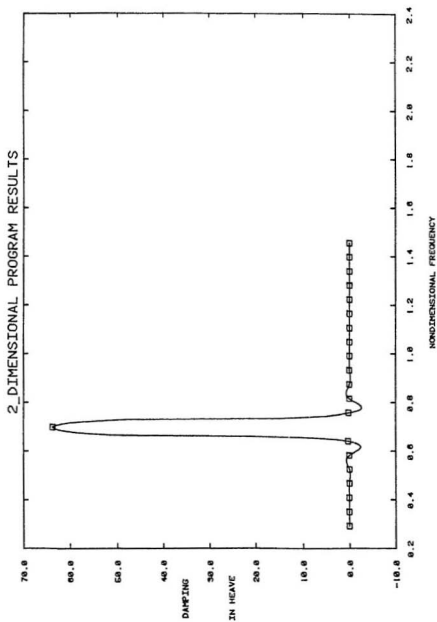


Figure 25b
2-D Numerical Results: Damping

THEORY/WATER ENTRAPPED/SURGE

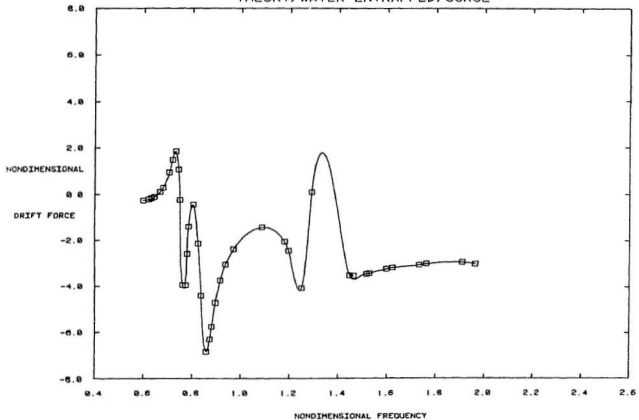


Figure 26a
 Plot of Computed Steady Drift Forces for Restricted
 Motions: Surge Motion Only

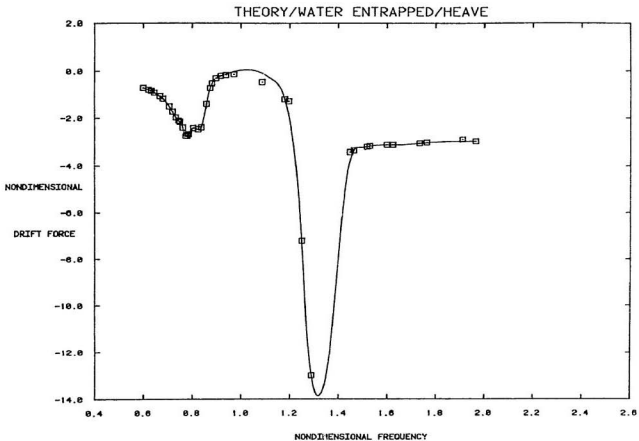


Figure 26b
 Plot of Computed Steady Drift Forces for Restricted
 Motions: Heave Motion Only

THEORY/WATER ENTRAPPED/PITCH

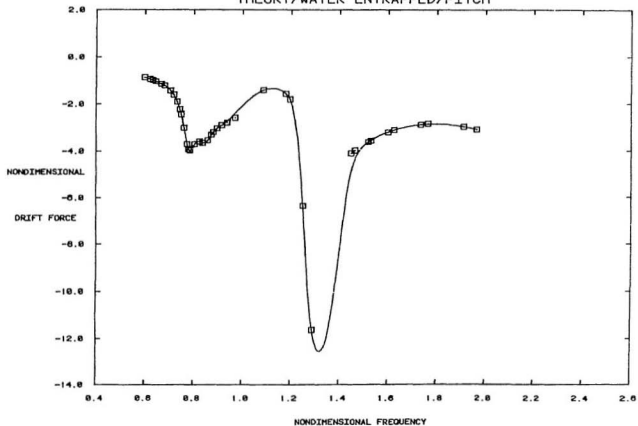


Figure 26c
Plot of Computed Steady Drift Forces for Restricted
Motions: Pitch Motion Only

THEORY/WATER ENTRAPPED/SURGE AND HEAVE

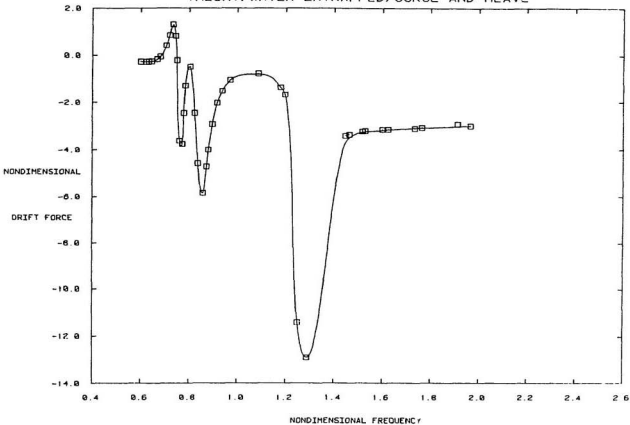


Figure 26d
 Plot of Computed Steady Drift Forces for Restricted
 Motions: Surge and Heave Motion Only

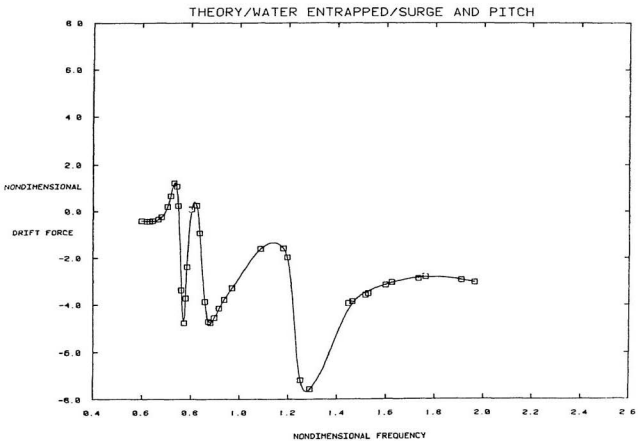


Figure 26e
Plot of Computed Steady Drift Forces for Restricted
Motions: Surge and Pitch Motion Only

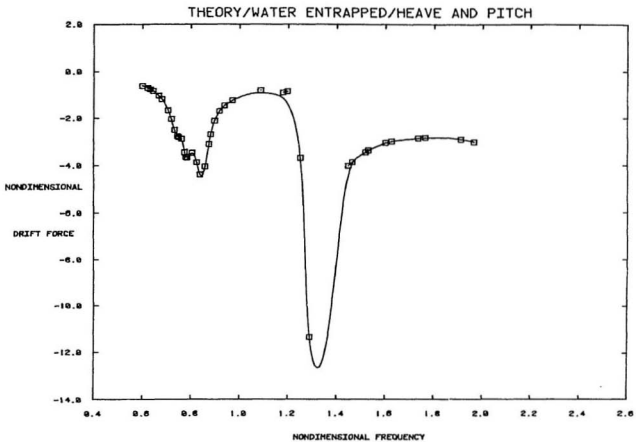


Figure 26f
Plot of Computed Steady Drift Forces for Restricted
Motions: Heave and Pitch Motion Only

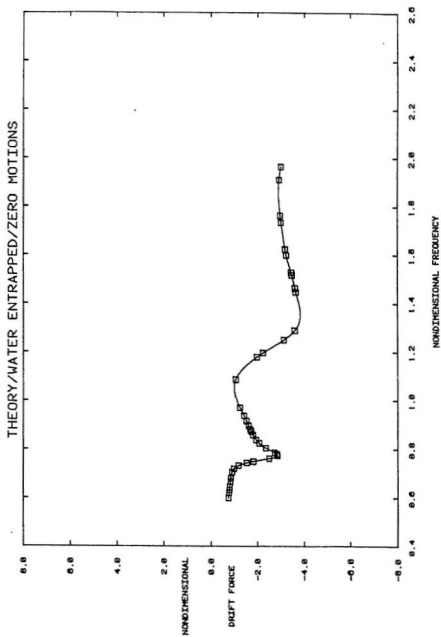


Figure 27
Plot of Computed Steady Drift Forces:
Fixed Body

THEORY/WATER ENTRAPPED/C(1,1)=1804000/SURGE ONLY

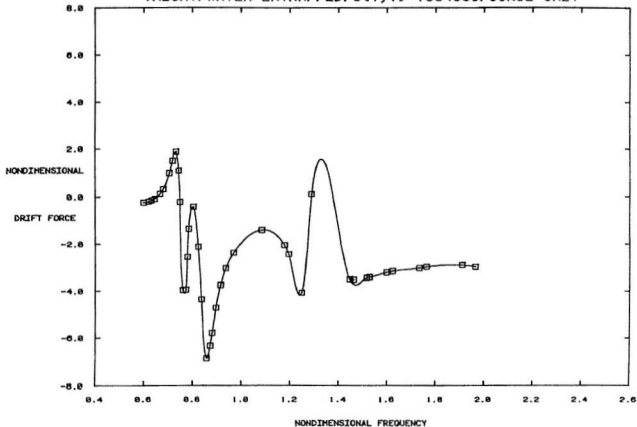


Figure 28a
Plot of Computed Steady Drift Forces: Surge Only;
Mooring #2 Stiffness Input to Program

THEORY/WATER ENTRAPPED/C(1,1)=3610000/SURGE ONLY

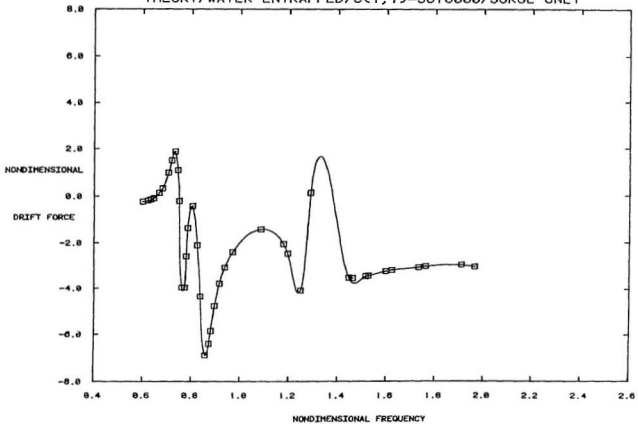


Figure 28b
Plot of Computed Steady Drift Forces: Surge Only;
Mooring #3 Stiffness Input to Program

THEORY/WATER ENTRAPPED/ALL MOTIONS/HEADING=240 DEG.

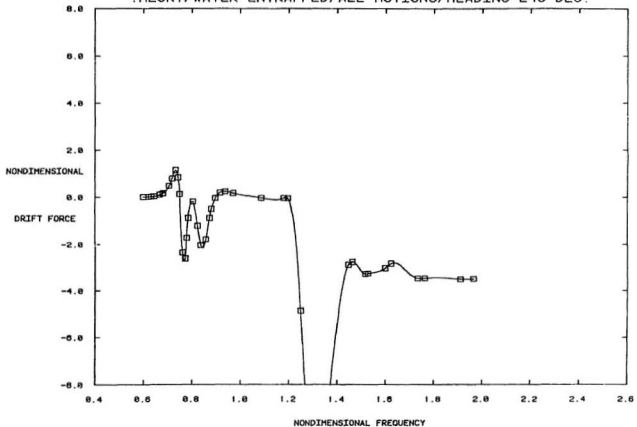


Figure 29a
Plot of Computed Steady Drift Forces:
Quartering Seas; Free Floating Body

THEORY/WATER ENTRAPPED/NO MOTIONS/HEADING=240 DEG.

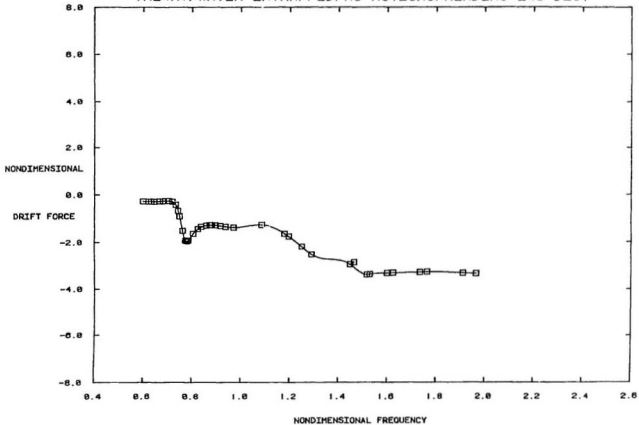


Figure 29b
Plot of Computed Steady Drift Forces:
Quartering Seas; Fixed Body

COMPARISON OF THEORY AND EXPERIMENT

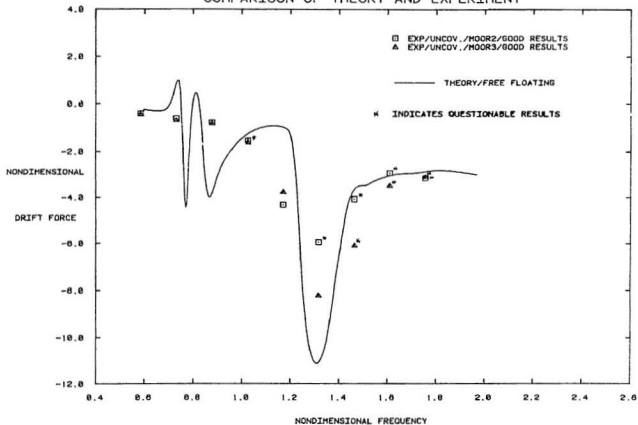


Figure 30
 Plot of Comparison of Steady Drift Forces:
 Computed Free Floating Structure .vs. Experimental
 Uncovered Model

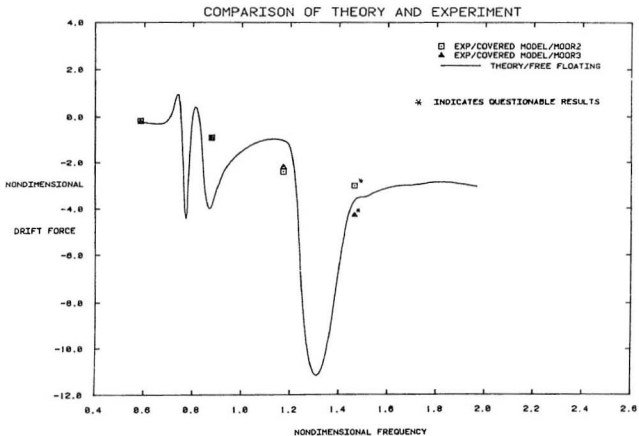


Figure 31
 Plot of Comparison of Steady Drift Forces:
 Computed Free Floating Structure .vs. Experimental
 Covered Model

COMPARISON OF THEORY AND EXPERIMENT

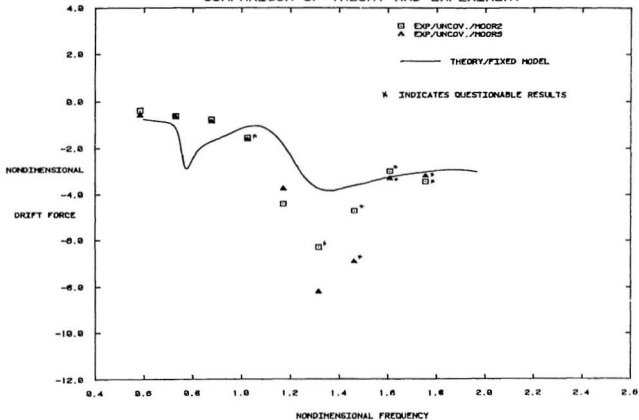


Figure 32
 Plot of Comparison of Steady Drift Forces:
 Computed Fixed Structure .vs. Experimental Uncovered
 Model

COMPARISON OF THEORY AND EXPERIMENT

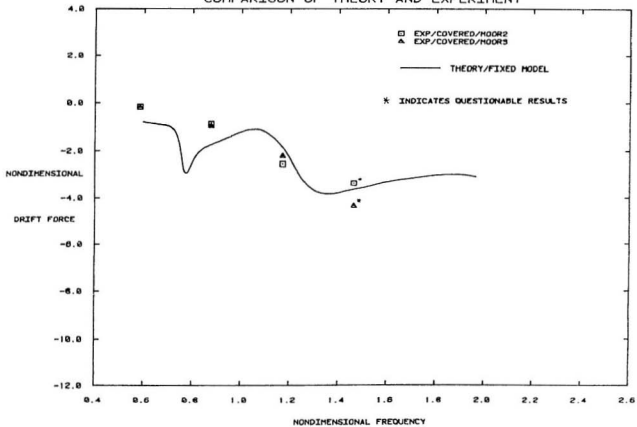
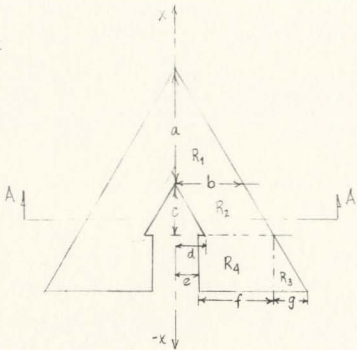


Figure 33
 Plot of Comparison of Steady Drift Forces:
 Computed Fixed Structure .vs. Experimental Covered
 Model

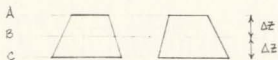
APPENDIX B

CALCULATIONS OF PARTICULARS OF THE MODEL

About x-x

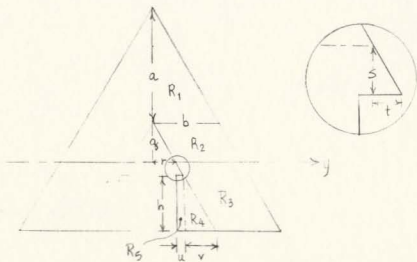


$$e + f = d + b$$



SECTION A-A

About y-y



DETERMINATION OF RADII OF GYRATION
1:200 SCALE MODEL

TABLE A1

DIM. (cm)	LEVEL		
	A	B	C
a	93	116	142
b	55	70	83
c	132	122	112
d	80	72	66
e	20	20	20
f	108	116	126
g	28	34	40
h	45	57.5	70
q	90	82	75
r	52	47	43
s	44	41	43
t	26	24	22
u	57	50	44
v	27	29	31
Δz	14	14	14

Calculation of Area for 1:200 scale model:

About x-x

TABLE A2

AREA (cm ²)	A	B	C
$R_1 = \frac{1}{2}ab$	2557.5	4060	5893
$R_2 = b \cdot c$	7260	8540	9296
$R_3 = \frac{1}{2}gh$	630	977.5	1400
$R_4 = f \cdot h$	4860	6670	8820
$A_T = \sum_{i=1}^4 R_i$	15307.5	20247.5	25409

About y-y

TABLE A3

AREA (cm ²)	A	B	C
$R_1 = \frac{1}{2}ab$	2557.5	4060	5893
$R_2 = b \cdot q$	4950	5740	6225
$R_3 = b(s+h)$	4895	6895	8964
$R_4 = \frac{1}{2}hv$	607.5	833.75	1085
$r_5 = hu$	2565	2875	3080
$A_T = \sum_{i=1}^5 R_i$	15575	20403.75	25247

TOTAL VOLUME AND MASS OF THE MODEL (without weights)

	(l)	(kg)
1 st deck (bottom)	7.1064	7.20
2 nd deck	5.4804	5.56
3 rd deck	4.6104	4.67
4 th deck (top)	3.8016	3.86
1 st web (bottom)	4.9320	5.01
2 nd web	4.212	4.28
3 rd web (top)	3.528	3.59
bottom buoyancy layer	89.0728	18.86
middle buoyancy layer	76.3481	16.17
top buoyancy layer	76.3481	16.17
	-----	-----
subtotals	275.44 l	85.37 kg
	0.275 m ³	

Adding on for additional materials (ie. plexiglass, plastic reinforcing, wood)

caps	4.17
harbour	10.0
other	16.5

Total Volume = 0.30 m³

Total mass = 116.0 kg

The model was weighed down such that the waterline was halfway up the second buoyancy layer. Steel bars were used for weights; total = 34 kgs (75 lbs)

VOLUME OF SUBMERGED PORTION ;

bottom layer of buoyancy cells	89.0728 l
50% of middle layer of buoyancy cells	38.175 l
72.9% of bottom deck	3.595 l
bottom deck	7.1064 l

subtotal	137.95 l
plastic reinforcing	2.0 l
harbour entrance reinforcing	10.0 l

Total submerged volume = 150 l

TOTAL MASS OF THE MODEL WITH WEIGHTS

Mass of the structure with weights = 150 kg

CENTER OF GRAVITY OF THE MODEL WITH WEIGHTS

Grouping weights as shown;

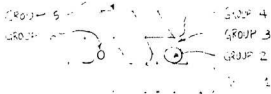


TABLE A4

DESCRIPTION	wt. (kg)	dist. from bottom (cm)	moment f x d (Nm)	dist. from c.g. (cm)
GROUP 1				
2 decks 7.2 + 5.56	70.8	4	27.8	-5.76
1 web 5.01				
2 layers of tubes 18.86 + 16.17				
harbour etc. 15				
caps 3				
GROUP 2				
1 layer tubes 16.17	17.4	10.4	17.75	0.64
caps 1.2				
GROUP 3				
1 web	4.28	12	5.04	2.24
GROUP 4				
2 decks 4.67 + 3.86	12.1	20	23.80	10.24
1 web 3.6				
GROUP 5				
plexiglass	10.5	27	27.8	17.24
GROUP 6				
steel bars	34.0	12	40.5	2.39
TOTALS	149.1		142.7	

CENTER OF GRAVITY OF THE MODEL

$$\text{c.g.} = \frac{\text{moment}}{\text{force}} = \frac{142.7 \text{ Nm}}{149.1 \text{ kg} \times 9.81 \text{ m/s}^2} = 9.76 \text{ cm from the bottom}$$

Using the waterline as the reference line...

$$9.76 - 5.95 = 3.81 \text{ cm} = 0.0381 \text{ m}$$

the coordinates of the center of gravity for the model are;

$$(0, 0, +0.0381)$$

For the prototype they are;

$$(0, 0, +7.62)$$

RADIOI OF GYRATION

$$I = \int y^2 \, dm = r^2 M$$

$$M = m_1 + m_2 + m_3 + \dots \quad r = \sqrt{\frac{I}{M}}$$

$$I_{xx} = m_1 x_1^2 + m_2 x_2^2 + m_3 x_3^2 + \dots$$

$$I_{yy} = m_1 y_1^2 + m_2 y_2^2 + m_3 y_3^2 + \dots$$

$$I_{zz} = m_1 z_1^2 + m_2 z_2^2 + m_3 z_3^2 + \dots$$

TABLE A7

GROUP	z	I_{yy}
1	.0145	15.99
2	.0705	4.51
3	.0755	0.93
4	.1655	3.13
5	.2105	2.65
6	.0755	27.71
7	.1045	3.76

		58.68

About z-z;
using TABLE A5 and;

TABLE A8

GROUP	x_1	x_2	x_3	x_4	I_{zz}
1	1.223	0.19	0.8967	0.78	32.96
2	1.207	0.21	0.7933	0.6975	9.16
3	1.207	0.21	0.7933	0.6975	2.16
4	1.21	0.24	0.74	0.665	5.84
5	1.21	0.24	0.74	0.665	4.8
6	1.80		0.90		60.49
7	0.70				4.49

					119.9

RADIO OF GYRATION OF MODEL WITHOUT WATER ENTRAPPED

$$I_{xx} = 2(62.45) = 124.9$$

$$I_{yy} = 2(58.68) = 117.36$$

$$M = 150 \text{ kg}$$

$$r_{xx}^2 = \frac{I_{xx}}{M} = \frac{124.9}{150}$$

$$r_{yy}^2 = \frac{I_{yy}}{M} = \frac{117.36}{150}$$

$$r_{xx} = 0.91 \text{ m}$$

$$r_{yy} = 0.88 \text{ m}$$

$$I_{zz} = 2(119.9) = 239.8$$

$$r_{zz}^2 = \frac{I_{zz}}{M} = \frac{239.8}{150}$$

$$r_{zz} = 1.26$$

	model	prototype
	-----	-----
r_{xx}	0.91	182
r_{yy}	0.88	176
r_{zz}	1.26	252

Taking moments about the bottom of the submerged portion;

$$\text{wt. of group 1} = 70.8 \text{ kg} \quad \text{moment} = 27.78 \text{ Nm}$$

subtracting half a layer of tubes above the waterline;

$$-5.12 \text{ Nm}$$

and subtracting 27.1% of the web above the waterline;

$$-1.15 \text{ Nm}$$

$$\text{moment} = 27.78 - 5.12 - 1.15 = 21.5 \text{ Nm}$$

$$\begin{aligned} \text{Total mass of submerged part is } (70.8 - 8.7 - 0.976) \text{ kg} \\ = 61.1 \text{ kg} \end{aligned}$$

$$d = \frac{M}{F} = \frac{21.5 \text{ Nm}}{61.1 \text{ kg} \cdot 9.81 \text{ m/s}^2} = 0.036 \text{ m} = 3.6 \text{ cm from bottom}$$

z-coordinate is;

$$-5.95 + 3.6 = -2.35 \text{ cm} \quad (\text{model})$$

$$\frac{-2.35 \text{ cm}}{100 \text{ cm/m}} (200) = -4.7 \text{ m} \quad (\text{prototype})$$

NATURAL FREQUENCY

spring stiffness' #2 4.6 kg/m = 45.1 N/m

#3 9.2 kg/m = 90.3 N/m

$$\omega_{0,2} = \sqrt{\frac{K}{M}}$$

$$M_V = (1+0.5)150 \text{ kg} \\ = 225 \text{ kg}$$

$$\omega_{0,2} = \sqrt{\frac{45.1}{225}} = 0.448 \text{ rads/sec (model)}$$

$$= 0.0317 \text{ rads/sec (prototype)}$$

$$f_{0,2} = 0.0713 \text{ Hz (model)}$$

$$= 0.005 \text{ Hz (prototype)}$$

$$\omega_{0,3} = \sqrt{\frac{90.2}{225}} = 0.633 \text{ rads/sec (model)}$$

$$= 0.0448 \text{ rads/sec (prototype)}$$

$$f_{0,3} = 0.101 \text{ Hz (model)}$$

$$= 0.007 \text{ Hz (prototype)}$$

WATER PLANE AREA

The waterline is halfway up the second layer of buoyancy tubes. So the ratio of cross sectional area to total area is;

$$\frac{4.5}{8.5} = 0.529$$

Thus, the buoyancy tubes take up approximately 52.9% of the water plane area. The linears also break the surface, so say approximately 55% of the total area is actually water plane area.

CALCULATIONS WITH WATER ENTRAPPED IN THE MODEL

VOLUME OF ENTRAPPED WATER

The volume estimated for the prototype of the submerged portion with water entrapped is 2,800,000 m³. In model scale this is 0.35 m³ which corresponds to 350 kg. The model weighs 150 kg so the entrapped water weighs 200 kg.

The volume of the submerged portion of the body is 150 l and the volume of entrapped water is 200 l. Therefore the ratio of body to water volume is:

$$\frac{\text{Volume of body}}{\text{Volume of water}} = \frac{150}{200} = 0.75$$

$$\frac{\text{volume of body}}{\text{Volume of water}} = \frac{150}{350} = 0.43$$

CENTER OF GRAVITY WITH WATER ENTRAPPED

Taking the centroid of mass of water at -4.0 cm on the z-axis, the moment about the bottom is;

$$\text{Moment} = f \times d = (200\text{kg})(9.81\text{m/s}^2)(0.02\text{m}) = 39.24 \text{ Nm}$$

The total moment is;

$$143.3 + 39.24 = 182.5 \text{ Nm}$$

The z centroid is located at 5.95 from the bottom so;

$$5.32 - 5.95 = -0.68 \text{ cm (model)}$$

$$-0.0063\text{m} \times (200) = -1.26 \text{ m (prototype)}$$

CENTER OF BUOYANCY WITH WATER ENTRAPPED

$$\text{Moment} = 21.5 + 39.24 = 60.74 \text{ Nm}$$

$$d = \frac{M}{f} = \frac{60.74 \text{ Nm}}{(200\text{kg} + 61.1\text{kg})(9.81\text{m/s}^2)} = 0.0237 \text{ m from bottom}$$

z-coordinate is;

$$2.37 \text{ cm} - 5.95 \text{ cm} = -3.58 \text{ cm} = -0.0358 \text{ m (model)}$$

$$-0.0358\text{m}(200) = -7.16 \text{ m (prototype)}$$

NATURAL FREQUENCY WITH WATER ENTRAPPED

spring stiffness' #2 = 4.6 kg/m = 45.1 N/m

#3 = 9.2 kg/m = 90.3 N/m

$$\omega_0 = \sqrt{\frac{K}{M_V}} \quad M_V = (1+0.5)(150\text{kg} + 200\text{kg}) = 525 \text{ kg}$$

$$\omega_{02} = \sqrt{\frac{45.1}{525}} = 0.293 \text{ rads/sec (model)}$$

$$= 0.0207 \text{ rads/sec (prototype)}$$

$$f_{02} = 0.047 \text{ Hz (model)}$$

$$= 0.003 \text{ Hz (prototype)}$$

$$\omega_{03} = \sqrt{\frac{90.2}{525}} = 0.414 \text{ rads/sec (model)}$$

$$= 0.0293 \text{ rads/sec (prototype)}$$

$$f_{03} = 0.066 \text{ Hz (model)}$$

$$= 0.005 \text{ Hz (prototype)}$$

RADII OF GYRATION WITH WATER ENTRAPPED

TABLE A9

M from A5	x	y	z	I _{xx}	I _{yy}	I _{zz}
46.4	1.223	0.473	0.03	10.42	69.44	79.78
73.2	0.19	0.735	0.03	39.61	2.71	42.19
11.0	0.8967	1.623	0.03	28.99	8.85	37.82
69.4	0.78	0.83	0.03	47.87	42.29	90.03
				-----	-----	-----
				124.9	117.36	239.62
				-----	-----	-----
			TOTALS	251.79	240.65	489.62

$$r_{xx}^2 = \frac{I_{xx}}{N} = \frac{251.79}{350} = 0.72 \text{ m}^2$$

$$r_{xx} = 0.85 \text{ m}$$

$$r_{yy}^2 = \frac{I_{yy}}{M} = \frac{240.65}{350} = 0.69 \text{ m}^2$$

$$r_{yy} = 0.83 \text{ m}$$

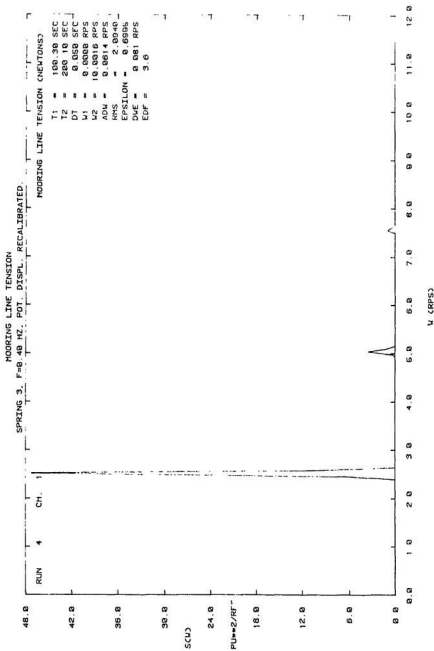
$$r_{zz}^2 = \frac{I_{zz}}{M} = \frac{489.62}{350} = 1.40 \text{ m}^2$$

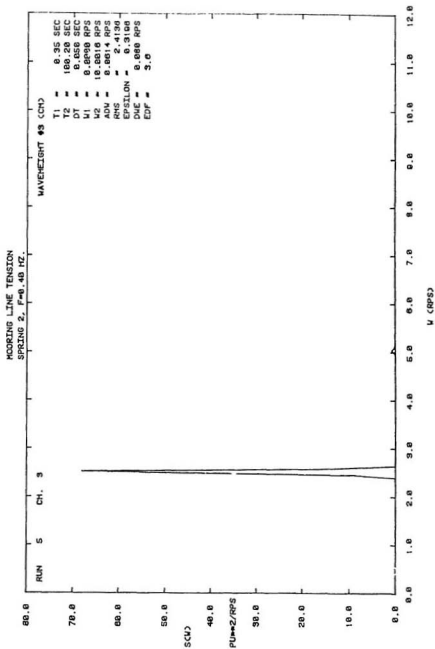
$$r_{zz} = 1.18 \text{ m}$$

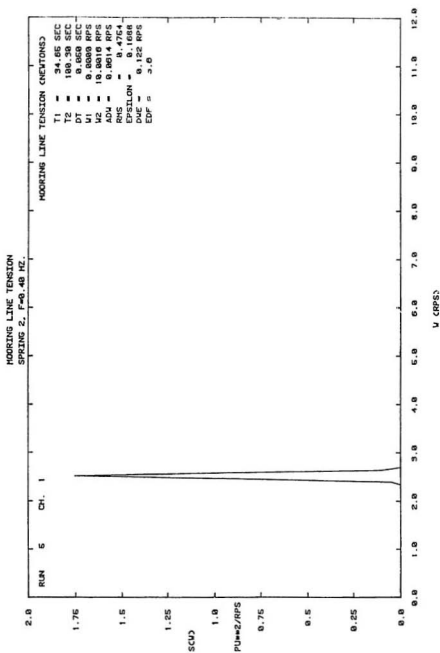
	model	prototype
r_{xx}	0.85 m	170 m
r_{yy}	0.83 m	166 m
r_{zz}	1.18 m	236 m

APPENDIX C

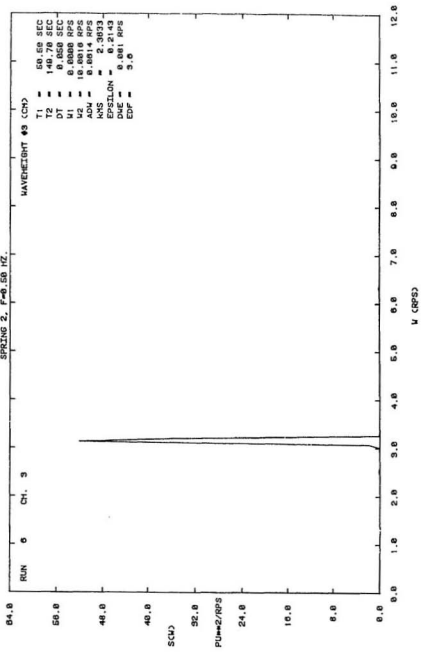
POWER SPECTRA OF WAVE AMPLITUDE AND MOORING FORCE



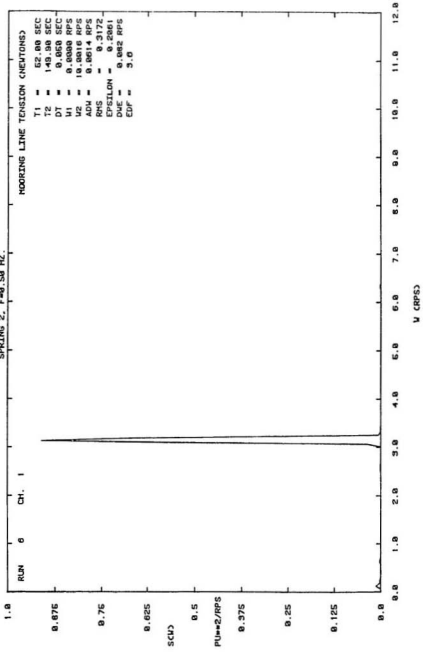


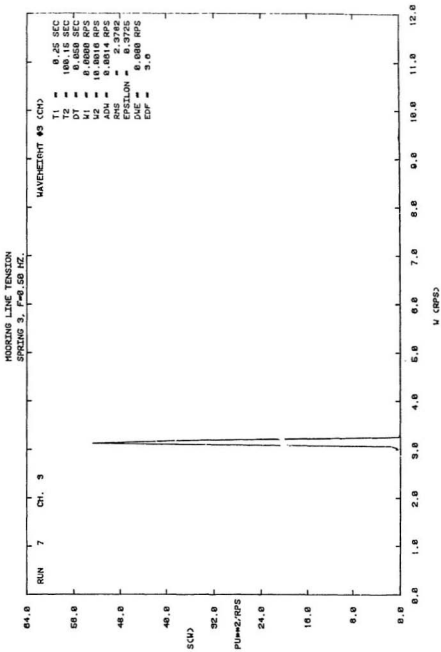


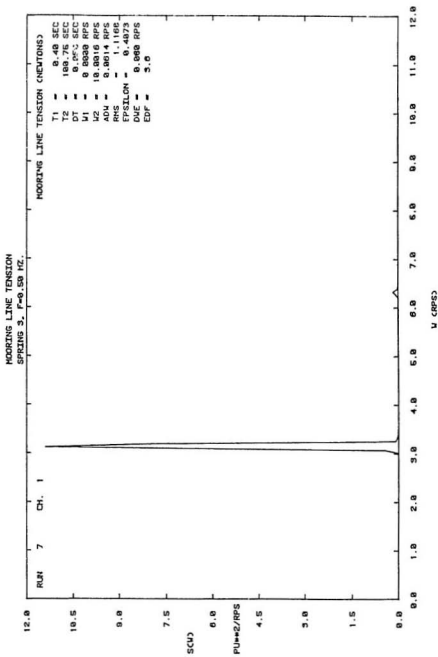
MOORE'S LINE TENSION
 SPRING 2, F=0.50 HZ.

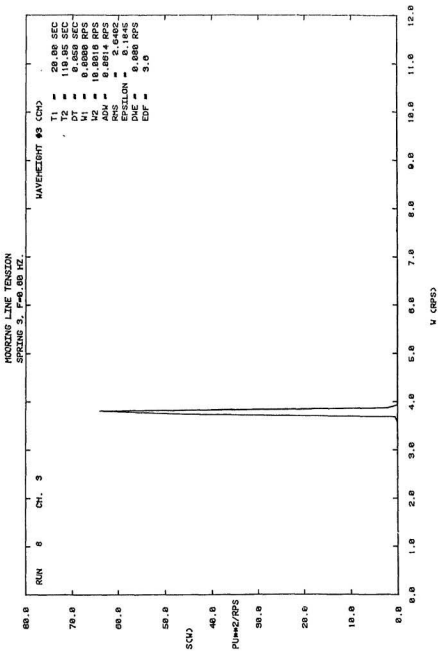


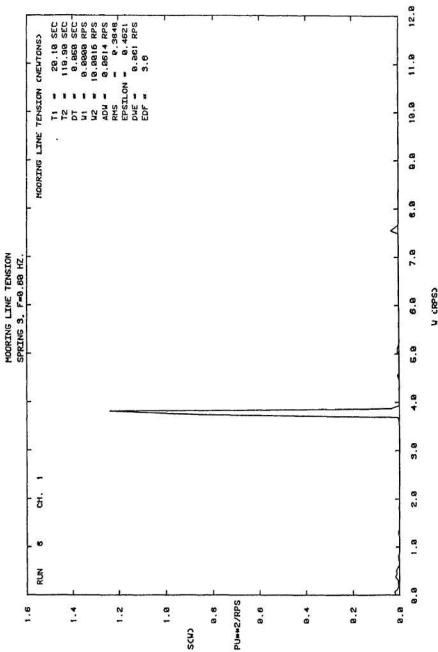
MOORING LINE TENSION
 SPRING 2, F=9.58 HZ.

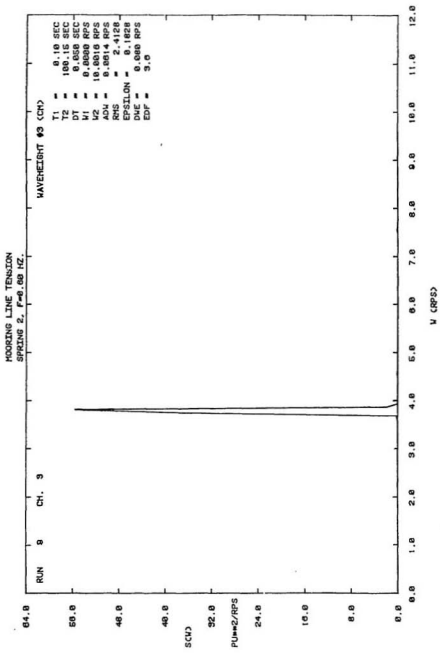


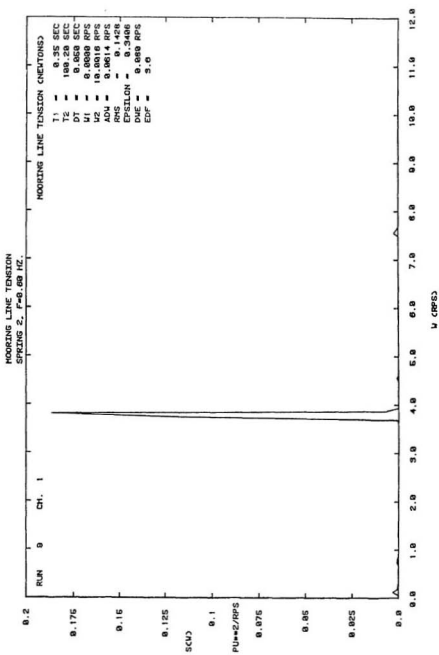




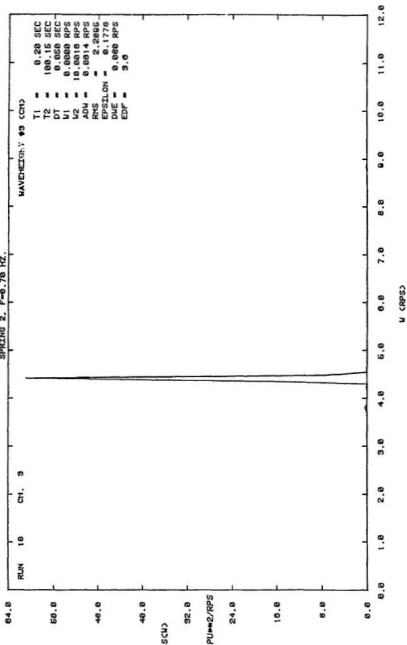




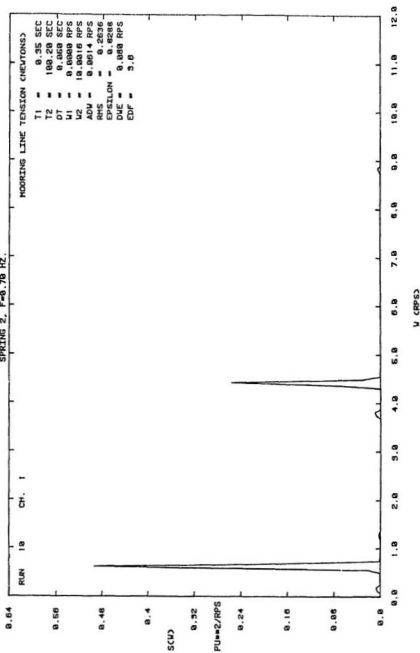




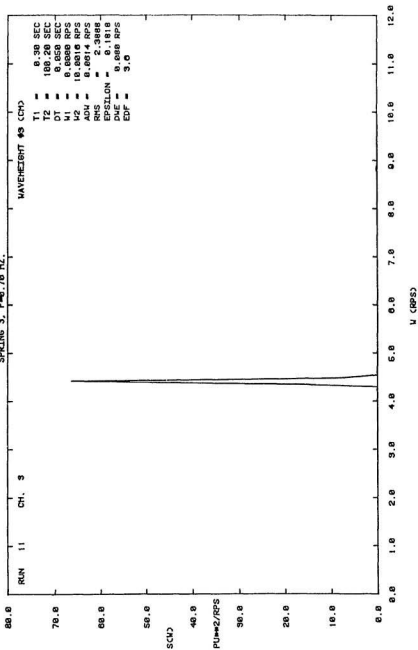
MOORING LINE TENSION
 SPRING 2, F=0.70 HZ.

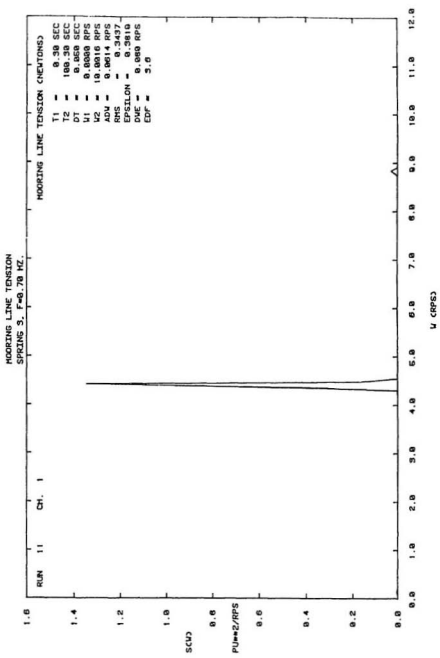


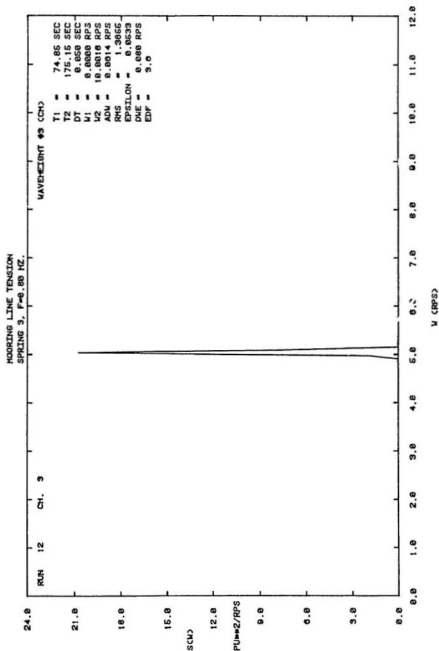
MOORING LINE TENSION
 SPRING 2, F=0.70 HZ.



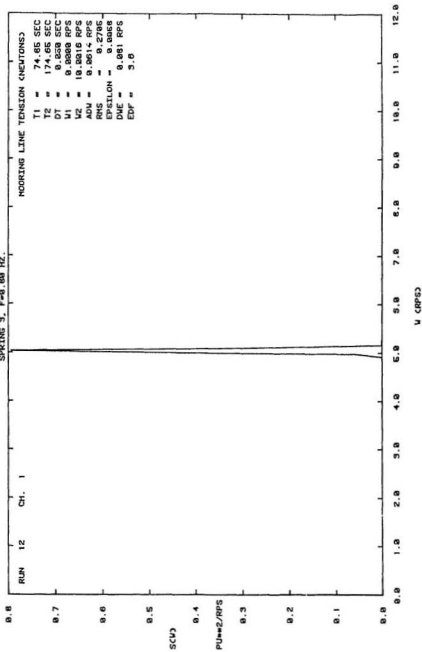
MOORING LINE TENSION
 SPRING 3, F=0.70 HZ.

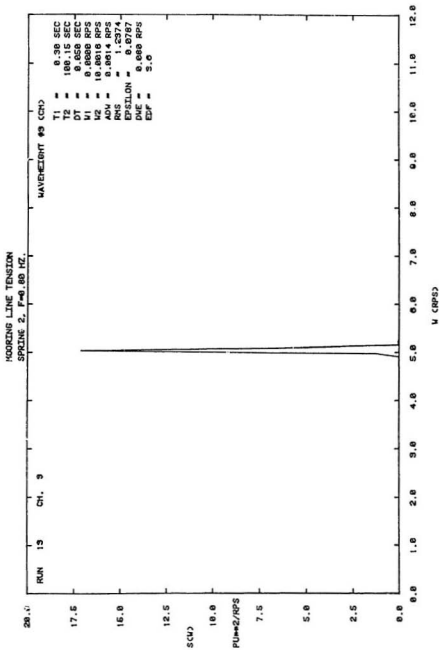




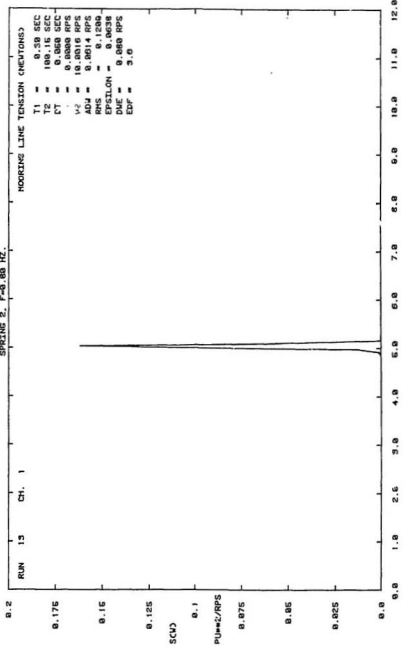


MOORING LINE TENSION
SPRING 3. F=0.89 HZ.

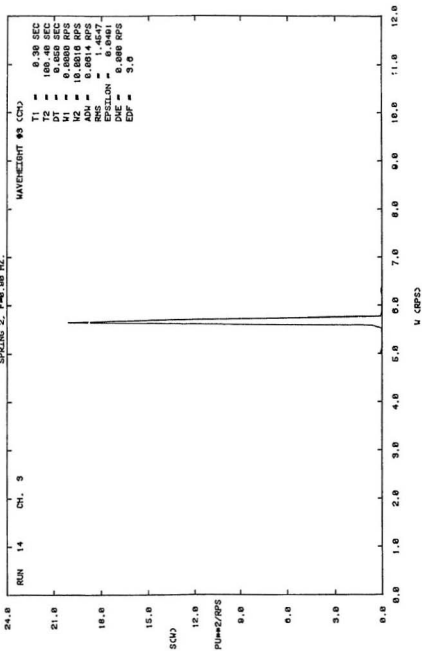


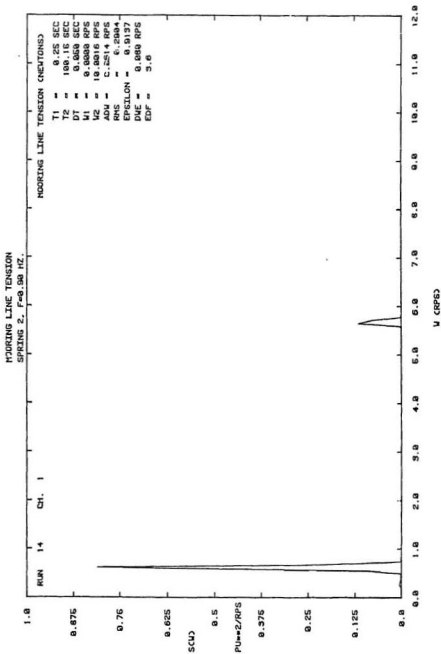


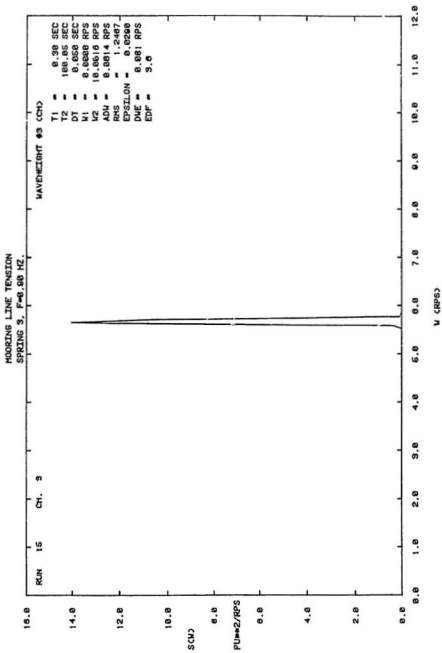
MOORING LINE TENSION
 SPRING 2, F=0.88 HZ.

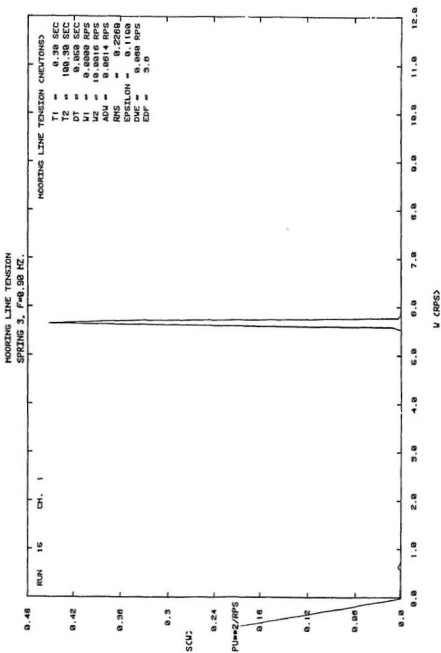


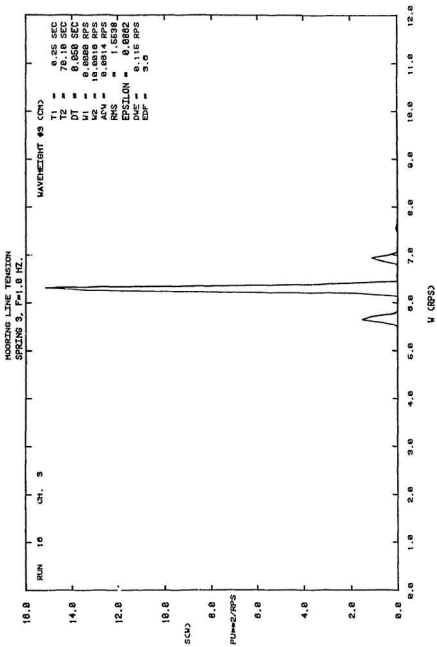
MOORING LINE TENSION
SPRING 2, F=6.68 HZ.

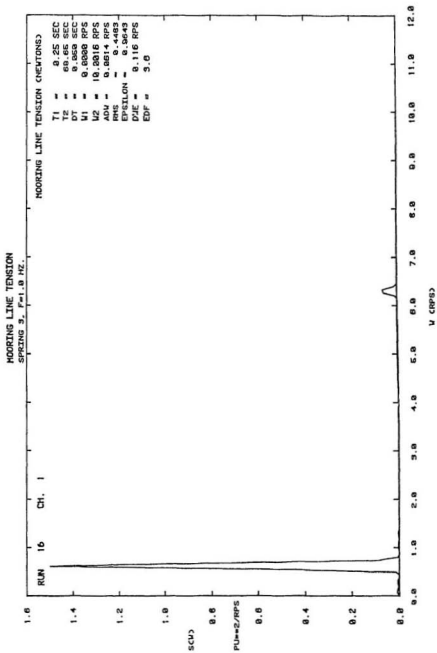


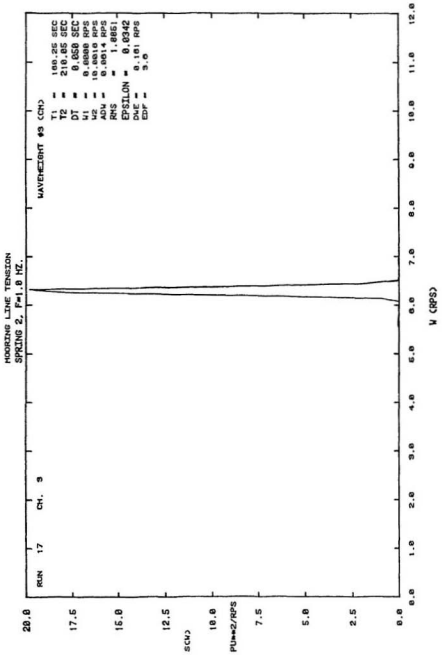


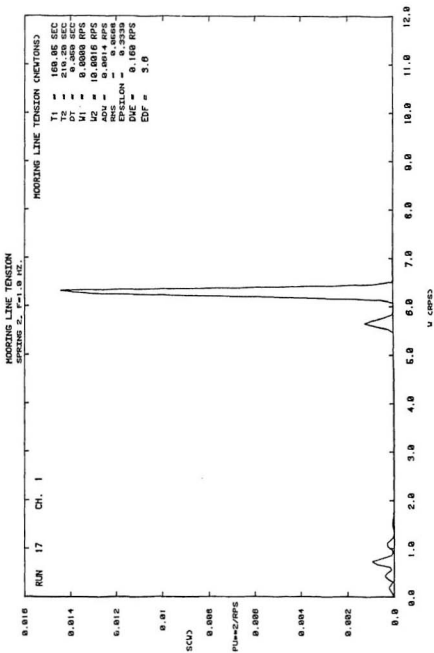




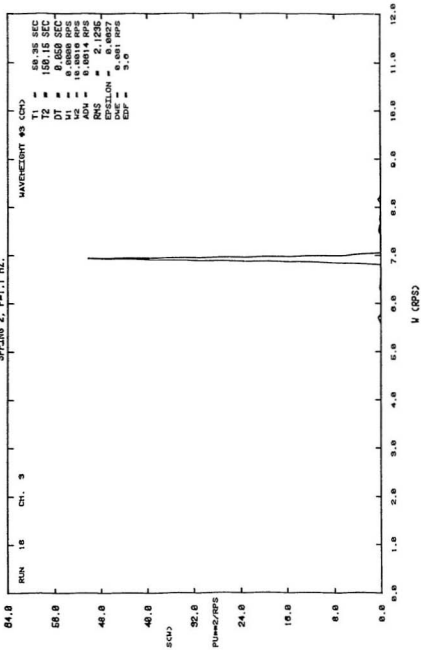


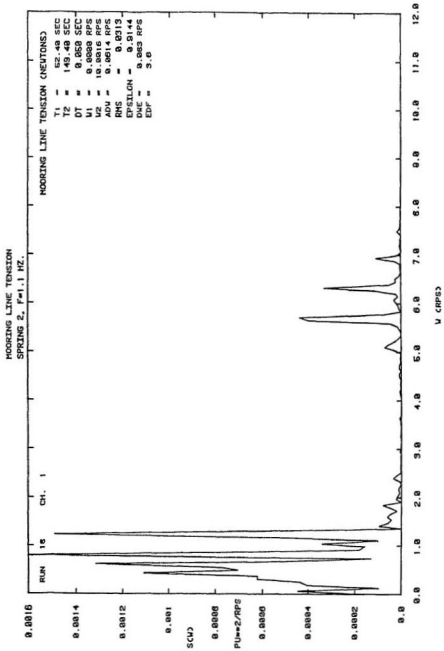


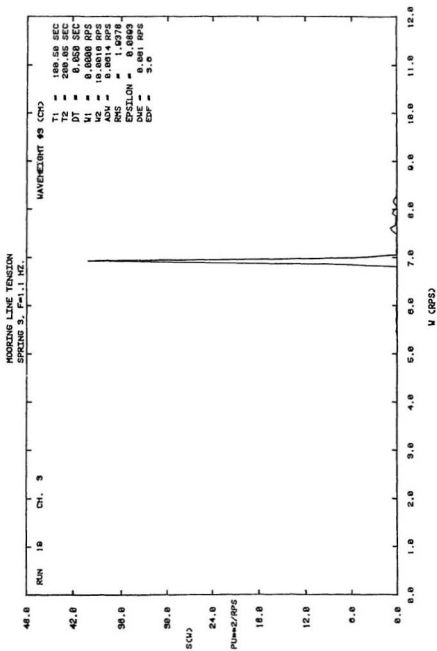


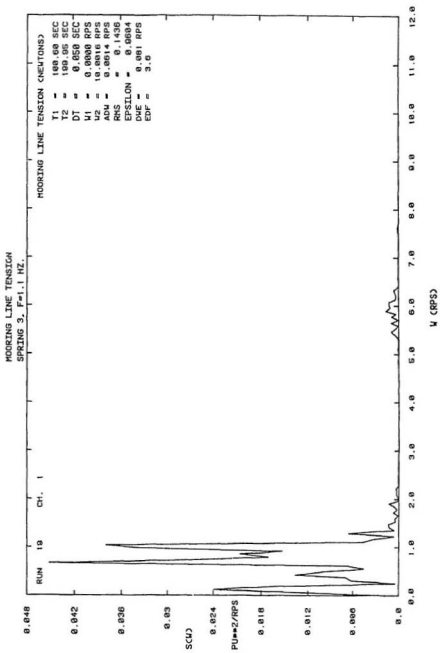


MOORING LINE TENSION
SPRING 2, F=1.1 HZ.









0.048

0.042

0.036

0.03

SCW)

0.024

PU=2/RPS

0.018

0.012

0.006

0.0

RUN 10 CH. 1

MOORING LINE TENSION (NEWTONS)

12.0

11.0

10.0

9.0

8.0

7.0

6.0

5.0

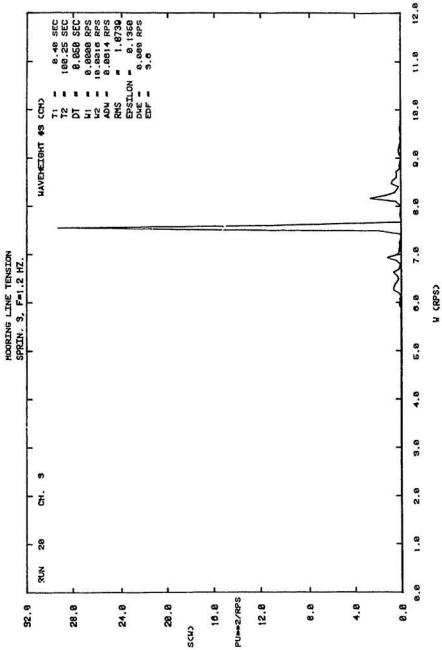
4.0

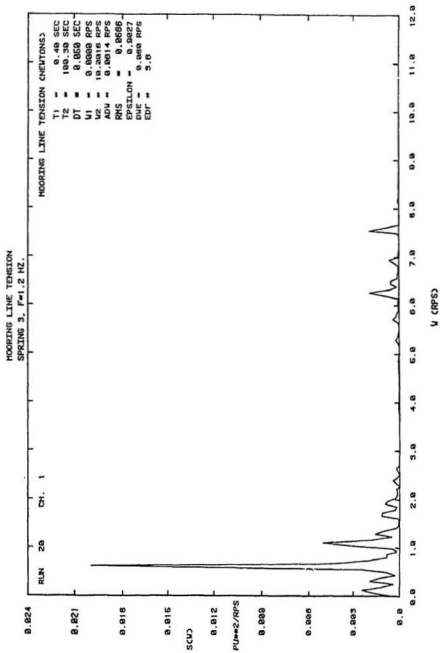
3.0

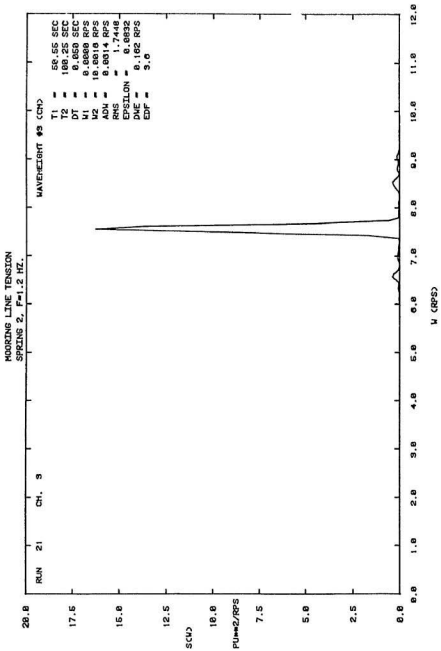
2.0

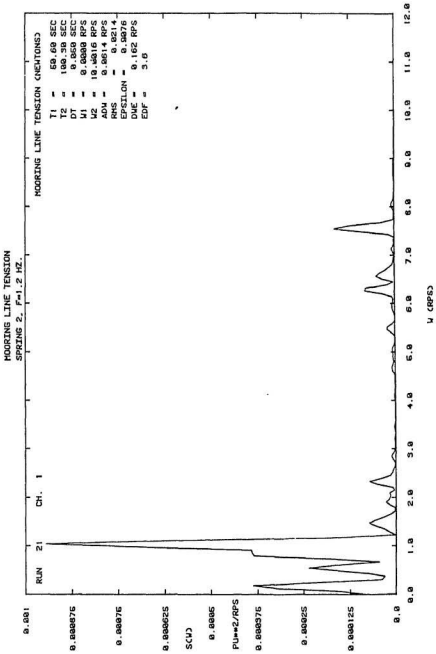
1.0

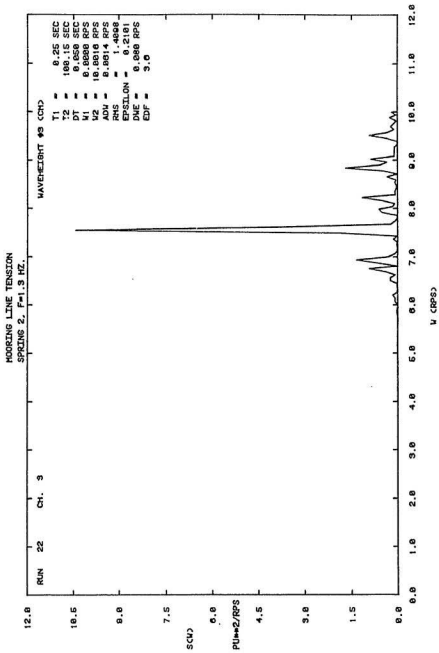
0.0

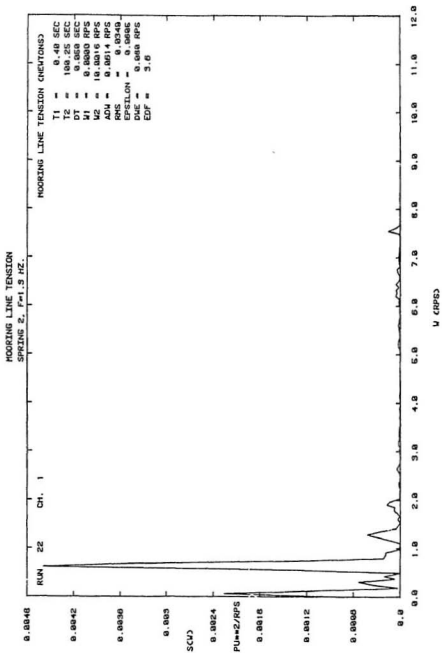


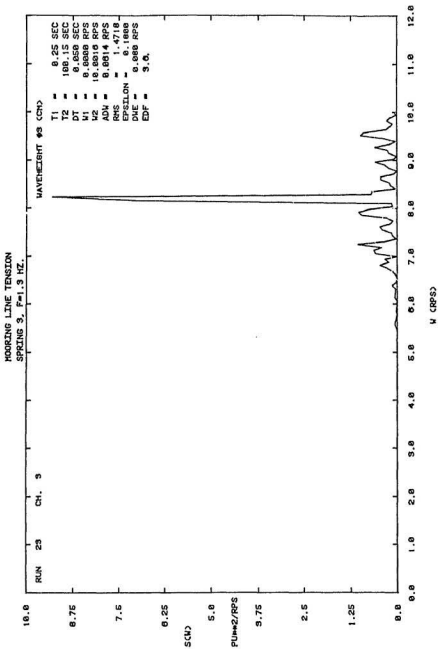


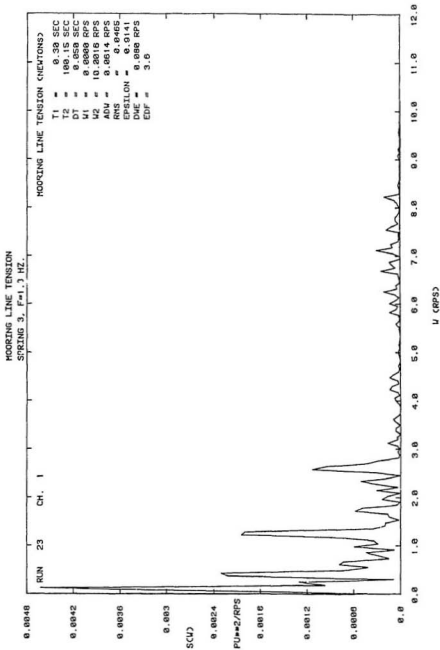


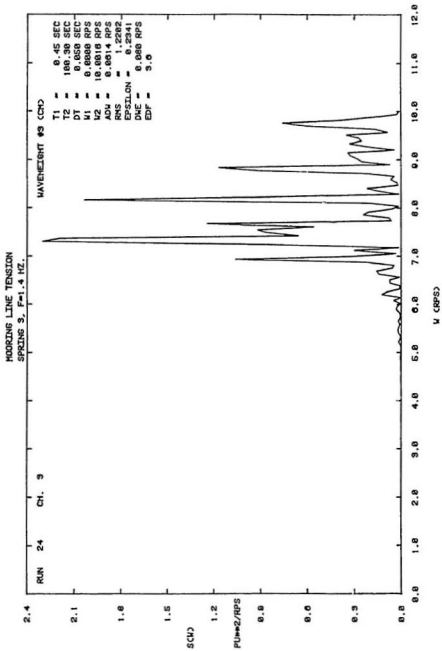


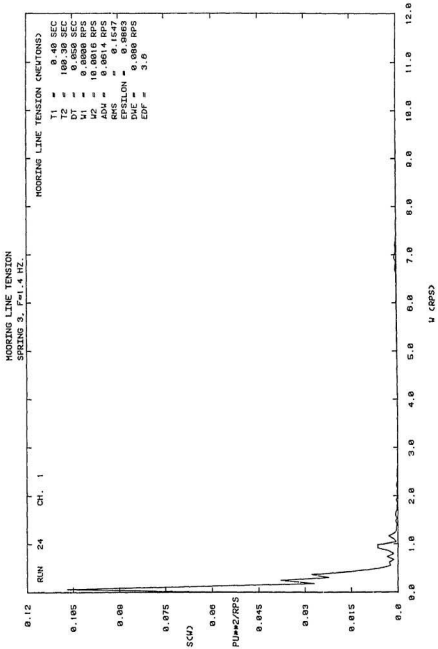




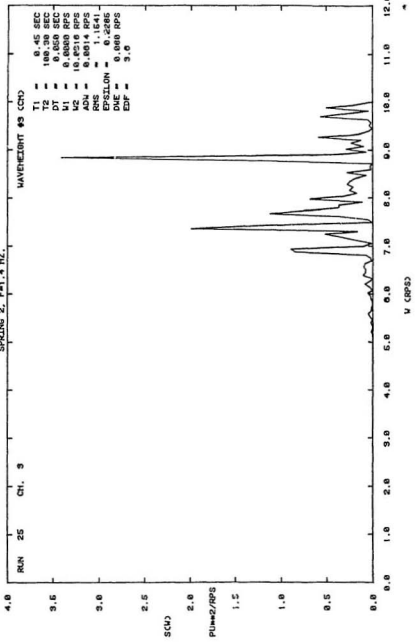




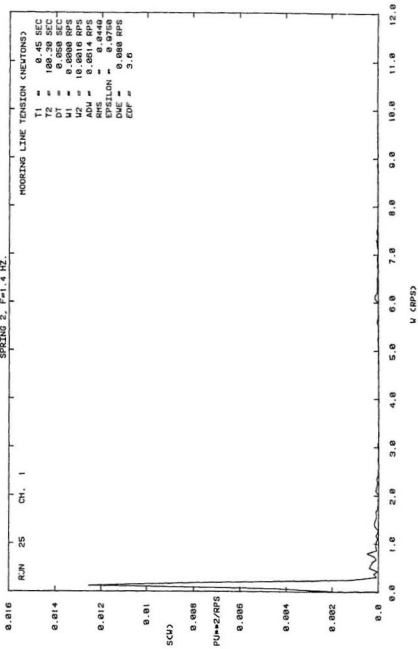


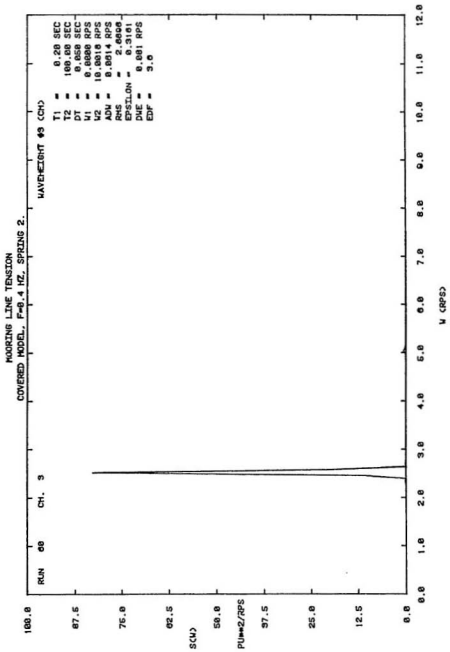


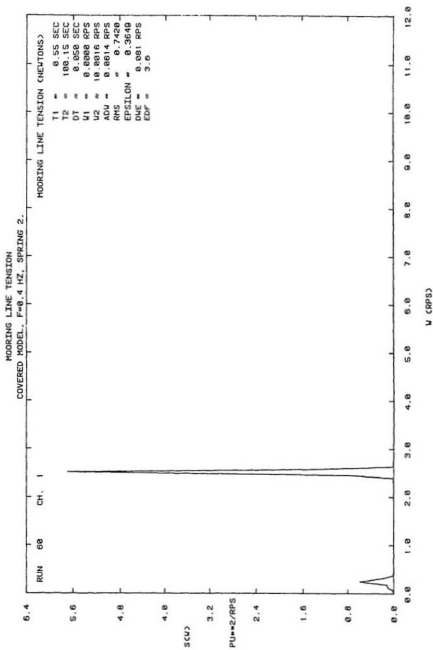
MOORING LINE TENSION
SPRING 2, F=1.4 HZ.

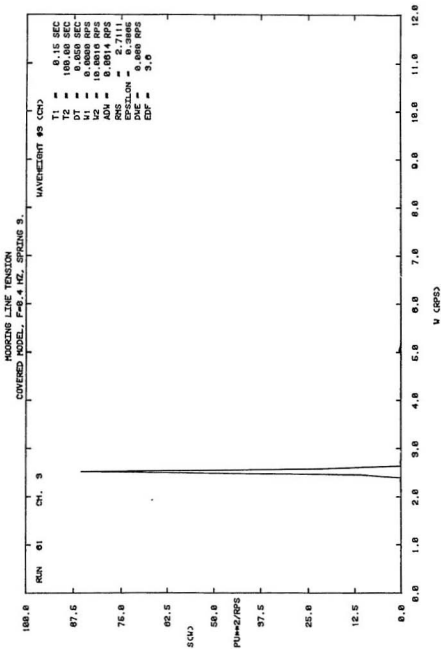


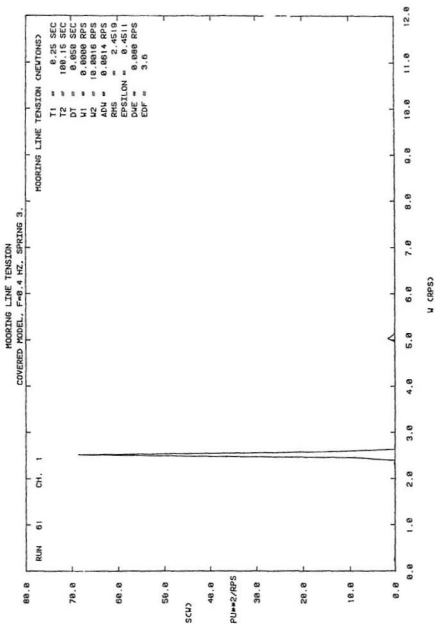
MOORING LINE TENSION
 SPRING 2, F=1.4 HZ.

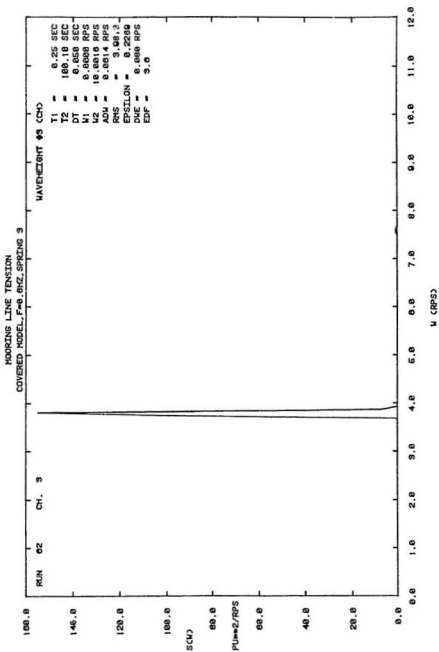


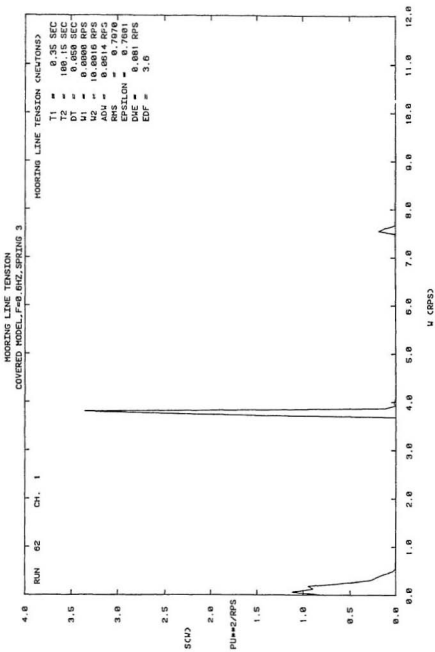


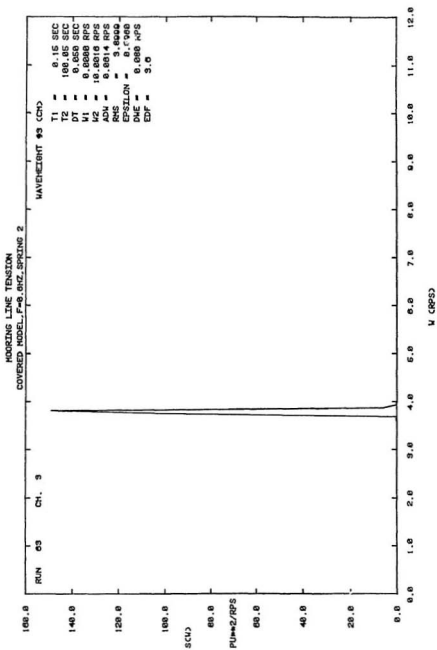


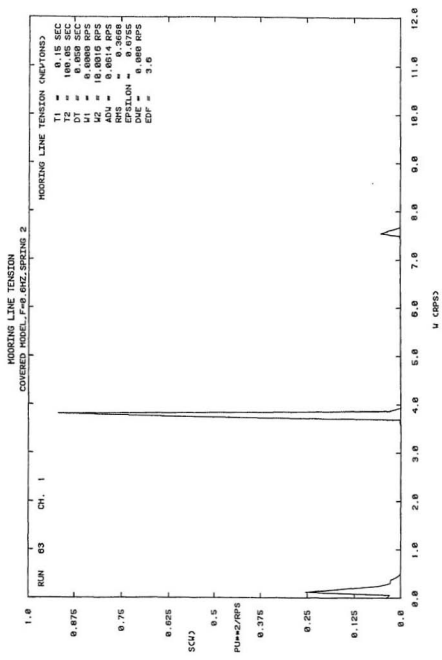


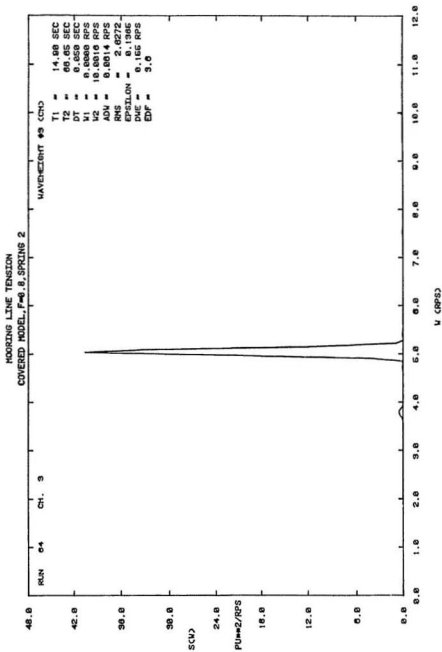


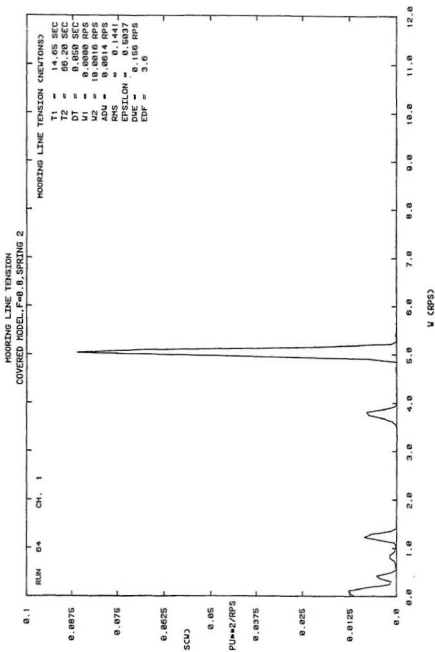




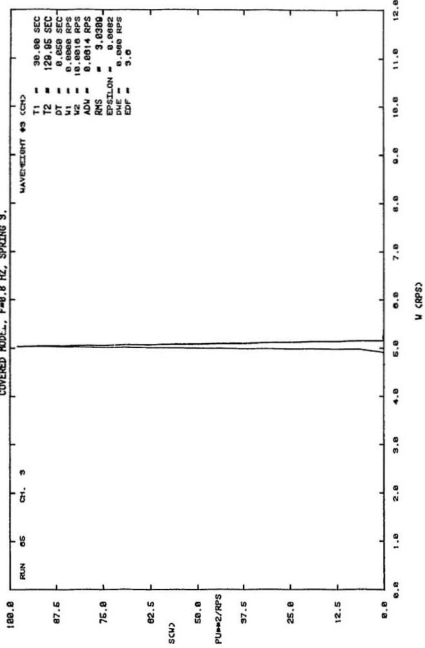


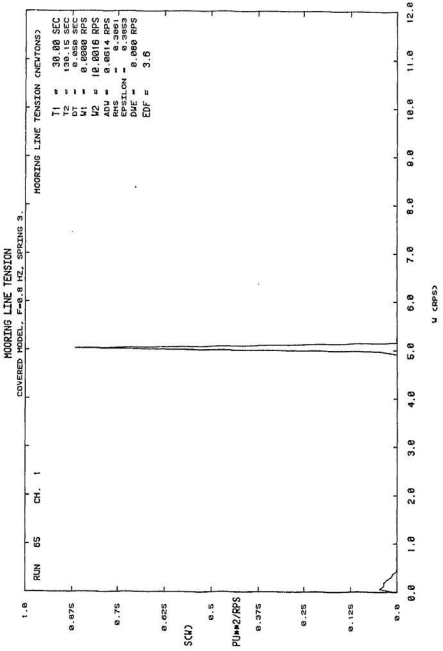


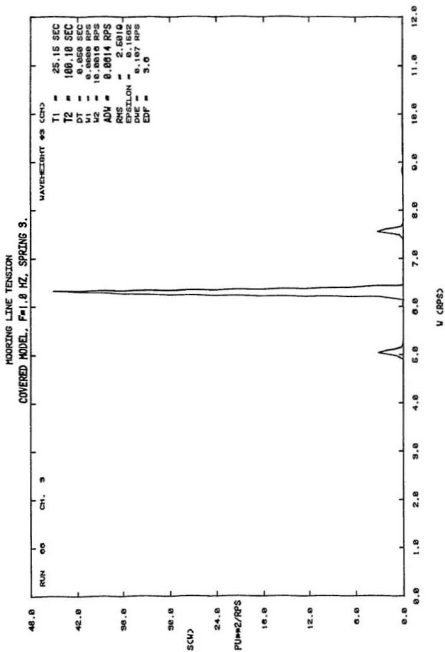


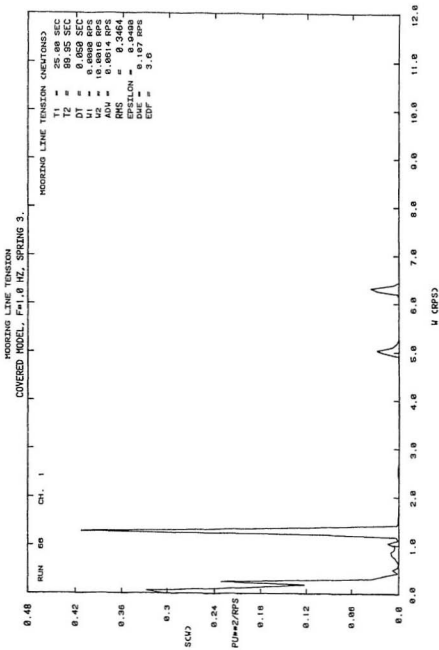


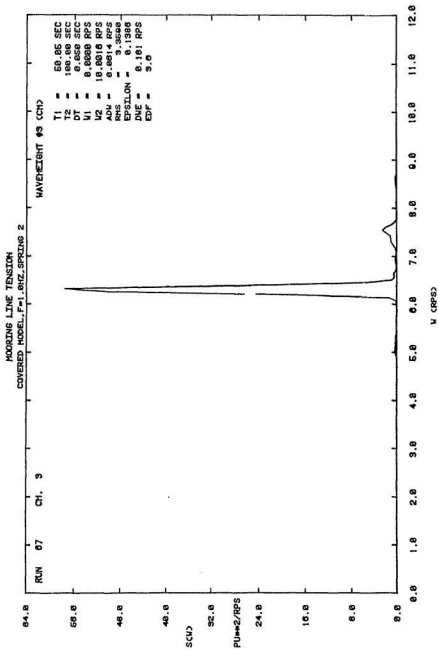
HOOBINS LINE TENSION
COVERED MODEL., F=0.8 HZ, SPRING 3.

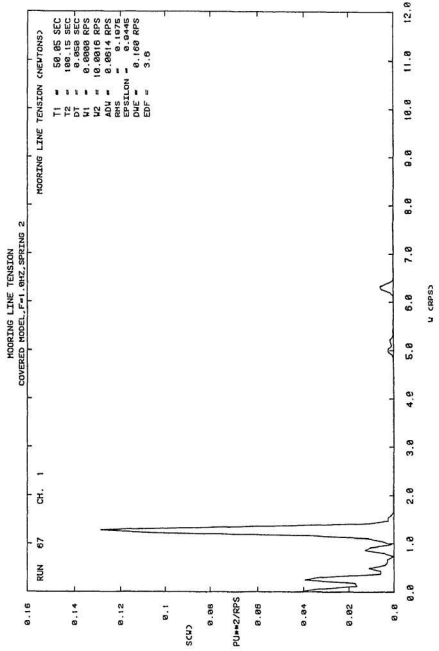


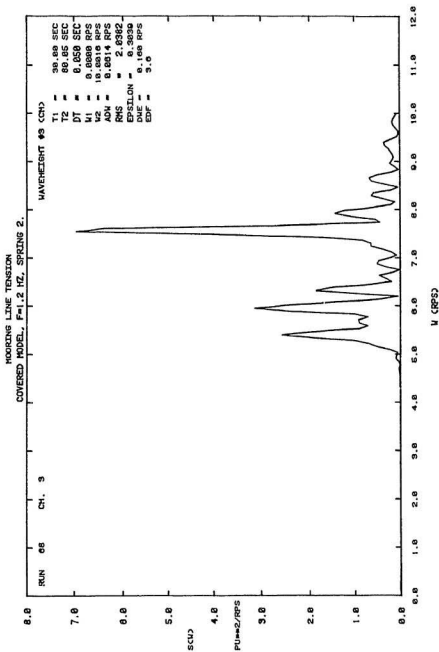


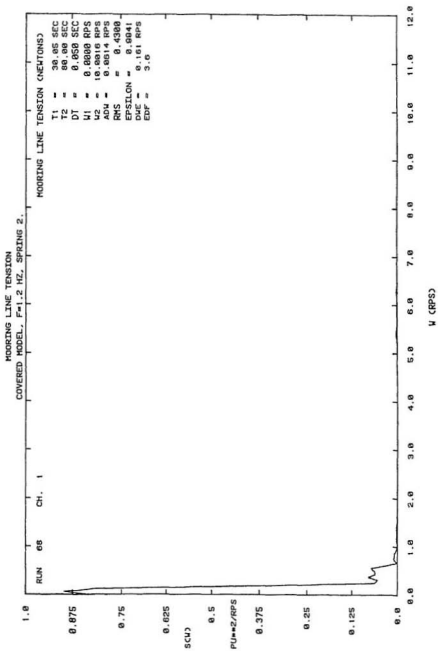


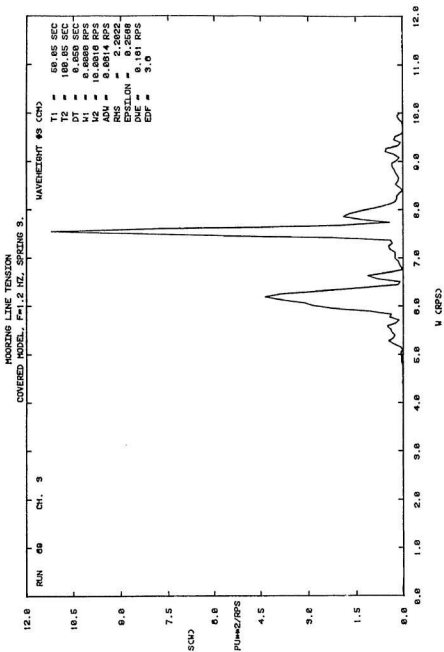




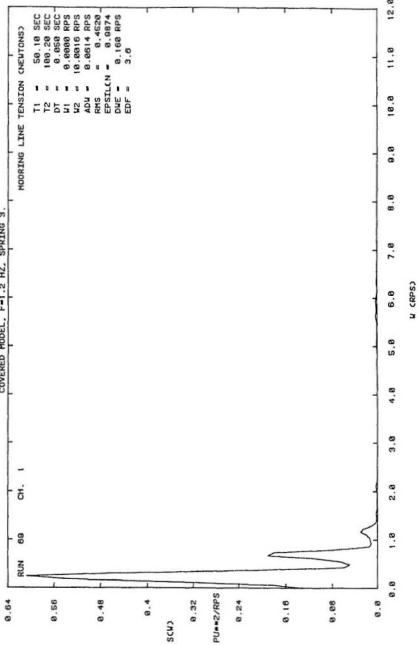


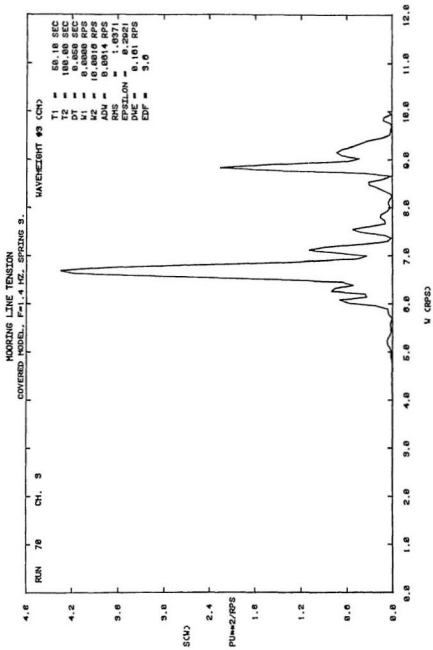


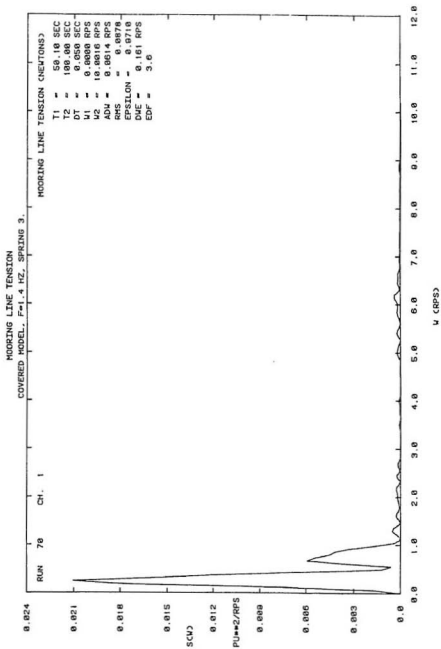


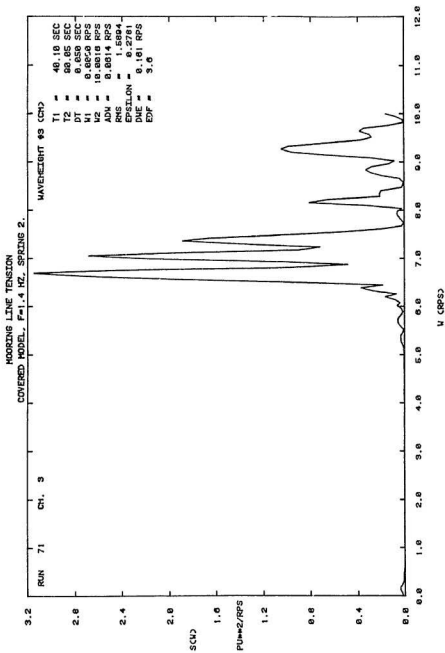


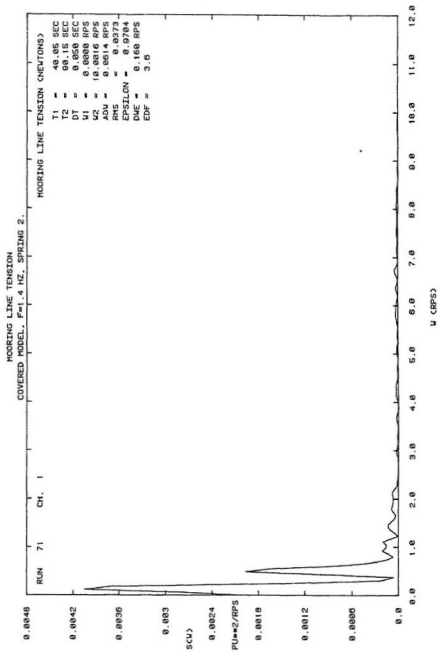
HOORING LINE TENSION
COVERED MODEL, F=1.2 HZ, SPRING 3.











APPENDIX D

PROGRAM LISTINGS: DPORT2.FOR AND OUTPORT2.FOR

```

DATA NSP/115/
DIMENSION PAN(115,3),UN(115,3),UNN(115,3),SUR(115),
1 DG11R(115,115),DG11I(115,115),DG12R(115,115),DG12I(115,115),
2 G11R(115,115),G11I(115,115),G12R(115,115),G12I(115,115),
3 PHI7R(115),PHI7I(115),PHI8R(115),PHI8I(115),QDF1(230),
3 QDF2(230),PT(100),
4 P0135(230,4),P0T246(230,4),Q135(230,4),Q246(230,4),
5 AM(6,6),DEMP(6,6),RM(6,6),C(6,6),FOR(12),AMP(12)
DIMENSION DA(230,230),DN(230,4),TTUN(115,6),P01R(115),P01I(115),
1 P02R(115),P02I(115),TPR(115,6),TPI(115,6),
2 VA(3),VB(3),VC(3),VD(3),VE(3),VF(3)

COMMON /C2/ GRAV,DEN,FREQ,DEPTH,WNUM,ANU,HEAD
COMMON /C3/ VOL,XB,YB,ZB,AREA,AREAWP,XG,YG,ZG
COMMON /CC/ RI44,RI55,RI66
COMMON /SER/ UK(1000),GAMMA(1000),ALPHA
DATA GRAV,DEN/9.8,1000.0/
DATA XG,YG,ZG/0.0,0.0,-1.26/
DATA RI44,RI55,RI66/170.0,166.0,236.0/
DATA DEPTH,HEAD/500.0,240.0/

CALL ASSIGN(1,'PRNT1 2.DAT')
CALL ASSIGN(2,'COM 2.DAT')
OPEN(UNIT=4,FILE='DEBUG1.OUT',STATUS='NEW')
HEAD=HEAD/180.0*3.14159
CALL CHART(NSP,PAN,UN,UNN,SUR,C,RM)
PT(1)=10.5
PT(2)=10.8
PT(3)=11.7
PT(4)=11.9
PT(5)=12.7
PT(6)=12.9
PT(7)=13.5
PT(8)=13.6
PT(9)=14.1
PT(10)=14.25
PT(11)=16.0
PT(12)=16.5
PT(13)=17.25
PT(14)=17.5
PT(15)=19.0
PT(16)=21.25
PT(17)=22.0
PT(18)=22.5
PT(19)=23.0
PT(20)=23.4
PT(21)=23.6
PT(22)=24.0
PT(23)=24.6
PT(24)=25.0
PT(25)=25.6
PT(26)=26.2
PT(27)=26.4
PT(28)=26.6
PT(29)=27.0
PT(30)=27.4
PT(31)=27.6
PT(32)=28.0
PT(33)=28.5

```

```

PT(34)=-29.0
PT(35)=-30.0
PT(36)=-30.5
PT(37)=-31.5
PT(38)=-32.0
PT(39)=-32.5
PT(40)=-33.5
CALL PRNT1(NSP,PAN,UN,UNN,SUR,C,RM)
DO 17 KI=1,40
TT=PT(KI)
WRITE(4,*)'PERIOD=',TT
WNUM=4.0*3.14159*3.14159/(GRAV*TT*TT)
CALL LINR1(NSP,PAN,UN,SUR,DG11R,DG11I,DG12R,DG12I,G11R,G11I,
1      G12R,G12I)
CALL PHI78(NSP,PAN,UN,PHI7R,PHI7I,PHI8R,PHI8I)
CALL GINVER(NSP,2*NSP,UN,UNN,PHI7R,PHI7I,PHI8R,PHI8I,DA,DN,
1      DG11R,DG11I,DG12R,DG12I,Q135,Q246)
CALL POTEN(NSP,2*NSP,G11R,G11I,G12R,G12I,Q135,Q246,DA,
1      POT135,POT246)
CALL AMASS(NSP,2*NSP,UN,UNN,SUR,POT135,POT246,TPR,TPI,TTUN,
1      AM,DEMP)
CALL EXFOR(NSP,2*NSP,PAN,UN,UNN,SUR,POT135,POT246,TTUN,P01R,
1      P01I,P02R,P02I,FOR)
CALL AMPL(AM,DEMP,RM,C,FOR,AMP)
CALL QTOTAL(NSP,2*NSP,Q135,Q246,AMP,QDF1,QDF2)
CALL DRIFT(NSP,2*NSP,PAN,SUR,QDF1,QDF2,DRIFX,DRIFY,DRMZ)
WRITE (2) PAN,SUR,FOR,AMP,AM,DEMP,C,RM,
1      GRAV,DEN,FREQ,DEPTH,WNUM,ANU,HEAD,DRIFX,DRIFY,DRMZ
17 CONTINUE
CLOSE(UNIT=4)
STOP
END

SUBROUTINE CHART(NSP,PAN,UN,UNN,SUR,C,RM)
C...COMPUTE THE CHARACTERISTICS OF THE FLOATING BODY
C...OUTPUT: PAN,UN,UNN,SUR,C; ALSO VOL, XB, AREA, AREAWP IN /C3/
DIMENSION PAN(NSP,3),UN(NSP,3),UNN(NSP,3),SUR(NSP),
1      C(6,6),RM(6,6)
DIMENSION VA(3),VB(3),VC(3),VD(3),VE(3),VF(3)
COMMON /C2/ GRAV,DEN,FREQ,DEPTH,WNUM,ANU,HEAD
COMMON /C3/ VOL,XB,YB,ZB,AREA,AREAWP,XG,YG,ZG
COMMON /CC/ RI44,RI55,RI66
CALL ASSIGN(5,'DELTA1_2.DAT')
N=NSP
DO 10 J=1,N
READ(5,*)X,Y,Z,UN1,UN2,UN3,S
TYPE*,X,Y,Z,UN1,UN2,UN3,S,J
PAN(J,1)=X
PAN(J,2)=Y
PAN(J,3)=Z
UN(J,1)=UN1
UN(J,2)=UN2
UN(J,3)=UN3
SUR(J)=S
10 CONTINUE
XB=0.0
YB=0.0
ZB=0.0
AREA=0.0

```

```

AREAWP=0.0
VOL=0.0
TEMP2=0.0
TEMP3=0.0
TEMP4=0.0
DO 40 I=1,NSP
VA(1)=PAN(I,1)
VA(2)=PAN(I,2)
VA(3)=PAN(I,3)
UNN(I,1)=VA(2)*UN(I,3)-VA(3)*UN(I,2)
UNN(I,2)=VA(3)*UN(I,1)-VA(1)*UN(I,3)
UNN(I,3)=VA(1)*UN(I,2)-VA(2)*UN(I,1)
VB(1)=UN(I,1)
VB(2)=UN(I,2)
VB(3)=UN(I,3)
CALL VDOT(VA,VB,TEMP1)
VOL=VOL+TEMP1*SUR(I)
XB=XB+VA(1)*VA(1)*VB(1)*SUR(I)
ZB=ZB+VA(3)*VA(3)*VB(3)*SUR(I)
AREA=AREA+SUR(I)
TEMP=VB(3)*SUR(I)
AREAWP=(AREAWP+TEMP)
TEMP2=TEMP2+VA(1)*TEMP
TEMP3=TEMP3+VA(1)*VA(1)*TEMP
TEMP4=TEMP4+VA(2)*VA(2)*TEMP
40 CONTINUE
DO 45 I=1,6
DO 45 J=1,6
C(I,J)=0.0
45 CONTINUE
VOL=2.0*(VOL/3.0)
C VOL=1200000.0
TYPE*, 'VOLUME', VOL
XB=XB/VOL
ZB=ZB/VOL
C XB=0.0
C ZB=-4.7
AREA=2.0*AREA
TYPE*, 'AREA', AREA
C AREAWP=-2.0*AREAWP*0.55
AREAWP=-2.0*AREAWP
TYPE*, 'AREAWP', AREAWP
TEMP=DEN*GRAV
C(1,1)=1804000
C(3,3)=TEMP*AREAWP
C(3,5)=0.55*(TEMP*2.0*TEMP2)
C(5,3)=C(3,5)
C(4,4)=TEMP*(VOL*(ZB-ZG)-2.0*TEMP4*0.55)
C(5,5)=TEMP*(VOL*(ZB-ZG)-2.0*TEMP3*0.55)
C(3,3)=TEMP*AREAWP
C(3,5)=(TEMP*2.0*TEMP2)
C(5,3)=C(3,5)
C(4,4)=TEMP*(VOL*(ZB-ZG)-2.0*TEMP4)
C(5,5)=TEMP*(VOL*(ZB-ZG)-2.0*TEMP3)
RM(1,1)=DEN*VOL
RM(2,2)=DEN*VOL
RM(3,3)=DEN*VOL
RM(4,4)=DEN*VOL*RI44*RI44
RM(5,5)=DEN*VOL*RI55*RI55
RM(6,6)=DEN*VOL*RI66*RI66

```

```

RM(1,5)=DEN*VOL*ZG
RM(5,1)=RM(1,5)
RM(2,4)=-DEN*VOL*ZG
RM(4,2)=RM(2,4)
RETURN
END

SUBROUTINE PRNT1(NSP,PAN,UN,UNN,SUR,C,RM)

DIMENSION PAN(NSP,3),UN(NSP,3),UNN(NSP,3),SUR(NSP),
1      C(6,6),RH(6,6)
COMMON /C2/ GRAV,DEN,FREQ,DEPTH,WNUM,ANU,HEAD
COMMON /C3/ VOL,XB,YB,ZB,AREA,AREAWP,XG,YG,ZG

WRITE(1,*)'DATA FOR TRIANGULAR MODEL'
WRITE(1,*)' '
WRITE(1,*)'VOL= ',VOL
WRITE(1,*)'AREA= ',AREA
WRITE(1,*)'CENTROID XB,YB,ZB : ',XB,YB,ZB
WRITE(1,*)'CENTER OF GRAVITY XG,YG,ZG : ',XG,YG,ZG
WRITE(1,*)'AREAWP= ',AREAWP
WRITE(1,*)'C(3,3)=',C(3,3)
WRITE(1,*)'PAN(I,K)'
DO 40 I=1,NSP
  WRITE(1,100) I,(PAN(I,K),K=1,3)
40 CONTINUE
WRITE(1,*)'UN(I,K)'
DO 50 I=1,NSP
  WRITE(1,500) I,(UN(I,K),K=1,3)
50 CONTINUE
WRITE(1,*)'UNN(I,K)'
DO 51 I=1,NSP
  WRITE(1,500) I,(UNN(I,K),K=1,3)
51 CONTINUE
WRITE(1,*)'SUR(I)'
DO 60 I=1,NSP
  WRITE(1,600) I,SUR(I)
60 CONTINUE
100  FORMAT(1X,'(',I3,'):',3F13.6)
500  FORMAT(1X,'(',I3,'):',3F13.6)
600  FORMAT(1X,'(',I3,'):',F13.6)
700  FORMAT(1X,6E14.5)
WRITE(1,*)'RESTORING COEFFICIENT'
DO 21 I=1,6
  WRITE(1,700) (C(I,J),J=1,6)
21 CONTINUE
WRITE(1,*)' '
WRITE(1,*)'REAL MASS MATRIX'
DO 22 I=1,6
  WRITE(1,700) (RM(I,J),J=1,6)
22 CONTINUE
CALL CLOSE (1)
RETURN
END

SUBROUTINE LINK1(N,PAN,UN,SUR,DG11R,DG11I,DG12R,DG12I,
1      G11R,G11I,G12R,G12I)
C...THIS PROGRAM COMPUTES THE ELEMENTS OF GREEN'S FUNCTION MATRIX
C...INPUT:N,PAN,UN,SUR

```

```

C...OUTPUT:DG11R,DG11I,DG12R,DG12I,G11R,G11I,G12R,G12I
DIMENSION PAN(N,3),UN(N,3),SUR(N)
DIMEX ...ON DG11R(N,N),DG11I(N,N),DG12R(N,N),DG12I(N,N),
1      G11R(N,N),G11I(N,N),G12R(N,N),G12I(N,N)

DIMENSION G(2),DGX(2),DGY(2),DGZ1(2),DGZ2(2),VA(3),VB(3),VC(3)
COMMON /C2/ GRAV,DEN,FREQ,DEPTH,WNUM,ANU,HEAD
COMMON /SER/ UK(1000),GAMMA(1000),ALPHA

ANU=WNUM*TANH(WNUM*DEPTH)
FREQ=SQRT(GRAV*ANU)
CALL ROOTUK(1000)
ALPHA=6.283185/(4.0*DEPTH*EXP(-2.0*WNUM*DEPTH)+ANU*
1      (1.0+EXP(-2.0*WNUM*DEPTH))/WNUM)**2.0)
DO 10 I=1,N
VA(1)=PAN(I,1)
VA(2)=PAN(I,2)
VA(3)=PAN(I,3)
DO 20 J=I,N
VB(1)=PAN(J,1)
VB(2)=PAN(J,2)
VB(3)=PAN(J,3)
CALL VSUB(VA,VB,VC)
IF(I .EQ. J)GO TO 11
R1=SQRT(VC(1)*VC(1)+VC(2)*VC(2))
IF(R1 .EQ. 0.0)GO TO 11
TEMP=2.0+10.0*DEPTH/(3.1416*R1)
IF(TEMP .GT. 1000.)GO TO 11
NTERM=TEMP

CALL GS2(VA,VB,G,DGX,DGY,DGZ1,DGZ2,NTERM)
GO TO 12
11  UMAX=-10.0/(VA(3)+VB(3))

12  CALL GI2(VA,VB,G,DGX,DGY,DGZ1,DGZ2,UMAX)
CONTINUE
G11R(I,J)=G(1)
G11I(I,J)=G(2)
DG11R(I,J)=DGX(1)*UN(I,1)+DGY(1)*UN(I,2)+(DGZ1(1)+DGZ2(1))
1      *UN(I,3)
DG11I(I,J)=DGX(2)*UN(I,1)+DGY(2)*UN(I,2)+(DGZ1(2)+DGZ2(2))
1      *UN(I,3)
IF (I .EQ. J)GO TO 20
G11R(J,I)=G(1)
G11I(J,I)=G(2)
DG11R(J,I)=-DGX(1)*UN(J,1)-DGY(1)*UN(J,2)+(DGZ1(1)-DGZ2(1))
1      *UN(J,3)
DG11I(J,I)=-DGX(2)*UN(J,1)-DGY(2)*UN(J,2)+(DGZ1(2)-DGZ2(2))
1      *UN(J,3)
20  CONTINUE
DO 30 J=I,N
VB(1)=PAN(J,1)
VB(2)=-PAN(J,2)
VB(3)=PAN(J,3)
CALL VSUB(VA,VB,VC)
R1=SQRT(VC(1)*VC(1)+VC(2)*VC(2))
TEMP=2.0+10.0*DEPTH/(3.1416*R1)
IF(TEMP .GT. 1000.) GO TO 31
NTERM=TEMP
NSER=NSER+1

```

```

CALL GS2(VA,VB,G,DGX,DGY,DGZ1,DGZ2,NTERM)
GO TO 32
31 UMAX=-10.0/(VA(3)+VB(3))
   NINTEG=NINTEG+1

CALL G12(VA,VB,G,DGX,DGY,DGZ1,DGZ2,UMAX)
32 CONTINUE
   G12R(I,J)=G(1)
   G12I(I,J)=G(2)
   DG12R(I,J)=DGX(1)*UN(I,1)+DGY(1)*UN(I,2)+(DGZ1(1)+DGZ2(1))
   1 *UN(I,3)
   DG12I(I,J)=DGX(2)*UN(I,1)+DGY(2)*UN(I,2)+(DGZ1(2)+DGZ2(2))
   1 *UN(I,3)
   IF(I .EQ. J)GO TO 30
   G12R(J,I)=G(1)
   G12I(J,I)=G(2)
   DG12R(J,I)=-DGX(1)*UN(J,1)+DGY(1)*UN(J,2)+(DGZ1(1)-DGZ2(1))
   1 *UN(J,3)
   DG12I(J,I)=-DGX(2)*UN(J,1)+DGY(2)*UN(J,2)+(DGZ1(2)-DGZ2(2))
   1 *UN(J,3)
30 CONTINUE
10 CONTINUE
C...COMBINE DG11 AND DG12 TO BE DG11 FOR DG135 MODE,
C...AND DG12 FOR DG246 MODE
   DO 40 I=1,N
   DO 40 J=1,N
   TEMP1=DG11R(I,J)+DG12R(I,J)
   TEMP2=DG11I(I,J)+DG12I(I,J)
   TEMP3=DG11R(I,J)-DG12R(I,J)
   TEMP4=DG11I(I,J)-DG12I(I,J)
   DG11R(I,J)=TEMP1*SUR(J)
   DG11I(I,J)=TEMP2*SUR(J)
   DG12R(I,J)=TEMP3*SUR(J)
   DG12I(I,J)=TEMP4*SUR(J)
40 CONTINUE
C...ADDING THE DIAGONAL TERM OF DG MATRIX
   DO 50 I=1,N
   DG11R(I,I)=DG11R(I,I)-6.28318
   DG12R(I,I)=DG12R(I,I)-6.28318
50 CONTINUE
C...COMBINE G11 AND G12 TO BE G11 FOR G135 MODE,AND G12 FOR G246 MODE
   DO 60 I=1,N
   DO 60 J=1,N
   TEMP1=G11R(I,J)+G12R(I,J)
   TEMP2=G11I(I,J)+G12I(I,J)
   TEMP3=G11R(I,J)-G12R(I,J)
   TEMP4=G11I(I,J)-G12I(I,J)
   G11R(I,J)=TEMP1*SUR(J)
   G11I(I,J)=TEMP2*SUR(J)
   G12R(I,J)=TEMP3*SUR(J)
   G12I(I,J)=TEMP4*SUR(J)
60 CONTINUE
C...ADDING THE DIAGONAL TERM OF G MATRIX
   DO 70 I=1,N
   TEMP=2.0*SQRT(SUR(I))*3.14159
   G11R(I,I)=G11R(I,I)+TEMP
   G12R(I,I)=G12R(I,I)+TEMP
70 CONTINUE
   RETURN

```

END

SUBROUTINE PHI78(N,PAN,UN,PHI7R,PHI7I,PHI8R,PHI8I)
 C... THIS PROGRAM CALCULATE THE PHI7:SYMMETRIC PART,PHI8:ANTI-SYM PART
 DIMENSION PAN(N,3),UN(N,3)
 DIMENSION PHI7R(N),PHI7I(N),PHI8R(N),PHI8I(N)
 COMMON /C2/ GRAV,DEN,FREQ,DEPTH,WNUM,ANU,HEAD

APHI=GRAV/(FREQ*(1.0+EXP(-2.0*WNUM*DEPTH)))
 AK1=WNUM*COS(HEAD)
 AK2=WNUM*SIN(HEAD)
 DO 10 I=1,N
 V1=PAN(I,1)
 V2=PAN(I,2)
 V3=PAN(I,3)
 XK1=V1*AK1
 YK2=V2*AK2
 ZH=V3+DEPTH
 XN=UN(I,1)
 YN=UN(I,2)
 ZN=UN(I,3)
 TEMPA=APHI*EXP(WNUM*V3)*(1.0+EXP(-2.0*WNUM*ZH))
 TEMPB=APHI*EXP(WNUM*V3)*(1.0-EXP(-2.0*WNUM*ZH))
 ARNX=TEMPA*AK1*XN
 ARNY=TEMPA*AK2*YN
 ARNZ=TEMPB*WNUM*ZN
 CY2=COS(YK2)
 SY2=SIN(YK2)
 CX1=COS(XK1)
 SX1=SIN(XK1)
 PHI7R(I)=-(-ARNX*CY2*SX1-ARNY*SY2*CX1+ARNZ*CY2*CX1)
 PHI7I(I)=-(- ARNX*CY2*CX1-ARNY*SY2*SX1+ARNZ*CY2*SX1)
 PHI8R(I)=-(-ARNX*SY2*CX1-ARNY*CY2*SX1-ARNZ*SY2*SX1)
 PHI8I(I)=-(-ARNX*SY2*SX1+ARNY*CY2*CX1+ARNZ*SY2*CX1)
 10 CONTINUE
 RETURN
 END

SUBROUTINE GINVER(N,NN,UN,UNN,PHI7R,PHI7I,PHI8R,PHI8I,DA,DN,
 1 DG135R,DG135I,DG246R,DG246I,Q135,Q246)
 C... THIS PROGRAM COMPUTES THE INVERSE OF MATRIX DG AND SOURCE Q
 C... INPUT:N,NN,UN,UNN,PHI, DG135,DG246
 C... OUTPUT:Q135,Q246
 C... DA AND DN IS FOR TEMPERARY USE,NN=2*N=2*NSP

DIMENSION UN(N,3),UNN(N,3),PHI7R(N),PHI7I(N),PHI8R(N),PHI8I(N),
 1 DG135R(N,N),DG135I(N,N),DG246R(N,N),DG246I(N,N),
 2 DA(NN,NN),DN(NN,4)
 DIMENSION Q135(NN,4),Q246(NN,4)

C... FORMATION OF THE REAL MATRIX DA*Q=UN FOR THE SYMMETRIC P/VT
 DO 10 I=1,N
 DN(I,1)=UN(I,1)
 DN(I,2)=UN(I,3)
 DN(I,3)=UNN(I,2)
 DN(I,4)=PHI7R(I)
 DN(I+N,1)=0.0
 DN(I+N,2)=0.0
 DN(I+N,3)=0.0
 DN(I+N,4)=PHI7I(I)

```

DO 10 J=1,N
DA(I,J)=DG135R(I,J)
DA(I+N,J)=+DG135I(I,J)
DA(I,J+N)=-DG135I(I,J)
DA(I+N,J+N)=DG135R(I,J)
10 CONTINUE
C...SOLVING Q BY INVERSION A*X=R, A:(M*M),R:(M*N),X(M*N) STORED IN R
CALL INV(DN,DA,NN,4)
DO 20 I=1,NN
DO 20 J=1,4
Q135(I,J)=DN(I,J)
20 CONTINUE
C...SOLVING Q246 (ANTISYMMETRIC PART)BY THE SIMILAR PROCESS AS ABOVE
DO 30 I=1,N
DN(I,1)=UN(I,2)
DN(I,2)=UNN(I,1)
DN(I,3)=UNN(I,3)
DN(I,4)=PHI8R(I)
DN(I+N,1)=0.0
DN(I+N,2)=0.0
DN(I+N,3)=0.0
DN(I+N,4)=PHI8I(I)
DO 30 J=1,N
DA(I,J)=DG246R(I,J)
DA(I+N,J)=+DG246I(I,J)
DA(I,J+N)=-DG246I(I,J)
DA(I+N,J+N)=DG246R(I,J)
30 CONTINUE
CALL INV(DN,DA,NN,4)
DO 40 I=1,NN
DO 40 J=1,4
Q246(I,J)=DN(I,J)
40 CONTINUE
RETURN
END

SUBROUTINE POTEN(N,NN,G135R,G135I,G246R,G246I,Q135,Q246,DA,
1 POT135,POT246)
C...COMPUTE THE POTENTIAL
C...INPUT:N,NN,G135,G246,Q135,Q246
C...OUTPUT:POT135,POT246
C...DA IS FOR TEMPERARY USE
DIMENSION G135R(N,N),G135I(N,N),G246R(N,N),G246I(N,N),Q135(NN,4),
1 Q246(NN,4),DA(NN,NN)
DIMENSION POT135(NN,4),POT246(NN,4)

DO 10 I=1,N
DO 10 J=1,N
DA(I,J)=G135R(I,J)
DA(I+N,J)=G135I(I,J)
DA(I,J+N)=-G135I(I,J)
DA(I+N,J+N)=G135R(I,J)
10 CONTINUE
CALL MPRD(DA,Q135,POT135,NN,NN,4)
DO 20 I=1,N
DO 20 J=1,N
DA(I,J)=G246R(I,J)
DA(I+N,J)=G246I(I,J)
DA(I,J+N)=-G246I(I,J)
DA(I+N,J+N)=G246R(I,J)

```

```

20  CONTINUE
    CALL MPRD(DA,Q246,POT246,NN,NN,4)
    RETURN
    END

    SUBROUTINE AMASS(N,NN,UN,UNN,SUR,POT135,POT246,TPR,TPI,TTUN,
1      AM,DEMP)
C... COMPUTE THE ADDED MASS AND DEMPING COEFFICIENT
C... INPUT:N,NN,UN,UNN,SUR,POT135,POT246
C... OUTPUT:AM,DEMP
C... TPR,TPI,TTUN IS FOR TEMPERARY USE
    DIMENSION UN(N,3),UNN(N,3),SUR(N),POT135(NN,4),POT246(NN,4),
1      TPR(N,6),TPI(N,6),TTUN(N,6),AM(6,6),DEMP(6,6)
    COMMON /C2/ GRAV,DEN,FREQ,DEPTH,WNUM,ANU,HEAD

    DO 5 I=1,N
    DO 5 K=1,3
    TTUN(I,K)=UN(I,K)
    TTUN(I,K+3)=UNN(I,K)
5    CONTINUE
    DO 10 J=1,N
    JJ=J+N
    DO 10 K=1,3
    TPR(J,2*K-1)=POT135(J,K)
    TPR(J,2*K) =POT246(J,K)
    TPI(J,2*K-1)=POT135(JJ,K)
    TPI(J,2*K) =POT246(JJ,K)
10   CONTINUE
    DO 20 J=1,5,2
    JJ=J+1
    DO 20 K=1,5,2
    KK=K+1
    S1R=0.0
    S1I=0.0
    S2R=0.0
    S2I=0.0
    DO 25 I=1,N
    S1R=S1R+TPR(I,J)*TTUN(I,K)*SUR(I)
    S1I=S1I+TPI(I,J)*TTUN(I,K)*SUR(I)
    S2R=S2R+TPR(I,JJ)*TTUN(I,KK)*SUR(I)
    S2I=S2I+TPI(I,JJ)*TTUN(I,KK)*SUR(I)
25   CONTINUE
    AM(J,K)   =-2.0*DEN*S1R
    AM(JJ,KK) =-2.0*DEN*S2R
    DEMP(J,K) =-2.0*DEN*FREQ*S1I
    DEMP(JJ,KK)=-2.0*DEN*FREQ*S2I
20   CONTINUE
    RETURN
    END

    SUBROUTINE EXFOR(N,NN,PAN,UN,UNN,SUR,POT135,POT246,TTUN,P01R,P01I,
1      P02R,P02I,FOR)
C... COMPUTE THE EXCITING FORCE
C... INPUT:N,UN,UNN,SUR,POT135,POT246
C... OUTPUT:FOR
C... TTUN,P01R,P01I,P02R,P02I IS FOR TEMPERARY USE
    DIMENSION PAN(N,3),UN(N,3),UNN(N,3),SUR(N),POT135(NN,4),POT246(NN,4),
1      TTUN(N,6),P01R(N),P01I(N),P02R(N),P02I(N),FOR(12)
    COMMON /C2/ GRAV,DEN,FREQ,DEPTH,WNUM,ANU,HEAD

```

```

DO 5 I=1,N
DO 5 K=1,3
TTUN(I,K)=UN(I,K)
TTUN(I,K+3)=UNN(I,K)
5 CONTINUE
DO 10 I=1,5,2
II=I+1
S7R=0.0
S7I=0.0
S8R=0.0
S8I=0.0
DO 20 J=1,N
JJ=J+N
S7R=S7R+POT135(J,4) *TTUN(J,I)*SUR(J)
S7I=S7I+POT135(JJ,4)*TTUN(J,I)*SUR(J)
S8R=S8R+POT246(J,4) *TTUN(J,II)*SUR(J)
S8I=S8I+POT246(JJ,4)*TTUN(J,II)*SUR(J)
20 CONTINUE
TEMP=2.0*FREQ*DEN
FOR(I) =TEMP*S7R
FOR(II)=TEMP*S8R
FOR(I+6) =TEMP*S7I
FOR(II+6)=TEMP*S8I
10 CONTINUE
APHI=GRAV/(FREQ*(1.0+EXP(-2.0*WNUM*DEPTH)))
AK1=WNUM*COS(HEAD)
AK2=WNUM*SIN(HEAD)
DO 30 J=1,N
X=PAN(J,1)
Y=PAN(J,2)
Z=PAN(J,3)
TEMP1=APHI*EXP(WNUM*Z)*(1.0+EXP(-2.0*WNUM*(Z+DEPTH)))*SUR(J)
TEMP2=AK1*X+AK2*Y
TEMP3=AK1*X-AK2*Y
P01R(J)=TEMP1*COS(TEMP2)
P01I(J)=TEMP1*SIN(TEMP2)
P02R(J)=TEMP1*COS(TEMP3)
P02I(J)=TEMP1*SIN(TEMP3)
30 CONTINUE
DO 40 I=1,6
II=I+6
SR=0.0
SI=0.0
TB=1.0
IF( (I/2)*2 .EQ. I) TB=-1.0
DO 50 J=1,N
SR=SR+P01R(J)*TTUN(J,I)+TB*P02R(J)*TTUN(J,I)
SI=SI+P01I(J)*TTUN(J,I)+TB*P02I(J)*TTUN(J,I)
50 CONTINUE
FOR(I)=FOR(I)+FREQ*DEN*SR
FOR(II)=FOR(II)+FREQ*DEN*SI
TEMP=FOR(I)
FOR(I)=+FOR(II)
FOR(II)=-TEMP
40 CONTINUE
RETURN
END

```

SUBROUTINE AMPL(AM,DEMP,RM,C,FOR,AMP)
C...COMPUTE THE RESPONSE AMPLITUDE

```

C...INPUT:AM,DEMP,RM,C,FOR
C...OUTPUT:AMP
C...DC AND DF IS FOR TEMPORARY USE
  DIMENSION AM(6,6),DEMP(6,6),RM(6,6),C(6,6),FOR(12),AMP(12),
  1      DC(12,12),DF(12)
  COMMON /C2/ GRAV,DEN,FREQ,DEPTH,WNUM,ANU,HEAD

  DO 10 I=1,6
  II=I+6
  DF(I)=FOR(I)
  DF(II)=FOR(II)
  DO 10 J=1,6
  JJ=J+6
  TEMP1=-FREQ*FREQ*(AM(I,J)+RM(I,J))+C(I,J)
  TEMP2=-FREQ*DEMP(I,J)
  DC(I,J)= TEMP1
  DC(II,JJ)=TEMP1
  DC(II,J)=-TEMP2
  DC(I,JJ)=-TEMP2
10  CONTINUE
  CALL INV(DF,DC,12,1)
  DO 20 I=1,12
  IF ((I.EQ.1).OR.(I.EQ.7)) GOTO 15
  IF ((I.EQ.3).OR.(I.EQ.9)) GOTO 15
  IF ((I.EQ.5).OR.(I.EQ.11)) GOTO 15
  AMP(I)=0.0
  GOTO 20
15  AMP(I)=DF(I)
20  CONTINUE
  RETURN
  END

  SUBROUTINE GI2(VX,VXX,G,DGX,DGY,DGZ1,DGZ2,UMAX)
  EXTERNAL FG1,FGE,FGX1,FGXE,FGZ11,FGZ1E,FGZ21,FGZ2E
  DIMENSION VX(3),VXX(3),G(2),DGX(2),DGY(2),DGZ1(2),DGZ2(2)
  COMMON /C2/ GRAV,DEN,FREQ,DEPTH,WNUM,ANU,HEAD
  COMMON /SER/ UK(1000),GAMMA(1000),ALPHA
  COMMON /G1/ ZH,ZZH,R1

C....THIS PROGRAM CALCULATE THE GREEN'S FUNCTION BY INTEGRAL FORM
C....F1 IS THE INTEGRAND; FE IS THE SYMMETRIC PART OF THE INTEGRAND
F21(X)=X*(EXP(X*(ZH+ZZH-2.0*DEPTH))-EXP(-X*(ZH+ZZH+2.0*DEPTH)))
F22(X)=X*(EXP(-X*(ZH-ZH+2.0*DEPTH))-EXP(-X*(ZH-ZZH+2.0*DEPTH)))
TEMP1=VX(1)-VXX(1)
TEMP2=VX(2)-VXX(2)
TEMP3=VX(3)-VXX(3)
R1=SQRT(TEMP1*TEMP1+TEMP2*TEMP2)
IF (R1 .LE. 1.0E-6) R1=0.0
TEMP4=R1*WNUM
ZH=VX(3)+DEPTH
ZZH=VXX(3)+DEPTH
R=SQRT(R1*R1+TEMP3*TEMP3)
IF (R .LE. 1.0E-6) R=0.0
R2H=SQRT(R1*R1+(ZH+ZZH)*(ZH+ZZH))
BJ0=BJ(TEMP4,0)
BJ1=BJ(TEMP4,1)
EZH=EXP(-2.0*WNUM*ZH)
EZZH=EXP(-2.0*WNUM*ZZH)
G(1)=1.0/R2H
IF (R .NE. 0.0)G(1)=G(1)+1.0/R
G(2)=ALPHA*(1.0+EZH)*(1.0+EZZH)*BJ0*EXP(WNUM*(VX(3)+VXX(3)))

```

```

DGX(1)=-1.0/R2H**3.0
IF(R .NE. 0.0)DGX(1)=DGX(1)-1.0/R**3.0
IF(R1 .EQ. 0.0) GO TO 1
DGX(2)=-ALPHA*(1.0+EZH)*(1.0+EZZH)*EXP(WNUM*(VX(3)+VXX(3)))
1 *BJ(TEMP4,1)*WNUM/R1
GO TO 2
1 DGX(2)=-ALPHA*(1.0+EZH)*(1.0+EZZH)*EXP(WNUM*(VX(3)+VXX(3)))
1 *0.5*WNUM*WNUM
2 DGZ1(1)=-((ZH+ZHZ)/R2H**3.0
DGZ1(2)=-ALPHA*FZ1(WNUM)*BJ0
DGZ2(1)=0.0
IF(R .NE. 0.0)DGZ2(1)=DGZ2(1)-(ZH-ZZH)/R**3.0
DGZ2(2)=-ALPHA*FZ2(WNUM)*BJ0
UINT=0.01*WNUM
CALL DG16(UINT,WNUM,FGE,SMG1)
CALL DG16(2.0*WNUM,UMAX,FG1,SMG2)
G(1)=G(1)+SMG1+SMG2+UINT*FGE(UINT)
CALL DG16(UINT,WNUM,FGXE,SMG1)
CALL DG16(2.0*WNUM,UMAX,FGX1,SMG2)
DGX(1)=DGX(1)+SMG1+SMG2+UINT*FGXE(UINT)
CALL DG16(UINT,WNUM,FGZ1E,SMG1)
CALL DG16(2.0*WNUM,UMAX,FGZ11,SMG2)
DGZ1(1)=DGZ1(1)+SMG1+SMG2+UINT*FGZ1E(UINT)
CALL DG16(UINT,WNUM,FGZ2E,SMG1)
CALL DG16(2.0*WNUM,UMAX,FGZ21,SMG2)
DGZ2(1)=DGZ2(1)+SMG1+SMG2+UINT*FGZ2E(UINT)
DGY(1)=DGX(1)*TEMP2
DGY(2)=DGX(2)*TEMP2
DGX(1)=DGX(1)*TEMP1
DGX(2)=DGX(2)*TEMP1
RETURN
END

FUNCTION FG1(X)
COMMON /C2/ GRAV,DEN,FREQ,DEPTH,WNUM,ANU,HEAD
COMMON /G1/ ZH,ZZH,R1
B=1.0/((X-ANU)/(X+ANU)-EXP(-2.0*X*DEPTH))
FG1=B*EXP(X*(ZH+ZZH-2.0*DEPTH))*(1.0+EXP(-2.0*X*ZH))*
1 (1.0+EXP(-2.0*X*ZZH))*BJ(X*R1,0)
RETURN
END

FUNCTION FGE(X)
COMMON /C2/ GRAV,DEN,FREQ,DEPTH,WNUM,ANU,HEAD
COMMON /G1/ ZH,ZZH,R1
FGE=FG1(X+WNUM)+FG1(-X+WNUM)
RETURN
END

FUNCTION FGX1(X)
COMMON /C2/ GRAV,DEN,FREQ,DEPTH,WNUM,ANU,HEAD
COMMON /G1/ ZH,ZZH,R1
B=-1.0/((X-ANU)/(X+ANU)-EXP(-2.0*X*DEPTH))
1 *EXP(X*(ZH+ZZH-2.0*DEPTH))*(1.0+EXP(-2.0*X*ZH))*
2 (1.0+EXP(-2.0*X*ZZH))
IF (R1 .EQ. 0.0) GO TO 10
FGX1=B*BJ(X*R1,1)*X/R1
RETURN
10 FGX1=B*0.5*X*X
RETURN

```

END

```

FUNCTION FGXE(X)
COMMON /C2/ GRAV,DEN,FREQ,DEPTH,WNUM,ANU,HEAD
COMMON /G1/ ZH,ZZH,R1
FGXE=FGX1(X+WNUM)+FGX1(-X+WNUM)
RETURN
END

```

```

FUNCTION FGZ11(X)
COMMON /C2/ GRAV,DEN,FREQ,DEPTH,WNUM,ANU,HEAD
COMMON /G1/ ZH,ZZH,R1
B=1.0/((X-ANU)/(X+ANU)-EXP(-2.0*X*DEPTH))
FGZ11=B*X*(EXP(X*(ZH+ZZH-2.0*DEPTH))-EXP(-X*(ZH+ZZH+2.0*DEPTH)))
1 *BJ(X*R1,0)
RETURN
END

```

```

FUNCTION FGZ1E(X)
COMMON /C2/ GRAV,DEN,FREQ,DEPTH,WNUM,ANU,HEAD
COMMON /G1/ ZH,ZZH,R1
FGZ1E=FGZ11(X+WNUM)+FGZ11(-X+WNUM)
RETURN
END

```

```

FUNCTION FGZ21(X)
COMMON /C2/ GRAV,DEN,FREQ,DEPTH,WNUM,ANU,HEAD
COMMON /G1/ ZH,ZZH,R1
B=1.0/((X-ANU)/(X+ANU)-EXP(-2.0*X*DEPTH))
FGZ21=B*X*(EXP(-X*(ZZH-ZH+2.0*DEPTH))-EXP(-X*(ZH-ZZH+2.0*DEPTH)))
1 *BJ(X*R1,0)
RETURN
END

```

```

FUNCTION FGZ2E(X)
COMMON /C2/ GRAV,DEN,FREQ,DEPTH,WNUM,ANU,HEAD
COMMON /G1/ ZH,ZZH,R1
FGZ2E=FGZ21(X+WNUM)+FGZ21(-X+WNUM)
RETURN
END

```

```

SUBROUTINE GS2(VX,VXX,G,DGX,DGY,DGZ1,DGZ2,NTERM)
DIMENSION VX(3),VXX(3),G(2),DGX(2),DGY(2),DGZ1(2),DGZ2(2)
COMMON /C2/ GRAV,DEN,FREQ,DEPTH,WNUM,ANU,HEAD
COMMON /SER/ UK(1000),GAMMA(1000),ALPHA
C.... THIS PROGRAM CALCULATE THE GREEN'S FUNCTION BY SERIES FORM
TEMP1=VX(1)-VXX(1)
TEMP2=VX(2)-VXX(2)
TEMP3=VX(3)-VXX(3)
R1=SQRT(TEMP1*TEMP1+TEMP2*TEMP2)
ZH=VX(3)+DEPTH
ZZH=VXX(3)+DEPTH
TEMP4=-ALPHA*(1.0+EXP(-2.0*WNUM*ZH))*(1.0+EXP(-2.0*WNUM*ZZH))
1 *EXP(WNUM*(ZH+ZZH-2.0*DEPTH))
TEMP5=WNUM*R1
TEMP6=TEMP4*WNUM/R1
BYO=BY(TEMP5,0)
BJO=BJ(TEMP5,0)
G(1)=TEMP4*BYO
G(2)=-TEMP4*BJO

```

```

DGX(1)=-TEMP6*BY(TEMP5,1)
DGX(2)=-TEMP6*BJ(TEMP5,1)
T21=-ALPHA*WNUM*EXP(WNUM*(ZH+Z2H-2.0*DEPTH))*
1 (1.0-EXP(-2.0*WNUM*(ZH+Z1H)))
T22=-ALPHA*WNUM*(EXP(WNUM*(ZH-Z2H-2.0*DEPTH))
1 -EXP(WNUM*(Z2H-ZH-2.0*DEPTH)))
DGZ1(1)=T21*BY0
DGZ1(2)=-T21*BJ0
DGZ2(1)=T22*BY0
DGZ2(2)=-T22*BJ0
SUMG=0.0
SUMGX=0.0
SUMGZ1=0.0
SUMGZ2=0.0
IF (NTERM.EQ. 0) GO TO 11
DO 10 I=1,NTERM
J=NTERM-I+1
TEMP7=UK(J)*R1
BK0=BK(TEMP7, 0)
S1=GAMMA(J)*COS(UK(J)*ZH)*COS(UK(J)*Z2H)
S2=GAMMA(J)*UK(J)*BK0
SG=S1*BK0
SGX=-S1*UK(J)*BK(TEMP7,1)
SGZ1=-S2*0.5*SIN(UK(J)*(ZH+Z2H))
SGZ2=-S2*0.5*SIN(UK(J)*(ZH-Z2H))
SUMG=SUMG+SG
SUMGX=SUMGX+SGX
SUMGZ1=SUMGZ1+SGZ1
SUMGZ2=SUMGZ2+SGZ2
10 CONTINUE
11 CONTINUE
G(1)=G(1)+SUMG
DGX(1)=DGX(1)+SUMGX/R1
DGY(1)=DGX(1)*TEMP2
DGY(2)=DGX(2)*TEMP2
DGX(1)=DGX(1)*TEMP1
DGX(2)=DGX(2)*TEMP1
DGZ1(1)=DGZ1(1)+SUMGZ1
DGZ2(1)=DGZ2(1)+SUMGZ2
RETURN
END

SUBROUTINE ROOTUK(N)
COMMON /C2/ GRAV,DEN,FREQ,DEPTH,WNUM,ANU,HEAD
COMMON /SER/ UK(1000),GAMMA(1000),ALPHA
F(X)=X*TAN(X*1.570796327)+BETA
ERR=1.0E-6
BETA=ANU*DEPTH/1.570796327
DO 20 J=1,N
DELTA=1.0E-2
5 A2=2*J-1+DELTA
Y1=F(A1)
Y2=F(A2)
IF (ABS(Y1).LE.ERR) GO TO 100
IF (ABS(Y2).LE.ERR) GO TO 200
IF (Y1)13,100,12
12 DELTA=DELTA/10.
A2=A1
GO TO 5

```

```

13  A3=(A1+A2)*0.5
    Y3=F(A3)
    IF (ABS(Y3).LE.ERR) GO TO 101
    IF (Y3 .LT. 0.0) A1=A3
    IF (Y3 .GT. 0.0) A2=A3
    RA=ABS((A2-A1)/A3)
    IF (RA .LE. ERR) GO TO 101
    GO TO 13
100  UK(J)=A1
    GO TO 10
200  UK(J)=A2
    GO TO 10
101  UK(J)=A3
10   UK(J)=UK(J)+1.570796327/DEPTH
20   CONTINUE
    TEMP1=ANU*ANU
    TEMP2=TEMP1*DEPTH-ANU
    DO 50 J=1,N
    TEMP3=UK(J)*UX(J)
    GAMMA(J)=4.0*(TEMP3+TEMP1)/(TEMP3*DEPTH+TEMP2)
50   CONTINUE
    RETURN
    END

```

```

FUNCTION BJ(X,N)
BJ=0.0
IF (N .EQ. 1 .AND. X .EQ. 0.0)GO TO 1
IF (N .EQ. 0 .AND. X .EQ. 0.0)GO TO 2
D=1.0E-4
IF (N)10,20,20
10   IER=1
    TYPE *,'SOMETHING WRONG IN BESJ IER = ',IER
    RETURN
2   BJ=1.0
    RETURN
20   IF (X)30,30,31
30   IER=2
    TYPE *,'SOMETHING WRONG IN BESJ IER = ',IER
    RETURN
31   IF (X-15.)32,32,34
32   NTEST=20.+10.*X-X** 2/3
    GO TO 36
34   NTEST=90.+X/2.
36   IF (N-NTEST)40,38,38
38   IER=4
    TYPE *,'SOMETHING WRONG IN BESJ IER = ',IER
    RETURN
40   IER=0
    N1=N+1
    BPREV=.0
C...COMPUTE STARTING VALUE OF M
    IF (X-5.)50,60,60
50   MA=X+6.
    GO TO 70
60   MA=1.4*X+60./X
70   MB=N+IFIX(X)/4+2
    MZERO=MAX0(MA,MB)
C...SET UPPER LIMIT OF M
    MMAX=NTEST
100  DO 190 M=MZERO,MMAX,3

```

```

C...SET F(M),F(M-1)
      FM1=1.0E-28
      FM=0.0
      ALPHA=0.0
110  IF(M-(M/2)*2)120,110,120
      JT=-1
120  GO TO 130
      JT=1
130  M2=M-2
      DO 160 K=1,M2
      MK=M-K
      BMK=2.*FLOAT(MK)*FM1/X-FM
      FM=FM1
      FM1=BMK
      IF(MK-N-1)150,140,150
140  BJ=BMK
150  JT=-JT
      S=1+JT
160  ALPHA=ALPHA+BMK*S
      BMK=2.*FM1/X-FM
      IF(N)180,170,180
170  BJ=BMK
180  ALPHA=ALPHA+BMK
      BJ=BJ/ALPHA
      IF(ABS(BJ-BPREV)-ABS(D*BJ))200,200,190
190  BPREV=BJ
      IER=3
      WRITE(4,*)'ERROR=3'
      TYPE *,'SOMETHING WRONG IN BESJ IER = ',IER
200  RETURN
      END

      FUNCTION BK(X,N)
      DIMENSION T(12)
      BK=0.0
      IF(N)10,11,11
10    IER=1
      TYPE *,'SOMETHING WRONG IN BESK IER = ',IER
      RETURN
11    IF(X)12,12,20
12    IER=2
      TYPE *,'SOMETHING WRONG IN BESK IER = ',IER
      RETURN
20    IF(X-170.0)22,22,21
21    IER=3
C...  ...TYPE *,'SOMETHING WRONG IN BESK IER = ',IER
      RETURN
22    IER=0
      IF(X-1.)36,36,25
25    A=EXP(-X)
      B=1./X
      C=SQRT(B)
      T(1)=B
      DO 26 L=2,12
26    T(L)=T(L-1)*B
      IF(N-1)27,29,27
C...  COMPUTE KO USING POLYNOMIAL APPROXIMATION
27    G0=A*(1.25331414-.15666418*T(1)+0.088111278*T(2)-0.091390954*T(3)
      2+-.13445962*T(4)-.22998503*T(5)+.37924097*T(6)-.52472773*T(7)
      3+.55753684*T(8)-.42626329*T(9)+.21845181*T(10)

```

```

      4-.066809767*T(11)+0.009189383*T(12))*C
      IF(N)20,28,29
28  BK=GO
      RETURN
C...COMPUTE K1 USING POLYNOMIAL APPROXIMATION
29  G1=A*(1.2533141+.46999270*T(1)-.14685830*T(2)+.12804226*T(3)
      2-.17364316*T(4)+.28476181*T(5)-.45943421*T(6)+.62833807*T(7)
      3-.66322954*T(8)+.50502386*T(9)-.25813038*T(10)+.078800012*T(11)
      4-.010824177*T(12))*C
      IF(N-1)20,30,31
30  BK=G1
      RETURN
C...FROM K0,K1 COMPUTE KN USING RECURRENCE RELATION
31  DO 35 J=2,N
      GJ=2.*(FLOAT(J)-1.)*G1/X+G0
      IF(GJ-1.0E38)33,33,32
32  IER=4
      TYPE *,'SOMETHING WRONG IN BESK IER = ',IER
      GO TO 34
33  G0=G1
34  G1=GJ
35  BK=GJ
36  RETURN
      B=X/2.
      A=.57721566+ALOG(B)
      C=B*B
      IF(N-1)37,43,37
C...COMPUTE K0 USING SERIES EXPANSION
37  G0=-A
      X2J=1.
      FACT=1.
      HJ=0.0
      DO 40 J=1,6
      RJ=1./FLOAT(J)
      X2J=X2J*C
      FACT=FACT*RJ*RJ
      HJ=HJ+RJ
40  G0=G0+X2J*FACT*(HJ-A)
      IF(N)43,42,43
42  BK=GO
      RETURN
C...COMPUTE K1 USING SERIES EXPANSION
43  X2J=B
      FACT=1.
      HJ=1.
      G1=1./X+X2J*(.5+A-HJ)
      DO 50 J=2,8
      X2J=X2J*C
      RJ=1./FLOAT(J)
      FACT=FACT*RJ*RJ
      HJ=HJ+RJ
50  G1=G1+X2J*FACT*(.5+(A-HJ)*FLOAT(J))
      IF(N-1)31,52,31
52  BK=G1
      RETURN
      END
      FUNCTION BY(X,N)
C...CHECK FOR ERRORS IN N AND X
      IF(N)180,10,10

```

```

10  IER=0
    IF(X)190,190,20
C...BRANCH IF X LESS THAN OR EQUAL 4
20  IF(X-.4)40,40,30
C...COMPUTE Y1 AND Y0 FOR X GREATER THAN 4.0
30  T1=4.0/X
    T2=T1*T1
    P0={((- .0000037043*T2+.0000173565)*T2-.0000487613)*T2
      1+.00017343)*T2-.001753062)*T2+.3989423
    Q0={(((.0000052312*T2-.0000142078)*T2+.0000342468)*T2
      1-.0000869791)*T2+.0004564324)*T2-.01246694
    P1={(((.0000042414*T2-.0000200920)*T2+.0000580759)*T2
      1-.000223203)*T2+.002921826)*T2+.3989423
    Q1={((- .0000036594*T2+.00001622)*T2-.0000398708)*T2
      1+.0001064741)*T2-.0006390400)*T2+.03740084
    A=2.0/SQRT(X)
    B=A*T1
    C=X-.7853982
    Y0=A*P0*SIN(C)+B*Q0*COS(C)
    Y1=-A*P1*COS(C)+B*Q1*SIN(C)
    GO TO 90
C...COMPUTE Y0 AND Y1 FOR X LESS OR EQUAL TO 4.0
40  XX=X/2.
    X2=XX*XX
    T=ALOG(XX)+.5772157
    SUM=0.0
    TERM=T
    Y0=T
    DO 70 L=1,15
    IF(L-1)50,60,50
    SUM=SUM+1./FLOAT(L-1)
60  FL=L
    TS=T-SUM
    TERM=(TERM*(-X2)/FL**2)*(1.-1./(FL*TS))
70  Y0=Y0+TERM
    TERM=XX*(T-.5)
    SUM=0.0
    Y1=TERM
    DO 80 L=2,16
    SUM=SUM+1./FLOAT(L-1)
    FL=L
    FL1=FL-1
    TS=T-SUM
    TERM=(TERM*(-X2)/(FL1*FL))*((TS-.5/FL)/(TS+.5/FL1))
80  Y1=Y1+TERM
    PI2=.6366198
    Y0=PI2*Y0
    Y1=-PI2/X+PI2*Y1
C...CHECK IF ONLY Y0 OR Y1 IS DESIRED
90  IF(N-1)100,100,130
C...RETURN EITHER Y0 OR Y1 AS REQUIRED
100 IF(N)110,120,110
110 BY=Y1
    GO TO 170
120 BY=Y0
    GO TO 170
C...PERFORM RECURRENCE OPERATIONS TO FIND YN(X)
130 YA=Y0
    YB=Y1
    K=1

```

```

140 T=FLOAT(2*K)/X
    YC=T*YB-YA
    IF(ABS(YC)-1.0E38)145,145,141
141 IER=3
    TYPE *, 'SOMETHING WRONG IN BESY IER = ', IER
    RETURN
145 K=K+1
    IF(K-N)150,160,150
150 YA=YB
    YB=YC
    GO TO 140
160 BY=YC
170 RETURN
180 IER=1
    TYPE *, 'SOMETHING WRONG IN BESY IER = ', IER
    RETURN
190 IER=2
    TYPE *, 'SOMETHING WRONG IN BESY IER = ', IER
    RETURN
    END

    SUBROUTINE DG16(XL,XU,FCT,SUM)
C... THIS PROGRAM COMPUTE INTEGRAL (FCT), SUMMED OVER X FROM
C... XL TO XU
C   DOUBLE PRECISION XL,XU,Y,A,B,C,FCT
    SUM0=0.0
    DO 10 I=1,10
        DELTA=(XU-XL)/I
        SUM=0.0
        DO 20 J=1,I
            X1=XL+(J-1)*DELTA
            X2=X1+DELTA
            A=.5E0*(X2+X1)
            B=DELTA
            C=.49470046749582497E0*B
            Y=.13576229705877047E-1*(FCT(A+C)+FCT(A-C))
            C=.47228751153661629E0*B
            Y=Y+.31126761969323946E-1*(FCT(A+C)+FCT(A-C))
            C=.43281560119391587E0*B
            Y=Y+.47579255841246392E-1*(FCT(A+C)+FCT(A-C))
            C=.37770220417750152E0*B
            Y=Y+.62314485627766936E-1*(FCT(A+C)+FCT(A-C))
            C=.30893812220132187E0*B
            Y=Y+.7479799440828837E-1*(FCT(A+C)+FCT(A-C))
            C=.22906838882861369E0*B
            Y=Y+.8457825969750127E-1*(FCT(A+C)+FCT(A-C))
            C=.14080177538962946E0*B
            Y=Y+.9130170752246179E-1*(FCT(A+C)+FCT(A-C))
            C=.47506254918818720E-1*B
            Y=B*(Y+.9472530522753425E-1*(FCT(A+C)+FCT(A-C)))
            SUM=SUM+Y
20   CONTINUE
        IF(ABS(SUM-SUM0) .LE. ABS(SUM*1.0E-2)) GO TO 100
        SUM0=SUM
10   CONTINUE
    TYPE *, '***FAIL TO CONVERGE IN DG16*** NO = 10'
100  CONTINUE
    RETURN
    END

```

```

SUBROUTINE MPRD(A,B,R,N,M,L)
C...THIS PROGRAM COMPUTES R=A*B,WHERE A(N*M),B(M*L)
DIMENSION A(1),B(1),R(1)
IR=0
IK=-M
DO 10 K=1,L
IK=IK+M
DO 10 J=1,N
IR=IR+1
JI=J-N
IB=IK
R(IR)=0.0
DO 10 I=1,M
JI=JI+N
IB=IB+1
10 R(IR)=R(IR)+A(JI)*B(IB)
RETURN
END

```

```

SUBROUTINE INV(R,A,M,N)
DIMENSION A(1),R(1)
EPS=1.0E-4
IF(M)23,23,1
C...SEARCH FOR GREATEST ELEMENT IN MATRIX A
1 IER=0
PIV=0.0E0
MM=M*M
NM=N*M
DO 3 L=1,MM
TB=ABS(A(L))
IF(TB-PIV)3,3,2
2 PIV=TB
I=L
3 CONTINUE
TOL=EPS*PIV
LST=1
DO 17 K=1,M
IF(PIV)23,23,4
4 IF(IER)7,5,7
5 IF(PIV-TOL)6,6,7
6 IER=K-1
7 PIVI=1.0E0/A(I)
J=(I-1)/M
I=I-J*M-K
J=J+1-K
DO 8 L=K,NM,M
LL=L+I
TB=PIVI*R(LL)
R(LL)=R(L)
8 R(L)=TB
IF(K-M)9,18,18
9 LEND=LST+M-K
IF(J)12,12,10
10 II=J*M
DO 11 L=LST,LEND
TB=A(L)
LL=L+II
A(L)=A(LL)
11 A(LL)=TB
12 DO 13 L=LST,MM,M

```

```

LL=L+I
TB=PIVI*A(LL)
A(LL)=A(L)
13 A(L)=TB
A(LST)=J
PIV=0.0E0
LST=LST+1
J=0
DO 10 II=LST,LEND
PIVI=-A(II)
IST=II+M
J=J+1
DO 15 L=IST,MM,M
LL=L-J
A(L)=A(L)+PIVI*A(LL)
TB=ABS(A(L))
IF(TB-PIV)15,15,14
14 PIV=TB
I=L
15 CONTINUE
DO 16 L=K,NM,M
LL=L+J
16 R(LL)=R(LL)+PIVI*R(L)
17 LST=LST+M
18 IF(M-1)23,22,19
19 IST=MM+M
LST=M+1
DO 21 I=2,M
II=LST-I
IST=IST-LST
L=IST-M
L=A(L)+0.5E0
DO 21 J=II,NM,M
TB=R(J)
LL=J
DO 20 K=IST,MM,M
LL=LL+1
20 TB=TB-A(K)*R(LL)
K=J+L
R(J)=R(K)
21 R(K)=TB
22 RETURN
23 IER=-1
TYPE *, '?????SOMETHING WRONG IN INV.FTN*****'
RETURN
END

```

```

SUBROUTINE VSUB(A,B,C)
DIMENSION A(3),B(3),C(3)
DO 10 I=1,3
10 C(I)=A(I)-B(I)
RETURN
END

```

```

SUBROUTINE VDOT(A,B,S)
DIMENSION A(3),B(3)
S=0.0
DO 10 I=1,3
10 S=S+A(I)*B(I)
RETURN

```

```

END

SUBROUTINE VCRO(A,B,C,S)
DIMENSION A(3),B(3),C(3)
C1=A(2)*B(3)-A(3)*B(2)
C2=A(3)*B(1)-A(1)*B(3)
C3=A(1)*B(2)-A(2)*B(1)
S=SQRT(C1*C1+C2*C2+C3*C3)
C(1)=C1
C(2)=C2
C(3)=C3
RETURN
END

SUBROUTINE VCOM(A,N1,N2,N3,C,I,J)
DIMENSION A(N1,N2,N3),C(N3)
DO 10 K=1,3
C(K)=A(I,J,K)
RETURN
END

FUNCTION FTAN(AR,AI)
D=ABS(AI/AR)
D=ATAN(D)/3.1416*180.0
IF(AI .GT. 0.0 .AND. AR .LT. 0.0) D=180.0-D
IF(AI .LT. 0.0 .AND. AR .GT. 0.0) D=-D
IF(AI .LT. 0.0 .AND. AR .LT. 0.0) D=-180.0+D
FTAN=D
RETURN
END

SUBROUTINE QTOTAL(NSP,NN,Q135,Q246,AMP,QDF1,QDF2)
C...THIS PROGRAM CALCULATE THE TOTAL Q FOR DRIFTING FORCE
C...INPUT: NSP,NN,Q135,Q246,AMP
C...OUTPUT: QDF1(SIDE 1),QDF2(SIDE 2)
DIMENSION Q135(NN,4),Q246(NN,4),QDF1(NN),QDF2(NN),AMP(12)
COMMON /C2/ GRAV,DEN,FREQ,DEPTH,WNUM,ANU,HEAD

DO 10 I=1,NSP
II=I+NSP
T1=0.0
T2=0.0
T3=0.0
T4=0.0
DO 20 J=1,3
J1=2*J-1
J2=J1+1
T1=T1+Q135(I,J)*AMP(J1+6)+Q135(II,J)*AMP(J1)
T2=T2+Q246(I,J)*AMP(J2+6)+Q246(II,J)*AMP(J2)
T3=T3+Q135(I,J)*AMP(J1)-Q135(II,J)*AMP(J1+6)
T4=T4+Q246(I,J)*AMP(J2)-Q246(II,J)*AMP(J2+6)
20 CONTINUE
QDF1(I)=Q135(I,4)+Q246(I,4)+FREQ*(T1+T2)
QDF2(I)=Q135(I,4)-Q246(I,4)+FREQ*(T1-T2)
QDF1(II)=Q135(II,4)+Q246(II,4)-FREQ*(T3+T4)
QDF2(II)=Q135(II,4)-Q246(II,4)-FREQ*(T3-T4)
C...TOT SOURCE STRENGTH WHICH MOTION IS NOT INCLUDED
C QD. I,I)=Q135(I,4)+Q246(I,4)
C QDF2(I)=Q135(I,4)-Q246(I,4)
C QDF1(II)=Q135(II,4)+Q246(II,4)

```

```

C   QDF2(II)-Q135(II,4)-Q246(II,4)
10  CONTINUE
    RETURN
    END

    SUBROUTINE SIR(N,NN,PAN,SUR,QDF1,QDF2,THETA,SR,SI,SCOS,SSIN,DSR,DSI,
1    DMENT)
C...THIS PROGRAM CALCULATE THE SR,SI...VALUES FOR DRIFTING FORCE
C...INPUT: N,NN,PAN,SUR,QDF1,QDF2,THETA
C...OUTPUT: SR,SI,SCOS,SSIN
    DIMENSION PAN(N,3),SUR(N),QDF1(NN),QDF2(NN)
    COMMON /C2/ GRAV,DEN,FREQ,DEPTH,WNUM,ANU,HEAD
    S1=0.0
    S2=0.0
    S3=0.0
    S4=0.0
    DS1=0.0
    DS2=0.0
    DS3=0.0
    DS4=0.0
    DO 10,I=1,N
    II=I+N
    CX=COS(THETA)*PAN(I,1)
    SY=SIN(THETA)*PAN(I,2)
    U1=WNUM*(CX+SY)+2.35619
    U2=WNUM*(CX-SY)+2.35619
    SX=SIN(THETA)*PAN(I,1)
    CY=COS(THETA)*PAN(I,2)
    DU1=WNUM*(SX-CY)
    DU2=WNUM*(SX+CY)
    Z=PAN(I,3)
    TZ=EXP(WNUM*Z)*(1.0+EXP(-2.0*WNUM*(Z+DEPTH)))*SUR(I)
    S1=S1+(QDF1(I)*COS(U1)+QDF1(II)*SIN(U1))*TZ
    S2=S2+(QDF2(I)*COS(U2)+QDF2(II)*SIN(U2))*TZ
    S3=S3+(QDF1(II)*COS(U1)-QDF1(I)*SIN(U1))*TZ
    S4=S4+(QDF2(II)*COS(U2)-QDF2(I)*SIN(U2))*TZ
    DS1=DS1+(QDF1(I)*SIN(U1)-QDF1(II)*COS(U1))*TZ*DU1
    DS2=DS2+(QDF2(I)*SIN(U2)-QDF2(II)*COS(U2))*TZ*DU2
    DS3=DS3+(QDF1(I)*COS(U1)+QDF1(II)*SIN(U1))*TZ*DU1
    DS4=DS4+(QDF2(I)*COS(U2)+QDF2(II)*SIN(U2))*TZ*DU2
10  CONTINUE
    SR=S1+S2
    SI=S3+S4
    DSR=DS1+DS2
    DSI=DS3+DS4
    SM=SR*SR+SI*SI
    SCOS=SM*COS(THETA)
    SSIN=SM*SIN(THETA)
    DMENT=SR*DSI-SI*DSR
    RETURN
    END

    SUBROUTINE DRIFT(NSP,NN,PAN,SUR,QDF1,QDF2,DRFX,DRFY,DRMZ)
C...CALCULATE THE DRIFTING FORCE
C...INPUT: NSP,NN,PAN,SUR,QDF1,QDF2
C...OUTPUT: DRFX,DRFY(DRIFTING FORCE IN X- AND Y-DIRECTION).
    DIMENSION PAN(NSP,3),SUR(NSP),QDF1(NN),QDF2(NN)
    COMMON /C2/ GRAV,DEN,FREQ,DEPTH,WNUM,ANU,HEAD

    HK=WNUM*DEPTH

```

```

E2=EXP(-2.0*HK)
E4=EXP(-4.0*HK)
T1=(WNUM*WNUM-ANU*ANU)*DEPTH+ANU
T2=1.0+4.0*HK*E2/(1.0-E4)
TEMP1=4.44288*DEN*WNUM*FREQ*T2/(T1*(1.0+E2))
TEMP2=-6.28318*(1.0-E2)*DEN*(WNUM**4.0)*T2/(T1*T1*(1.0+E2)**3.0)
C...DRIFTING FORCE DUE TO THE INCOME WAVE EFFECT
CALL SIR(NSP,2*NSP,PAN,SUR,QDF1,QDF2,HEAD,SR,SI,SCOS,SSIN,DSR,DSI,TM)
DRFX=TEMP1*(SR-SI)*COS(HEAD)
DRFY=TEMP1*(SR-SI)*SIN(HEAD)
DRMZ=TEMP1*(DSR+DSI)/WNUM
C...USING GUASSIAN 16 POINTS FORMULAR TO INTEGRATE THE DRIFTING FORCE
C...DUE THE MOTION EFFECT
DELTA=6.28318/4.0
SUMX=0.0
SUMY=0.0
SUMMEN=0.0
DO 20 J=1,4
X1=(J-1)*DELTA
X2=X1+DELTA
A=.5E0*(X2+X1)
B=DELTA
C=.49470046749582497E0*B
CALL SIR(NSP,2*NSP,PAN,SUR,QDF1,QDF2,A+C,SR,SI,APCC,APCS,TEM1,TEM2,DM1)
CALL SIR(NSP,2*NSP,PAN,SUR,QDF1,QDF2,A-C,SR,SI,AMCC,AMCS,TEM1,TEM2,DM2)
FX=.13576229705877047E-1*(APCC+AMCC)
FY=.13576229705877047E-1*(APCS+AMCS)
FMEN=.13576229705877047E-1*(DM1+DM2)
C=.47228751153661629E0*B
CALL SIR(NSP,2*NSP,PAN,SUR,QDF1,QDF2,A+C,SR,SI,APCC,APCS,TEM1,TEM2,DM1)
CALL SIR(NSP,2*NSP,PAN,SUR,QDF1,QDF2,A-C,SR,SI,AMCC,AMCS,TEM1,TEM2,DM2)
FX=FX+.31126761969373946E-1*(APCC+AMCC)
FY=FY+.31126761969373946E-1*(APCS+AMCS)
FMEN=FMEN+.31126761969373946E-1*(DM1+DM2)
C=.43281560119391587E0*B
CALL SIR(NSP,2*NSP,PAN,SUR,QDF1,QDF2,A+C,SR,SI,APCC,APCS,TEM1,TEM2,DM1)
CALL SIR(NSP,2*NSP,PAN,SUR,QDF1,QDF2,A-C,SR,SI,AMCC,AMCS,TEM1,TEM2,DM2)
FX=FX+.47579255841246392E-1*(APCC+AMCC)
FY=FY+.47579255841246392E-1*(APCS+AMCS)
FMEN=FMEN+.47579255841246392E-1*(DM1+DM2)
C=.37770220417750152E0*B
CALL SIR(NSP,2*NSP,PAN,SUR,QDF1,QDF2,A+C,SR,SI,APCC,APCS,TEM1,TEM2,DM1)
CALL SIR(NSP,2*NSP,PAN,SUR,QDF1,QDF2,A-C,SR,SI,AMCC,AMCS,TEM1,TEM2,DM2)
FX=FX+.62314485627766936E-1*(APCC+AMCC)
FY=FY+.62314485627766936E-1*(APCS+AMCS)
FMEN=FMEN+.62314485627766936E-1*(DM1+DM2)
C=.30893812220132187E0*B
CALL SIR(NSP,2*NSP,PAN,SUR,QDF1,QDF2,A+C,SR,SI,APCC,APCS,TEM1,TEM2,DM1)
CALL SIR(NSP,2*NSP,PAN,SUR,QDF1,QDF2,A-C,SR,SI,AMCC,AMCS,TEM1,TEM2,DM2)
FX=FX+.7479799440828837E-1*(APCC+AMCC)
FY=FY+.7479799440828837E-1*(APCS+AMCS)
FMEN=FMEN+.7479799440828837E-1*(DM1+DM2)
C=.22900838882861369E0*B
CALL SIR(NSP,2*NSP,PAN,SUR,QDF1,QDF2,A+C,SR,SI,APCC,APCS,TEM1,TEM2,DM1)
CALL SIR(NSP,2*NSP,PAN,SUR,QDF1,QDF2,A-C,SR,SI,AMCC,AMCS,TEM1,TEM2,DM2)
FX=FX+.8457825969750127E-1*(APCC+AMCC)
FY=FY+.8457825969750127E-1*(APCS+AMCS)
FMEN=FMEN+.8457825969750127E-1*(DM1+DM2)
C=.14080177538962946E0*B
CALL SIR(NSP,2*NSP,PAN,SUR,QDF1,QDF2,A+C,SR,SI,APCC,APCS,TEM1,TEM2,DM1)

```

```
CALL SIR(NSP,2*NSP,PAN,SUR,QDF1,QDF2,A-C,SR,SI,AMCC,AMCS,TEM1,TEM2,DM2)
FX=FX+.9130170752246179E-1*(APCC+AMCC)
FY=FY+.9130170752246179E-1*(APCS+AMCS)
FMEN=FMEN+.9130170752246179E-1*(DM1+DM2)
C=.47506254918818720E-1*B
CALL SIR(NSP,2*NSP,PAN,SUR,QDF1,QDF2,A+C,SR,SI,APCC,APCS,TEM1,TEM2,DM1)
CALL SIR(NSP,2*NSP,PAN,SUR,QDF1,QDF2,A-C,SR,SI,AMCC,AMCS,TEM1,TEM2,DM2)
FX=B*(FX+.9472530522753425E-1*(APCC+AMCC))
FY=B*(FY+.9472530522753425E-1*(APCS+AMCS))
FMEN=B*(FMEN+.9472530522753425E-1*(DM1+DM2))
SUMX=SUMX+FX
SUMY=SUMY+FY
SUMMEN=SUMMEN+FMEN
20 CONTINUE
C...TOTAL DRIFTING FORCE AND MOMENT
DRFX=DRFX+TEMP2*SUMX
DRFY=DRFY+TEMP2*SUMY
DRMZ=DRMZ+TEMP2*SUMMEN
RETURN
END
```

```

PROGRAM OUT72
DIMENSION PAN(115,3),UN(115,3),UNN(115,3),SUR(115),
1 DG11R(115,115),DG11I(115,115),DG12R(115,115),DG12I(115,115),
2 G11R(115,115),G11I(115,115),G12R(115,115),G12I(115,115),
3 PH17R(115),PH17I(115),PH18R(115),PH18I(115),QDF1(230),
4 QDF2(230),
5 POT135(230,4),POT246(230,4),Q135(230,4),Q246(230,4),
AM(6,6),DEMP(6,6),RM(6,6),C(6,6),FOR(12),AMP(12)

COMMON /C2/ GRAV,DEN,FREQ,DEPTH,WNUM,ANU,HEAD
COMMON /C3/ VOL,XB,YB,ZB,AREA,AREAWP,XG,YG,ZG
COMMON /SER/ UK(1000),GAMMA(1000),ALPHA
DATA DEN,GRAV/1000.,9.8/
DATA XG,YG,ZG/0.0,0.0,-1.26/
DATA RI44,RI55,RI66/170.0,166.0,236.0/
DATA DEPTH,HEAD/500.0,240.0/
DATA NSP/115/

C*****
VOL=3054270.0
SLL=200.0
AA1=DEN*VOL
BB1=DEN*VOL*SQRT(GRAV/SLL)
AA5=AA1*SLL*SLL
BB5=BB1*SLL*SLL
C*****
CALL ASSIGN (2,'COM 2.DAT')
CALL ASSIGN (3,'PRNT2 2.DAT')
OPEN (UNIT=7,TYPE='NEW',NAME='POINT2',FORM='FORMATTED')
C OPEN (UNIT=8,TYPE='NEW',NAME='SURGE MOTION2',FORM='FORMATTED')
C OPEN (UNIT=9,TYPE='NEW',NAME='HEAVE MOTION2',FORM='FORMATTED')
C OPEN (UNIT=10,TYPE='NEW',NAME='PITCH MOTION2',FORM='FORMATTED')
OPEN (UNIT=11,TYPE='NEW',NAME='ADDED MASS',FORM='FORMATTED')
OPEN (UNIT=12,TYPE='NEW',NAME='DAMPING',FORM='FORMATTED')

WRITE(3,*)'*****'
WRITE(3,*)'RESULT OF 115 PANELS FOR DELTA SHAPE'
WRITE(3,*)'WATER ENTRAPPED IN MODEL IS CONSIDERED'
WRITE(3,*)'*****'
DO 17 KI=1,40
READ (2) PAN,SUR,FOR,AMP,AM,DEMP,C,RM,
1 GRAV,DEN,FREQ,DEPTH,WNUM,ANU,HEAD,DRIFX,DRIFY,DRMZ

C*****
WRITE (3,*) 'PERIOD = ',2.0*3.14159/FREQ
WRITE (3,*) 'HEADING = ',HEAD*180./3.14159
WRITE (3,*) ' '

WRITE (3,*) 'A(11) = ',AM(1,1)/AA1,' A(33) = ',AM(3,3)/AA1
WRITE (3,*) 'A(55) = ',AM(5,5)/AA5,' A(66) = ',AM(6,6)/AA5
WRITE (3,*) 'B(11) = ',DEMP(1,1)/BB1,' B(33) = ',DEMP(3,3)/BB1
WRITE (3,*) 'B(55) = ',DEMP(5,5)/BB5,' B(66) = ',DEMP(6,6)/BB5

FREQND=(FREQ)*(VOL**0.333/9.81)**0.5
PHASE=90.0-FTAN(AMP(1),AMP(7))
AMIG =SQRT(AMP(1)*AMP(1)+AMP(7)*AMP(7))
WRITE (3,*) 'SURGE MOTION = ',AMIG,' PHASE = ',PHASE
C WRITE (8,*) AMIG,PHASE,FREQND
C
PHASE=90.0-FTAN(AMP(3),AMP(9))

```

```

AMIG =SQRT(AMP(3)*AMP(3)+AMP(9)*AMP(9))
WRITE (3,*) 'HEAVE MOTION =',AMIG,' PHASE =',PHASE
C
WRITE (9,*) AMIG,PHASE,FREQND
C
PHASE=90.0-FTAN(AMP(5),AMP(11))
AMIG =SQRT(AMP(5)*AMP(5)+AMP(11)*AMP(11))
WRITE (3,*) 'PITCH MOTION =',AMIG*SLL,' PHASE =',PHASE
C
WRITE (10,*) AMIG*SLL,PHASE,FREQND
C
PHASE=90.0-FTAN(FOR(1),FOR(7))
AMIG =SQRT(FOR(1)*FOR(1)+FOR(7)*FOR(7))
WRITE (3,*) 'SURGE EX. FORCE =',AMIG/(GRAV*AA1/SLL),' PHASE =',PHASE

PHASE=90.0-FTAN(FOR(3),FOR(9))
AMIG =SQRT(FOR(3)*FOR(3)+FOR(9)*FOR(9))
WRITE (3,*) 'HEAVE EX. FORCE =',AMIG/(GRAV*AA1/SLL),' PHASE =',PHASE

PHASE=90.0-FTAN(FOR(5),FOR(11))
AMIG =SQRT(FOR(5)*FOR(5)+FOR(11)*FOR(11))
WRITE (3,*) 'PITCH EX. FORCE =',AMIG/(GRAV*AA1),' PHASE =',PHASE

WRITE (3,*)'DRIFT FORCE(X) =', DRIFX/(DEN*GRAV*SLL)
WRITE (3,*)'DRIFT FORCE(Y) =', DRIFY/(DEN*GRAV*SLL)
WRITE (3,*)'DRIFT MOMENT(Z) =', DRMZ/(DEN*GRAV*SLL*SLL)
WRITE (3,*)'-----'
WRITE (3,*)'NONDIM.DRIFT FORCE(X) =', DRIFX/(0.5*DEN*GRAV*VOL**0.333)
WRITE (3,*)'NONDIM.DRIFT FORCE(Y) =', DRIFY/(0.5*DEN*GRAV*VOL**0.333)
WRITE (3,*)'DRIFT FORCE(X) =', DRIFX
WRITE (12,*) 2*3.14159/FREQ,DEMP(1,1)/BB1,DEMP(3,3)/BB1
+ ,DEMP(5,5)/BB5,DEMP(6,6)/BB5
WRITE (11,*) 2*3.14159/FREQ,AM(1,1)/AA1,AM(3,3)/AA1,
+ AM(5,5)/AA5,AM(6,6)/AA5
WRITE (7,*) 2*3.14159/FREQ,DRIFX
WRITE (3,*)'DRIFT FORCE(Y) =', DRIFY
WRITE (3,*)'*****'
WRITE (3,*) ' '

17 CONTINUE
CLOSE(UNIT=11)
CLOSE(UNIT=12)
CLOSE(UNIT=7)
STOP
END

FUNCTION FTAN(AR,AI)
C.....THIS FUNCTION COMPUTE THE ARGUMENT OF (AR,AI) IN THE RANGE
C.....FROM -90 DEG. TO +270 DEG.
D=ABS(AI/AR)
D=ATAN(D)/3.1416*180.0
IF(AI .GT. 0.0 .AND. AR .LT. 0.0) D=180.0-D
IF(AI .LT. 0.0 .AND. AR .GT. 0.0) D=-D
IF(AI .LT. 0.0 .AND. AR .LT. 0.0) D=+180.0+D
FTAN=D
RETURN
END

```

APPENDIX E

PROGRAM LISTING: SHAPE.FOR

```

C *****
C
C PROGRAM TO CALCULATE PANELS FOR DELTAPORT GEOMETRY
C THE OUTPUT FILE IS DELTA1.DAT.
C *****
C
C REAL I
C DIMENSION X1(200),X2(200),Y1(200),Y2(200),XINT1(50),Z(200)
C DIMENSION XX(200),Y(200),YY(200),XINT2(50)
C OPEN(UNIT=6,FILE='DELTA1.DAT',STATUS='NEW')
C OPEN(UNIT=7,FILE='DELTA2.DAT',STATUS='NEW')
C
C FIRST CALCULATE BOTTOM PANEL GEOMETRY (triangular panels)
C
C TYPE*, 'BOTTOM PANEL GEOMETRY'
C TYPE*, ' '
C XL=430.0
C YL=370.0
C NX=6
C NY=9
C DY=YL/NY
C DX=XL/NX
C
C ROUTINE TO CALCULATE Y COORDINATE OF THE CENTROID
C
C DO 20 I=1,NY
C Y1(I)=370-(2*DY/3.0)-((I-1)*DY)
C Y2(I)=370-(DY/3)-((I-1)*DY)
20 CONTINUE
C
C CALCULATE THE EQUATION OF EACH CENTROID LINE
C
C SLOPE=-1.726
C DO 30 I=1,NX
C XINT1(I)=(430.0-(DX/3.0))-((I-1)*DX)
C XINT2(I)=430-(2*DX/3)-(I-1)*DX
30 CONTINUE
C
C CALCULATE EACH PANEL AREA
C
C AREA=DX*DY/2
C
C CALCULATE X COORDINATE USING STRAIGHT EQUATION
C X=mY + a
C NOTE - Z=-11.9 m FOR ALL PANELS
C THE FOLLOWING LOOP ALSO WRITES TO FILE DELTA1.DAT
C
C DO 40 I=1,NX
C DO 40 J=1,NY
C X1(J)=SLOPE*Y1(J)+XINT1(I)
C IF (X1(J).LT.-216.) GOTO 35
C IF ((X1(J).GT.-76.).AND.(X1(J).LT.(SLOPE*Y1(J)+150))) GOTO 35
C WRITE(6,*) X1(J),Y1(J),-11.9,0.0,0.0,-1.0,AREA
C WRITE(7,*) X1(J),Y1(J)
C PB=PB+1
35 X2(J)=SLOPE*Y2(J)+XINT2(I)
C IF (X2(J).LT.-216) GOTO 40
C IF ((X2(J).GT.-76.).AND.(X2(J).LT.(SLOPE*Y2(J)+150))) GOTO 40
C WRITE(6,*) X2(J),Y2(J),-11.9,0.0,0.0,-1.0,AREA

```

```

        WRITE(7,*) X2(J),Y2(J)
        PB=PB+1
40    CONTINUE
C
C    PB=TOTAL NUMBER OF PANELS ON THE BOTTOM SIDE
C
C    *****
C
C    GEOMETRY FOR OUTSIDE PANELS (RECTANGULAR + TWO TRIANGULAR END PANELS )
C
C    *****
C    TAKING A RECTANGLE DOWN FROM THE WATER LINE...
        NH=25
        NZ=1
        XL=615
        YL=350
        ZL=11.9
        DZ=ZL/NZ
        DX=XL/NH
        DY=YL/NH
C
C    CALCULATION OF X AND Y FOR VERTICAL SIDES
        DO 100 I=1,NH
        X(I)=(395.0-(DX/2.0))-((I-1)*DX)
        XX(I)=X(I)
        Y(I)=(DY/2.0)+((I-1)*DY)
        YY(I)=Y(I)
100    CONTINUE
C
C    CALCULATION OF Z
C
        DO 110 I=1,NZ
        Z(I)=-((DZ/2.0)+((I-1)*DZ))
110    CONTINUE
C
C    CHANGE VERTICAL SIDES TO SLOPED SIDES
        DO J=1,NZ
        DO I=1,NH
        IF (X(I).LT.395.) Y(I)=Y(I)-2.1
        END DO
        END DO
C
C    CALCULATE PANEL AREA
C
        TAREA=705*25
        AREA=TAREA/(NH*NZ)
C
C    WRITE PANELS TO FILE
C
        DO 130 I=1,NZ
        DO 130 J=1,NH
        WRITE(6,*) X(J),Y(J),Z(I),.5,.866,0.3,AREA
130    CONTINUE
        WRITE(6,*) 423.7,2.4,-7.93,0.5,0.866,0.3,45.4
        WRITE(6,*) -215.3,365.9,-7.93,0.5,0.866,0.3,15.3
C
C    PO=NUMBER OF OUTSIDE PANELS
C
        PO=NH*NZ+2
C
C    *****
C

```

```

C GEOMETRY FOR INSIDE PANELS (RECTANGULAR PANELS)
C SIDE SECTION
C *****
C TYPE*, ' '
DO 200 I=1,NH

IF ((XX(I).GT.-76).AND.(XX(I).LT.150)) Y(I)=YY(I)-140
IF ((XX(I).GT.-216).AND.(XX(I).LT.-76)) Y(I)=YY(I)-230

200 CONTINUE
C
C WRITE TO FILE
C
DO 210 I=1,NZ
DO 210 J=1,NH
IF (XX(J).LT.-216) GO TO 210
IF (XX(J).GT.150) GO TO 210
WRITE(6,*) XX(J),Y(J),Z(I),-.5,-.866,0.0,AREA
PIS=PIS+1
210 CONTINUE
C
C *****
C INSIDE-BACK SECTION
C
NY=2
NZ=1
YL=80.0
ZL=11.9
DY=YL/NY
DZ=ZL/NZ
DO 250 I=1,NZ
DO 250 J=1,NY
Y(I)=130.-DY/2.-((I-1)*DY
Z(I)=-((DZ/2.)+(I-1)*DZ)
AREA=DY*DZ
WRITE(6,*)-76.,Y(J),Z(I),1.0,0.0,0.0,AREA
250 CONTINUE
PIB=NY*NZ
C NO. OF INSIDE-BACK PANELS=PIB
C
C
C *****
C GEOMETRY FOR THE BACK PANELS (RECTANGULAR PANELS + ONE TRIANGULAR PANEL)
C *****
C
NY=6
YL=225
DY=YL/NY
NZ=1
ZL=11.9
DZ=ZL/NZ
DO 300 I=1,NY
Y(I)=(370.0-(DY/2.0))-((I-1)*DY)
300 CONTINUE
C
C CALCULATE PANEL AREA

```

```
C
  TAREA=VL*ZL
  AREA=DY*DZ
C
C WRITE TO FILE
C
  DO 310 I=1,NZ
  DO 310 J=1,NY
  WRITE(6,*) -216.0,Y(J),Z(I),-1.0,0.0,0.0,AREA
310 CONTINUE
C
  WRITE(6,*)-216.0,366.8,-7.93,-1.0,0.0,0.0,28.9
C PS=NUMBER OF PANELS ON THE BACK SIDE
C
  PS=NY*NZ+1
C
C PRINT OUT PANEL DATA
C
  TYPE*, ' '
  TYPE*, 'NUMBER OF BOTTOM PANELS',PB
  TYPE*, 'NUMBER OF OUTSIDE PANELS',PO
  TYPE*, 'NUMBER OF INSIDE-BACK PANELS',PIB
  TYPE*, 'NUMBER OF INSIDE-SIDE PANELS',PIS
  TYPE*, 'NUMBER OF BACKSIDE PANELS',PS
  TYPE*, ' '
  TP=PB+PO+PIS+PS+PIB
  TYPE*, 'TOTAL NUMBER OF PANELS',TP
  END
```

APPENDIX F

INPUT PANEL DATA

-185.2037	342.5926	-11.90000	0.0000000E+00	0.0000000E+00
-1.000000	1473.148			
-114.2459	301.4815	-11.90000	0.0000000E+00	0.0000000E+00
-1.000000	1473.148			
-161.7874	315.1852	-11.90000	0.0000000E+00	0.0000000E+00
-1.000000	1473.148			
-43.28812	260.3704	-11.90000	0.0000000E+00	0.0000000E+00
-1.000000	1473.148			
-90.82959	274.0741	-11.90000	0.0000000E+00	0.0000000E+00
-1.000000	1473.148			
27.66965	219.2593	-11.90000	0.0000000E+00	0.0000000E+00
-1.000000	1473.148			
-19.87183	232.9630	-11.90000	0.0000000E+00	0.0000000E+00
-1.000000	1473.148			
98.62741	178.1481	-11.90000	0.0000000E+00	0.0000000E+00
-1.000000	1473.148			
51.08594	191.8519	-11.90000	0.0000000E+00	0.0000000E+00
-1.000000	1473.148			
169.5852	137.0370	-11.90000	0.0000000E+00	0.0000000E+00
-1.000000	1473.148			
122.0437	150.7407	-11.90000	0.0000000E+00	0.0000000E+00
-1.000000	1473.148			
240.5430	95.92592	-11.90000	0.0000000E+00	0.0000000E+00
-1.000000	1473.148			
193.0015	109.6296	-11.90000	0.0000000E+00	0.0000000E+00
-1.000000	1473.148			
311.5007	54.81482	-11.90000	0.0000000E+00	0.0000000E+00
-1.000000	1473.148			
263.9593	68.51852	-11.90000	0.0000000E+00	0.0000000E+00
-1.000000	1473.148			
382.4585	13.70370	-11.90000	0.0000000E+00	0.0000000E+00
-1.000000	1473.148			
334.9171	27.40741	-11.90000	0.0000000E+00	0.0000000E+00
-1.000000	1473.148			
-185.9125	301.4815	-11.90000	0.0000000E+00	0.0000000E+00
-1.000000	1473.148			
-114.9548	260.3704	-11.90000	0.0000000E+00	0.0000000E+00
-1.000000	1473.148			
-162.4962	274.0741	-11.90000	0.0000000E+00	0.0000000E+00
-1.000000	1473.148			
-43.99701	219.2593	-11.90000	0.0000000E+00	0.0000000E+00
-1.000000	1473.148			
-91.53848	232.9630	-11.90000	0.0000000E+00	0.0000000E+00
-1.000000	1473.148			
26.96075	178.1481	-11.90000	0.0000000E+00	0.0000000E+00
-1.000000	1473.148			
-20.58072	191.8519	-11.90000	0.0000000E+00	0.0000000E+00
-1.000000	1473.148			
97.91855	137.0370	-11.90000	0.0000000E+00	0.0000000E+00
-1.000000	1473.148			
50.37708	150.7407	-11.90000	0.0000000E+00	0.0000000E+00
-1.000000	1473.148			
168.8763	95.92592	-11.90000	0.0000000E+00	0.0000000E+00
-1.000000	1473.148			
121.3349	109.6296	-11.90000	0.0000000E+00	0.0000000E+00
-1.000000	1473.148			
239.8341	54.81482	-11.90000	0.0000000E+00	0.0000000E+00
-1.000000	1473.148			
192.2926	68.51852	-11.90000	0.0000000E+00	0.0000000E+00
-1.000000	1473.148			

310.7919	13.70370	-11.90000	0.0000000E+00	0.0000000E+00
-1.000000	1473.148			
263.2504	27.40741	-11.90000	0.0000000E+00	0.0000000E+00
-1.000000	1473.148			
-186.6214	260.3704	-11.90000	0.0000000E+00	0.0000000E+00
-1.000000	1473.148			
-115.6637	219.2593	-11.90000	0.0000000E+00	0.0000000E+00
-1.000000	1473.148			
-163.2052	232.9630	-11.90000	0.0000000E+00	0.0000000E+00
-1.000000	1473.148			
-44.70590	178.1481	-11.90000	0.0000000E+00	0.0000000E+00
-1.000000	1473.148			
-92.24739	191.8519	-11.90000	0.0000000E+00	0.0000000E+00
-1.000000	1473.148			
26.25189	137.0370	-11.90000	0.0000000E+00	0.0000000E+00
-1.000000	1473.148			
-21.28960	150.7407	-11.90000	0.0000000E+00	0.0000000E+00
-1.000000	1473.148			
97.20967	95.92592	-11.90000	0.0000000E+00	0.0000000E+00
-1.000000	1473.148			
49.66818	109.6296	-11.90000	0.0000000E+00	0.0000000E+00
-1.000000	1473.148			
168.1674	54.81482	-11.90000	0.0000000E+00	0.0000000E+00
-1.000000	1473.148			
120.6259	68.51852	-11.90000	0.0000000E+00	0.0000000E+00
-1.000000	1473.148			
239.1252	13.70370	-11.90000	0.0000000E+00	0.0000000E+00
-1.000000	1473.148			
191.5837	27.40741	-11.90000	0.0000000E+00	0.0000000E+00
-1.000000	1473.148			
-187.3304	219.2593	-11.90000	0.0000000E+00	0.0000000E+00
-1.000000	1473.148			
-116.3726	178.1481	-11.90000	0.0000000E+00	0.0000000E+00
-1.000000	1473.148			
-163.9141	191.8519	-11.90000	0.0000000E+00	0.0000000E+00
-1.000000	1473.148			
-45.41479	137.0370	-11.90000	0.0000000E+00	0.0000000E+00
-1.000000	1473.148			
-92.95627	150.7407	-11.90000	0.0000000E+00	0.0000000E+00
-1.000000	1473.148			
25.54298	95.92592	-11.90000	0.0000000E+00	0.0000000E+00
-1.000000	1473.148			
-21.99849	109.6296	-11.90000	0.0000000E+00	0.0000000E+00
-1.000000	1473.148			
96.50074	54.81482	-11.90000	0.0000000E+00	0.0000000E+00
-1.000000	1473.148			
48.95926	68.51852	-11.90000	0.0000000E+00	0.0000000E+00
-1.000000	1473.148			
167.4585	13.70370	-11.90000	0.0000000E+00	0.0000000E+00
-1.000000	1473.148			
119.9170	27.40741	-11.90000	0.0000000E+00	0.0000000E+00
-1.000000	1473.148			
-188.0392	178.1481	-11.90000	0.0000000E+00	0.0000000E+00
-1.000000	1473.148			
-117.0815	137.0370	-11.90000	0.0000000E+00	0.0000000E+00
-1.000000	1473.148			
-164.6229	150.7407	-11.90000	0.0000000E+00	0.0000000E+00
-1.000000	1473.148			
-93.66515	109.6296	-11.90000	0.0000000E+00	0.0000000E+00
-1.000000	1473.148			

-188.7481	137.0370	-11.90000	0.0000000E+00	0.0000000E+00
-1.000000	1473.148			
-117.7903	95.92592	-11.90000	0.0000000E+00	0.0000000E+00
-1.000000	1473.148			
-165.3318	109.6296	-11.90000	0.0000000E+00	0.0000000E+00
-1.000000	1473.148			
-94.37405	68.51852	-11.90000	0.0000000E+00	0.0000000E+00
-1.000000	1473.148			
382.7000	4.900000	-5.950000	0.5000000	0.8660000
0.3000000	705.0000			
358.1000	18.90000	-5.950000	0.5000000	0.8660000
0.3000000	705.0000			
333.5000	32.90000	-5.950000	0.5000000	0.8660000
0.3000000	705.0000			
308.9000	46.90000	-5.950000	0.5000000	0.8660000
0.3000000	705.0000			
284.3000	60.90000	-5.950000	0.5000000	0.8660000
0.3000000	705.0000			
259.7000	74.90000	-5.950000	0.5000000	0.8660000
0.3000000	705.0000			
235.1000	88.90000	-5.950000	0.5000000	0.8660000
0.3000000	705.0000			
210.5000	102.9000	-5.950000	0.5000000	0.8660000
0.3000000	705.0000			
185.9000	116.9000	-5.950000	0.5000000	0.8660000
0.3000000	705.0000			
161.3000	130.9000	-5.950000	0.5000000	0.8660000
0.3000000	705.0000			
136.7000	144.9000	-5.950000	0.5000000	0.8660000
0.3000000	705.0000			
112.1000	158.9000	-5.950000	0.5000000	0.8660000
0.3000000	705.0000			
87.50000	172.9000	-5.950000	0.5000000	0.8660000
0.3000000	705.0000			
62.89999	186.9000	-5.950000	0.5000000	0.8660000
0.3000000	705.0000			
38.30002	200.9000	-5.950000	0.5000000	0.8660000
0.3000000	705.0000			
13.70001	214.9000	-5.950000	0.5000000	0.8660000
0.3000000	705.0000			
-10.89999	228.9000	-5.950000	0.5000000	0.8660000
0.3000000	705.0000			
-35.50000	242.9000	-5.950000	0.5000000	0.8660000
0.3000000	705.0000			
-60.10001	256.9000	-5.950000	0.5000000	0.8660000
0.3000000	705.0000			
-84.69998	270.9000	-5.950000	0.5000000	0.8660000
0.3000000	705.0000			
-109.3000	284.9000	-5.950000	0.5000000	0.8660000
0.3000000	705.0000			
-133.9000	298.9000	-5.950000	0.5000000	0.8660000
0.3000000	705.0000			
-158.5000	312.9000	-5.950000	0.5000000	0.8660000
0.3000000	705.0000			
-183.1000	326.9000	-5.950000	0.5000000	0.8660000
0.3000000	705.0000			
-207.7000	340.9000	-5.950000	0.5000000	0.8660000
0.3000000	705.0000			
423.7000	2.400000	-7.930000	0.5000000	0.8660000
0.3000000	45.40000			

-215.3000	365.9000	-7.930000	0.5000000	0.8660000
0.3000000	15.30000			
136.7000	7.000000	-5.950000	-0.5000000	-0.8660000
0.0000000E+00	705.0000			
112.1000	21.00000	-5.950000	-0.5000000	-0.8660000
0.0000000E+00	705.0000			
87.50000	35.00000	-5.950000	-0.5000000	-0.8660000
0.0000000E+00	705.0000			
62.89999	49.00000	-5.950000	-0.5000000	-0.8660000
0.0000000E+00	705.0000			
38.30002	63.00000	-5.950000	-0.5000000	-0.8660000
0.0000000E+00	705.0000			
13.70001	77.00000	-5.950000	-0.5000000	-0.8660000
0.0000000E+00	705.0000			
-10.89999	91.00000	-5.950000	-0.5000000	-0.8660000
0.0000000E+00	705.0000			
-35.50000	105.0000	-5.950000	-0.5000000	-0.8660000
0.0000000E+00	705.0000			
-60.10001	119.0000	-5.950000	-0.5000000	-0.8660000
0.0000000E+00	705.0000			
-84.69998	43.00000	-5.950000	-0.5000000	-0.8660000
0.0000000E+00	705.0000			
-109.3000	57.00000	-5.950000	-0.5000000	-0.8660000
0.0000000E+00	705.0000			
-133.9000	71.00000	-5.950000	-0.5000000	-0.8660000
0.0000000E+00	705.0000			
-158.5000	85.00000	-5.950000	-0.5000000	-0.8660000
0.0000000E+00	705.0000			
-183.1000	99.00000	-5.950000	-0.5000000	-0.8660000
0.0000000E+00	705.0000			
-207.7000	113.0000	-5.950000	-0.5000000	-0.8660000
0.0000000E+00	705.0000			
-76.00000	110.0000	-5.950000	1.000000	0.0000000E+00
0.0000000E+00	476.0000			
-76.00000	18.90000	-5.950000	1.000000	0.0000000E+00
0.0000000E+00	476.0000			
-216.0000	351.2500	-5.950000	-1.000000	0.0000000E+00
0.0000000E+00	446.2500			
-216.0000	313.7500	-5.950000	-1.000000	0.0000000E+00
0.0000000E+00	446.2500			
-216.0000	276.2500	-5.950000	-1.000000	0.0000000E+00
0.0000000E+00	446.2500			
-216.0000	238.7500	-5.950000	-1.000000	0.0000000E+00
0.0000000E+00	446.2500			
-216.0000	201.2500	-5.950000	-1.000000	0.0000000E+00
0.0000000E+00	446.2500			
-216.0000	163.7500	-5.950000	-1.000000	0.0000000E+00
0.0000000E+00	446.2500			
-216.0000	366.8000	-7.930000	-1.000000	0.0000000E+00
0.0000000E+00	28.90000			

APPENDIX G

RESULTS OF PROGRAM OUTPORT2.FOR

 RESULT OF 115 PANELS FOR DELTA SHAPE
 WATER ENTRAPPED IN MODEL IS CONSIDERED

 PERIOD = 10.50000
 HEADING = 180.0000

A(11) = 0.1051111 A(33) = 3.264185
 A(55) = 1.322998 A(66) = 7.0522197E-02
 B(11) = 0.3095694 B(33) = 1.963395
 B(55) = 0.9624655 B(66) = 0.6856030
 SURGE MOTION = 3.0399682E-02 PHASE = 10.40342
 HEAVE MOTION = 4.0052738E-02 PHASE = 109.7882
 PITCH MOTION = 7.0765868E-02 PHASE = -127.6289
 SURGE EX.FORCE = 0.1779432 PHASE = -161.1657
 HEAVE EX.FORCE = 0.6456119 PHASE = -82.98737
 PITCH EX.FORCE = 0.6801304 PHASE = 29.22635
 DRIFT FORCE(X) = -0.7990930
 DRIFT FORCE(Y) = 5.4137622E-06
 DRIFT MOMENT(Z) = -3.8294975E-06

 NONDIM.DRIFT FORCE(X) = -2.214028
 NONDIM.DRIFT FORCE(Y) = 1.4999783E-05
 DRIFT FORCE(X) = -1566222.
 DRIFT FORCE(Y) = 10.61097

PERIOD = 10.80000
 HEADING = 180.0000

A(11) = 7.5390019E-02 A(33) = 3.082586
 A(55) = 1.280156 A(66) = 2.9582383E-02
 B(11) = 0.3214764 B(33) = 2.048813
 B(55) = 1.021827 B(66) = 0.6598853
 SURGE MOTION = 4.4834834E-02 PHASE = 4.990059
 HEAVE MOTION = 2.7377877E-02 PHASE = 105.6903
 PITCH MOTION = 0.1025326 PHASE = -142.5691
 SURGE EX.FORCE = 0.2593369 PHASE = -163.6033
 HEAVE EX.FORCE = 0.2441363 PHASE = -87.04454
 PITCH EX.FORCE = 0.8155283 PHASE = 15.49182
 DRIFT FORCE(X) = -0.7740943
 DRIFT FORCE(Y) = 5.2098894E-06
 DRIFT MOMENT(Z) = -4.4709400E-06

 NONDIM.DRIFT FORCE(X) = -2.144765
 NONDIM.DRIFT FORCE(Y) = 1.4434917E-05
 DRIFT FORCE(X) = -1517225.
 DRIFT FORCE(Y) = 10.21138

PERIOD = 11.70000
 HEADING = 180.0000

A(11) = 0.1275623 A(33) = 3.062597
 A(55) = 1.149684 A(66) = -5.5931669E-02
 B(11) = 0.3798601 B(33) = 2.787801
 B(55) = 1.121208 B(66) = 0.9045595
 SURGE MOTION = 7.2363958E-02 PHASE = 2.395897
 HEAVE MOTION = 3.2951895E-02 PHASE = -68.69910
 PITCH MOTION = 0.1872946 PHASE = -157.9673

SURGE EX.FORCE = 0.2638972 PHASE = -140.4422
HEAVE EX.FORCE = 0.8396516 PHASE = 73.97691
PITCH EX.FORCE = 0.8002200 PHASE = -12.14268
DRIFT FORCE(X) = -0.7553183
DRIFT FORCE(Y) = 5.5422320E-06
DRIFT MOMENT(Z) = -4.4382136E-06

NONDIM.DRIFT FORCE(X) = -2.092743
NONDIM.DRIFT FORCE(Y) = 1.5355732E-05
DRIFT FORCE(X) = -1480424.
DRIFT FORCE(Y) = 10.86277

PERIOD = 11.90000
HEADING = 180.0000

A(11) = 0.1286606 A(33) = 3.113638
A(55) = 1.120250 A(66) = -6.7451335E-02
B(11) = 0.3043473 B(33) = 2.730379
B(55) = 1.194106 B(66) = 0.9537278
SURGE MOTION = 7.2394930E-02 PHASE = 12.62360
HEAVE MOTION = 4.6865162E-02 PHASE = -76.86198
PITCH MOTION = 0.1839830 PHASE = -158.6190
SURGE EX.FORCE = 0.2564688 PHASE = -130.9018
HEAVE EX.FORCE = 1.029890 PHASE = 68.88496
PITCH EX.FORCE = 0.6901658 PHASE = -19.72369
DRIFT FORCE(X) = -0.7697544
DRIFT FORCE(Y) = 4.9187415E-06
DRIFT MOMENT(Z) = -4.5415172E-06

NONDIM.DRIFT FORCE(X) = -2.132740
NONDIM.DRIFT FORCE(Y) = 1.3628242E-05
DRIFT FORCE(X) = -1508719.
DRIFT FORCE(Y) = 9.640734

PERIOD = 12.70000
HEADING = 180.0000

A(11) = 8.5477225E-02 A(33) = 3.087097
A(55) = 1.294403 A(66) = -7.8644283E-02
B(11) = 0.2824962 B(33) = 1.811906
B(55) = 1.553260 B(66) = 1.150317
SURGE MOTION = 4.9662489E-02 PHASE = 109.6301
HEAVE MOTION = 0.1341617 PHASE = -85.77682
PITCH MOTION = 9.8325081E-02 PHASE = 140.2582
SURGE EX.FORCE = 0.3125671 PHASE = -99.10809
HEAVE EX.FORCE = 1.528415 PHASE = 60.53459
PITCH EX.FORCE = 0.2145327 PHASE = -142.5464
DRIFT FORCE(X) = -0.7965198
DRIFT FORCE(Y) = 5.1752227E-06
DRIFT MOMENT(Z) = -3.7233426E-06

NONDIM.DRIFT FORCE(X) = -2.206899
NONDIM.DRIFT FORCE(Y) = 1.4338867E-05
DRIFT FORCE(X) = -1561179.
DRIFT FORCE(Y) = 10.14344

PERIOD = 12.90000

HEADING = 180.0000

A(11) = 8.2183912E-02	A(33) = 3.000446
A(55) = 1.306777	A(66) = -7.5303462E-02
B(11) = 0.2680535	B(33) = 1.863812
B(55) = 1.440465	B(66) = 1.192955
SURGE MOTION = 5.6202713E-02	PHASE = 118.0304
HEAVE MOTION = 0.1516181	PHASE = -86.18277
PITCH MOTION = 8.8638440E-02	PHASE = 125.8443
SURGE EX. FORCE = 0.3202340	PHASE = -93.74649
HEAVE EX. FORCE = 1.502329	PHASE = 57.46931
PITCH EX. FORCE = 0.3629216	PHASE = -175.2769
DRIFT FORCE(X) = -0.8146660	
DRIFT FORCE(Y) = 5.6693329E-06	
DRIFT MOMENT(Z) = -4.2205820E-06	

NONDIM.DRIFT FORCE(X) = -2.257176
 NONDIM.DRIFT FORCE(Y) = 1.5707887E-05
 DRIFT FORCE(X) = -1596745.
 DRIFT FORCE(Y) = 11.11189

PERIOD = 13.50000
 HEADING = 180.0000

A(11) = 6.3735440E-02	A(33) = 2.910211
A(55) = 1.311278	A(66) = -7.5386621E-02
B(11) = 0.2730480	B(33) = 1.962360
B(55) = 1.325711	B(66) = 1.202362
SURGE MOTION = 0.1164308	PHASE = 137.1028
HEAVE MOTION = 0.2134472	PHASE = -86.82231
PITCH MOTION = 0.1288437	PHASE = 31.53979
SURGE EX. FORCE = 0.3174717	PHASE = -77.22083
HEAVE EX. FORCE = 1.274757	PHASE = 49.84913
PITCH EX. FORCE = 1.031610	PHASE = 151.3049
DRIFT FORCE(X) = -0.8979943	
DRIFT FORCE(Y) = 4.9705914E-06	
DRIFT MOMENT(Z) = -4.9093337E-06	

NONDIM.DRIFT FORCE(X) = -2.488052
 NONDIM.DRIFT FORCE(Y) = 1.3771900E-05
 DRIFT FORCE(X) = -1760069.
 DRIFT FORCE(Y) = 9.742359

PERIOD = 13.60000
 HEADING = 180.0000

A(11) = 6.1713424E-02	A(33) = 2.902458
A(55) = 1.312975	A(66) = -9.9771023E-02
B(11) = 0.2770682	B(33) = 1.969082
B(55) = 1.315140	B(66) = 1.161969
SURGE MOTION = 0.1306963	PHASE = 139.7508
HEAVE MOTION = 0.2253373	PHASE = -86.43748
PITCH MOTION = 0.1595439	PHASE = 23.13982
SURGE EX. FORCE = 0.3120337	PHASE = -73.67905
HEAVE EX. FORCE = 1.210189	PHASE = 48.91330
PITCH EX. FORCE = 1.146368	PHASE = 148.2650
DRIFT FORCE(X) = -0.9162641	
DRIFT FORCE(Y) = 4.6864425E-06	

DRIFT MOMENT(Z) = -3.9931879E-06

 NONDIM.DRIFT FORCE(X) = -2.538671
 NONDIM.DRIFT FORCE(Y) = 1.2984616E-05
 DRIFT FORCE(X) = -1795878.
 DRIFT FORCE(Y) = 9.185428

PERIOD = 14.10000
 HEADING = 180.0000

A(11) = 5.5993572E-02 A(33) = 2.876217
 A(55) = 1.322083 A(66) = -1.9312166E-03
 B(11) = 0.2993926 B(33) = 1.977532
 B(55) = 1.270134 B(66) = 1.951465
 SURGE MOTION = 0.2188288 PHASE = 151.8098
 HEAVE MOTION = 0.2953013 PHASE = -81.64592
 PITCH MOTION = 0.3624818 PHASE = 3.766045
 SURGE EX.FORCE = 0.2793047 PHASE = -50.07932
 HEAVE EX.FORCE = 0.7984636 PHASE = 46.68737
 PITCH EX.FORCE = 1.679868 PHASE = 137.2020
 DRIFT FORCE(X) = -1.018692
 DRIFT FORCE(Y) = 4.3319069E-06
 DRIFT MOMENT(Z) = -2.7723227E-06

 NONDIM.DRIFT FORCE(X) = -2.822466
 NONDIM.DRIFT FORCE(Y) = 1.2002312E-05
 DRIFT FORCE(X) = -1996636.
 DRIFT FORCE(Y) = 8.490538

PERIOD = 14.25000
 HEADING = 180.0000

A(11) = 5.5427682E-02 A(33) = 2.870785
 A(55) = 1.324567 A(66) = 4.0451944E-02
 B(11) = 0.3062447 B(33) = 1.971868
 B(55) = 1.258561 B(66) = 1.795429
 SURGE MOTION = 0.2510734 PHASE = 155.1524
 HEAVE MOTION = 0.3211171 PHASE = -79.23471
 PITCH MOTION = 0.4339815 PHASE = 0.8754120
 SURGE EX.FORCE = 0.2741729 PHASE = -40.95905
 HEAVE EX.FORCE = 0.6529942 PHASE = 47.78205
 PITCH EX.FORCE = 1.813980 PHASE = 134.7364
 DRIFT FORCE(X) = -1.051563
 DRIFT FORCE(Y) = 4.0517939E-06
 DRIFT MOMENT(Z) = -2.4545088E-06

 NONDIM.DRIFT FORCE(X) = -2.913539
 NONDIM.DRIFT FORCE(Y) = 1.1226210E-05
 DRIFT FORCE(X) = -2061063.
 DRIFT FORCE(Y) = 7.941516

PERIOD = 16.00000
 HEADING = 180.0000

A(11) = 8.5236453E-02 A(33) = 2.706505
 A(55) = 1.342509 A(66) = 0.2879294
 B(11) = 0.3743421 B(33) = 1.640025

B(55) = 1.170005 B(66) = 2.038930
 SURGE MOTION = 1.475824 PHASE = 173.7053
 HEAVE MOTION = 2.023552 PHASE = -61.86287
 PITCH MOTION = 2.557307 PHASE = -45.17549
 SURGE EX.FORCE = 0.5328630 PHASE = 33.67559
 HEAVE EX.FORCE = 1.657130 PHASE = -166.9177
 PITCH EX.FORCE = 1.866152 PHASE = 113.5337
 DRIFT FORCE(X) = -2.875366
 DRIFT FORCE(Y) = 9.9298522E-06
 DRIFT MOMENT(Z) = 3.5075020E-05

 NONDIM.DRIFT FORCE(X) = -7.966710
 NONDIM.DRIFT FORCE(Y) = 2.7512408E-05
 DRIFT FORCE(X) = -5635718.
 DRIFT FORCE(Y) = 19.46251

PERIOD = 16.50001
 HEADING = 180.0000

A(11) = 0.1081260 A(33) = 2.536057
 A(55) = 1.341339 A(66) = 0.4472590
 B(11) = 0.3714243 B(33) = 1.543343
 B(55) = 1.176442 B(66) = 2.080369
 SURGE MOTION = 1.298066 PHASE = 101.4107
 HEAVE MOTION = 2.200881 PHASE = -149.9867
 PITCH MOTION = 2.109569 PHASE = -140.9731
 SURGE EX.FORCE = 0.5817218 PHASE = 43.32428
 HEAVE EX.FORCE = 2.289949 PHASE = -161.9712
 PITCH EX.FORCE = 1.337995 PHASE = 102.1139
 DRIFT FORCE(X) = -2.063266
 DRIFT FORCE(Y) = 9.0077401E-06
 DRIFT MOMENT(Z) = 4.7552326E-06

 NONDIM.DRIFT FORCE(X) = -5.716641
 NONDIM.DRIFT FORCE(Y) = 2.4957531E-05
 DRIFT FORCE(X) = -4044001.
 DRIFT FORCE(Y) = 17.65517

PERIOD = 17.25002
 HEADING = 180.0000

A(11) = 0.1367698 A(33) = 2.153826
 A(55) = 1.364162 A(66) = 0.7261683
 B(11) = 0.3309265 B(33) = 1.704884
 B(55) = 1.209355 B(66) = 2.002148
 SURGE MOTION = 0.3292714 PHASE = 123.7356
 HEAVE MOTION = 0.5414751 PHASE = -174.1050
 PITCH MOTION = 0.3810202 PHASE = -113.2448
 SURGE EX.FORCE = 0.5178511 PHASE = 53.28951
 HEAVE EX.FORCE = 2.741764 PHASE = -152.8523
 PITCH EX.FORCE = 0.8636039 PHASE = 39.21546
 DRIFT FORCE(X) = -0.3292271
 DRIFT FORCE(Y) = 1.1852021E-06
 DRIFT MOMENT(Z) = 9.5720065E-07

 NONDIM.DRIFT FORCE(X) = -0.9121819
 NONDIM.DRIFT FORCE(Y) = 3.2838116E-06
 DRIFT FORCE(X) = -645285.2

DRIFT FORCE(Y) = 2.322996

PERIOD = 17.50003
HEADING = 180.0000

A(11) = 0.1416370 A(33) = 2.028884
A(55) = 1.376932 A(66) = 0.8209674
B(11) = 0.3122578 B(33) = 1.874900
B(55) = 1.214462 B(66) = 1.930450
SURGE MOTION = 0.2744223 PHASE = 134.0133
HEAVE MOTION = 0.3797341 PHASE = -178.2793
PITCH MOTION = 0.4059136 PHASE = -86.58398
SURGE EX.FORCE = 0.4666619 PHASE = 54.49652
HEAVE EX.FORCE = 2.714680 PHASE = -149.9380
PITCH EX.FORCE = 1.052823 PHASE = 16.38687
DRIFT FORCE(X) = -0.2763058
DRIFT FORCE(Y) = 1.0781397E-06
DRIFT MOMENT(Z) = 2.8424613E-06

NONDIM.DRIFT FORCE(X) = -0.7655540
NONDIM.DRIFT FORCE(Y) = 2.9871760E-06
DRIFT FORCE(X) = -541559.4
DRIFT FORCE(Y) = 2.113154

PERIOD = 19.00027
HEADING = 180.0000

A(11) = 0.1234272 A(33) = 1.929877
A(55) = 1.448314 A(66) = 1.181565
B(11) = 0.2266916 B(33) = 3.372746
B(55) = 1.248812 B(66) = 1.211903
SURGE MOTION = 0.2306647 PHASE = 100.8427
HEAVE MOTION = 0.1623340 PHASE = 89.10593
PITCH MOTION = 0.8923169 PHASE = -57.07552
SURGE EX.FORCE = 0.1920011 PHASE = 5.935051
HEAVE EX.FORCE = 1.238492 PHASE = -151.4523
PITCH EX.FORCE = 2.930676 PHASE = -17.20961
DRIFT FORCE(X) = -0.2641097
DRIFT FORCE(Y) = 1.7598387E-07
DRIFT MOMENT(Z) = 3.5563983E-06

NONDIM.DRIFT FORCE(X) = -0.7317626
NONDIM.DRIFT FORCE(Y) = 4.8759432E-07
DRIFT FORCE(X) = -517655.1
DRIFT FORCE(Y) = 0.3449284

PERIOD = 21.25284
HEADING = 180.0000

A(11) = 5.7348430E-02 A(33) = 3.148585
A(55) = 1.704662 A(66) = 1.142604
B(11) = 0.2016275 B(33) = 4.050815
B(55) = 1.290293 B(66) = 0.4669055
SURGE MOTION = 0.8787446 PHASE = 81.45818
HEAVE MOTION = 0.3370308 PHASE = 63.92249
PITCH MOTION = 1.133340 PHASE = -57.62869
SURGE EX.FORCE = 0.4218294 PHASE = -74.37808

HEAVE EX.FORCE = 1.751667 PHASE = 101.5117
 PITCH EX.FORCE = 3.991448 PHASE = -26.86558
 DRIFT FORCE(X) = -0.4685003
 DRIFT FORCE(Y) = 4.4941976E-07
 DRIFT MOMENT(Z) = -2.3120779E-07

 NONDIM.DRIFT FORCE(X) = -1.298063
 NONDIM.DRIFT FORCE(Y) = 1.2451967E-06
 DRIFT FORCE(X) = -918260.5
 DRIFT FORCE(Y) = 0.8808627

PERIOD = 22.00534
 HEADING = 180.0000

A(11) = 2.1457324E-02 A(33) = 3.575503
 A(55) = 1.820381 A(66) = 1.094582
 B(11) = 0.2024144 B(33) = 3.837221
 B(55) = 1.256968 B(66) = 0.3480621
 SURGE MOTION = 1.226404 PHASE = 82.55656
 HEAVE MOTION = 0.3781213 PHASE = 66.15347
 PITCH MOTION = 1.167558 PHASE = -59.84427
 SURGE EX.FORCE = 0.5462714 PHASE = -83.33867
 HEAVE EX.FORCE = 2.112711 PHASE = 96.65406
 PITCH EX.FORCE = 4.053880 PHASE = -31.01726
 DRIFT FORCE(X) = -0.5858364
 DRIFT FORCE(Y) = 7.8166238E-07
 DRIFT MOMENT(Z) = -1.4671841E-06

 NONDIM.DRIFT FORCE(X) = -1.623163
 NONDIM.DRIFT FORCE(Y) = 2.1657333E-06
 DRIFT FORCE(X) = -1148239.
 DRIFT FORCE(Y) = 1.532058

PERIOD = 22.50788
 HEADING = 180.0000

A(11) = -1.0220896E-02 A(33) = 3.834136
 A(55) = 1.903265 A(66) = 1.063304
 B(11) = 0.2093822 B(33) = 3.623490
 B(55) = 1.223420 B(66) = 0.2894277
 SURGE MOTION = 1.549247 PHASE = 85.13668
 HEAVE MOTION = 0.4001127 PHASE = 70.91006
 PITCH MOTION = 1.202109 PHASE = -61.32797
 SURGE EX.FORCE = 0.6325737 PHASE = -87.03609
 HEAVE EX.FORCE = 2.262950 PHASE = 93.94488
 PITCH EX.FORCE = 4.074016 PHASE = -33.78485
 DRIFT FORCE(X) = -0.6958893
 DRIFT FORCE(Y) = 1.1538474E-06
 DRIFT MOMENT(Z) = -1.9713486E-06

 NONDIM.DRIFT FORCE(X) = -1.928084
 NONDIM.DRIFT FORCE(Y) = 3.1969378E-06
 DRIFT FORCE(X) = -1363943.
 DRIFT FORCE(Y) = 2.261541

PERIOD = 23.01134
 HEADING = 180.0000

A(11) = -4.9484234E-02 A(33) = 4.074243
 A(55) = 1.991956 A(66) = 1.033653
 B(11) = 0.2244929 B(33) = 3.362293
 B(55) = 1.181004 B(66) = 0.2429007
 SURGE MOTION = 1.993473 PHASE = 90.78033
 HEAVE MOTION = 0.4120668 PHASE = 80.27769
 PITCH MOTION = 1.260365 PHASE = -62.16077
 SURGE EX.FORCE = 0.7183252 PHASE = -89.62651
 HEAVE EX.FORCE = 2.359040 PHASE = 91.40507
 PITCH EX.FORCE = 4.082949 PHASE = -36.37818
 DRIFT FORCE(X) = -0.8484316
 DRIFT FORCE(Y) = 1.4485050E-06
 DRIFT MOMENT(Z) = -2.4086157E-06

 NONDIM.DRIFT FORCE(X) = -2.350729
 NONDIM.DRIFT FORCE(Y) = 4.0133386E-06
 DRIFT FORCE(X) = -1662926.
 DRIFT FORCE(Y) = 2.839070

PERIOD = 23.41493
 HEADING = 180.0000

A(11) = -8.7135443E-02 A(33) = 4.255849
 A(55) = 2.068672 A(66) = 1.011464
 B(11) = 0.2445227 B(33) = 3.120078
 B(55) = 1.140095 B(66) = 0.2125662
 SURGE MOTION = 2.455363 PHASE = 99.10499
 HEAVE MOTION = 0.4044102 PHASE = 93.32715
 PITCH MOTION = 1.330886 PHASE = -61.43149
 SURGE EX.FORCE = 0.7860499 PHASE = -91.20207
 HEAVE EX.FORCE = 2.402791 PHASE = 89.57306
 PITCH EX.FORCE = 4.082338 PHASE = -38.24988
 DRIFT FORCE(X) = -0.9904994
 DRIFT FORCE(Y) = 2.3797968E-06
 DRIFT MOMENT(Z) = -3.1949023E-06

 NONDIM.DRIFT FORCE(X) = -2.744353
 NONDIM.DRIFT FORCE(Y) = 6.5936465E-06
 DRIFT FORCE(X) = -1941379.
 DRIFT FORCE(Y) = 4.664402

PERIOD = 23.61706
 HEADING = 180.0000

A(11) = -0.1084876 A(33) = 4.344030
 A(55) = 2.109493 A(66) = 1.000826
 B(11) = 0.2580944 B(33) = 2.984919
 B(55) = 1.116828 B(66) = 0.1992414
 SURGE MOTION = 2.710971 PHASE = 105.2011
 HEAVE MOTION = 0.3889936 PHASE = 102.8247
 PITCH MOTION = 1.372282 PHASE = -60.14774
 SURGE EX.FORCE = 0.8200877 PHASE = -91.87019
 HEAVE EX.FORCE = 2.413011 PHASE = 88.78129
 PITCH EX.FORCE = 4.078914 PHASE = -39.09654
 DRIFT FORCE(X) = -1.046431
 DRIFT FORCE(Y) = 2.6374098E-06
 DRIFT MOMENT(Z) = -3.5638466E-06

```

-----
NONDIM.DRIFT FORCE(X) = -2.899321
NONDIM.DRIFT FORCE(Y) = 7.3074093E-06
DRIFT FORCE(X) = -2051004.
DRIFT FORCE(Y) = 5.169323
*****

```

```

PERIOD = 24.02203
HEADING = 180.0000

```

```

A(11) = -0.1569304      A(33) = 4.515299
A(55) = 2.197542      A(66) = 0.9807277
B(11) = 0.2946613      B(33) = 2.679369
B(55) = 1.063038      B(66) = 0.1758455
SURGE MOTION = 3.144349      PHASE = 122.0770
HEAVE MOTION = 0.3206529      PHASE = 130.6197
PITCH MOTION = 1.436704      PHASE = -54.92307
SURGE EX.FORCE = 0.8896191      PHASE = -93.01843
HEAVE EX.FORCE = 2.405713      PHASE = 87.55592
PITCH EX.FORCE = 4.064487      PHASE = -40.57574
DRIFT FORCE(X) = -1.006484
DRIFT FORCE(Y) = 2.6873013E-06
DRIFT MOMENT(Z) = -3.7133782E-06
-----

```

```

NONDIM.DRIFT FORCE(X) = -2.788640
NONDIM.DRIFT FORCE(Y) = 7.4456420E-06
DRIFT FORCE(X) = -1972708.
DRIFT FORCE(Y) = 5.267110
*****

```

```

PERIOD = 24.63164
HEADING = 180.0000

```

```

A(11) = -0.2464055      A(33) = 4.751124
A(55) = 2.351381      A(66) = 0.9531407
B(11) = 0.3850290      B(33) = 2.092865
B(55) = 0.9550079      B(66) = 0.1472435
SURGE MOTION = 2.981128      PHASE = 153.9076
HEAVE MOTION = 0.1731873      PHASE = -152.1879
PITCH MOTION = 1.339232      PHASE = -43.54454
SURGE EX.FORCE = 1.003944      PHASE = -94.25017
HEAVE EX.FORCE = 2.296605      PHASE = 87.08833
PITCH EX.FORCE = 4.014759      PHASE = -42.10704
DRIFT FORCE(X) = -0.3716392
DRIFT FORCE(Y) = 1.0126490E-06
DRIFT MOMENT(Z) = -2.6656157E-06
-----

```

```

NONDIM.DRIFT FORCE(X) = -1.029692
NONDIM.DRIFT FORCE(Y) = 2.8057225E-06
DRIFT FORCE(X) = -728412.8
DRIFT FORCE(Y) = 1.984792
*****

```

```

PERIOD = 25.03972
HEADING = 180.0000

```

```

A(11) = -0.3176007      A(33) = 4.869928
A(55) = 2.473764      A(66) = 0.9362532
B(11) = 0.4853886      B(33) = 1.565150
B(55) = 0.8505877      B(66) = 0.1315560

```

SURGE MOTION = 2.387126 PHASE = 171.7274
 HEAVE MOTION = 0.1716435 PHASE = -90.12004
 PITCH MOTION = 1.176655 PHASE = -38.80847
 SURGE EX.FORCE = 1.094362 PHASE = -94.56596
 HEAVE EX.FORCE = 2.114875 PHASE = 88.23347
 PITCH EX.FORCE = 3.948908 PHASE = -42.50642
 DRIFT FORCE(X) = 1.2398577E-02
 DRIFT FORCE(Y) = -1.2122415E-07
 DRIFT MOMENT(Z) = -2.0393297E-06

 NONDIM.DRIFT FORCE(X) = 3.4352444E-02
 NONDIM.DRIFT FORCE(Y) = -3.3587287E-07
 DRIFT FORCE(X) = 24301.21
 DRIFT FORCE(Y) = -0.2375993

PERIOD = 25.65485
 HEADING = 180.0000

A(11) = -0.4231663 A(33) = 4.838224
 A(55) = 2.687837 A(66) = 0.9134930
 B(11) = 0.7524582 B(33) = 0.4305249
 B(55) = 0.5892703 B(66) = 0.1121489
 SURGE MOTION = 1.442527 PHASE = -167.8974
 HEAVE MOTION = 0.2185616 PHASE = -51.36612
 PITCH MOTION = 0.9490985 PHASE = -36.04193
 SURGE EX.FORCE = 1.270255 PHASE = -93.34892
 HEAVE EX.FORCE = 1.520293 PHASE = 93.84814
 PITCH EX.FORCE = 3.744205 PHASE = -41.81175
 DRIFT FORCE(X) = 8.3404429E-02
 DRIFT FORCE(Y) = -6.5206387E-07
 DRIFT MOMENT(Z) = -1.3196238E-06

 NONDIM.DRIFT FORCE(X) = 0.2310867
 NONDIM.DRIFT FORCE(Y) = -1.8066579E-06
 DRIFT FORCE(X) = 163472.7
 DRIFT FORCE(Y) = -1.278045

PERIOD = 26.27417
 HEADING = 180.0000

A(11) = -0.3827319 A(33) = 3.918275
 A(55) = 2.844638 A(66) = 0.8929142
 B(11) = 1.264261 B(33) = -1.165203
 B(55) = 6.1639268E-02 B(66) = 9.6358091E-02
 SURGE MOTION = 0.4844470 PHASE = -142.3473
 HEAVE MOTION = 0.2461486 PHASE = -51.9919C
 PITCH MOTION = 0.7136692 PHASE = -35.89342
 SURGE EX.FORCE = 1.507113 PHASE = -87.19568
 HEAVE EX.FORCE = 0.1256306 PHASE = 119.9101
 PITCH EX.FORCE = 3.231782 PHASE = -39.98450
 DRIFT FORCE(X) = -0.5610173
 DRIFT FORCE(Y) = 9.1934874E-07
 DRIFT MOMENT(Z) = -9.8334442E-07

 NONDIM.DRIFT FORCE(X) = -1.554397
 NONDIM.DRIFT FORCE(Y) = 2.5472177E-06
 DRIFT FORCE(X) = -1099594.
 DRIFT FORCE(Y) = 1.801924

PERIOD = 26.48167
HEADING = 180.0000

A(11) = -0.2563965	A(33) = 3.173485
A(55) = 2.811890	A(66) = 0.8865432
B(11) = 1.480782	B(33) = -1.622577
B(55) = -0.1925129	B(66) = 9.1763414E-02
SURGE MOTION = 0.1334889	PHASE = -109.4232
HEAVE MOTION = 0.2757234	PHASE = -57.32018
PITCH MOTION = 0.6220089	PHASE = -38.10844
SURGE EX.FORCE = 1.583952	PHASE = -83.16145
HEAVE EX.FORCE = 0.6359894	PHASE = -69.05405
PITCH EX.FORCE = 2.942208	PHASE = -40.28313
DRIFT FORCE(X) = -0.9183218	
DRIFT FORCE(Y) = 2.1762523E-06	
DRIFT MOMENT(Z) = -3.5625231E-07	

NONDIM.DRIFT FORCE(X) = -2.544373
NONDIM.DRIFT FORCE(Y) = 6.0296911E-06
DRIFT FORCE(X) = -1799911.
DRIFT FORCE(Y) = 4.265455

PERIOD = 26.68975
HEADING = 180.0000

A(11) = -3.2991078E-02	A(33) = 2.165104
A(55) = 2.686208	A(66) = 0.8803591
B(11) = 1.670278	B(33) = -1.813437
B(55) = -0.4545512	B(66) = 8.7442666E-02
SURGE MOTION = 0.2893263	PHASE = 33.08762
HEAVE MOTION = 0.3296922	PHASE = -61.19234
PITCH MOTION = 0.5344391	PHASE = -43.90807
SURGE EX.FORCE = 1.637496	PHASE = -77.94830
HEAVE EX.FORCE = 1.546403	PHASE = -58.41347
PITCH EX.FORCE = 2.605600	PHASE = -42.70970
DRIFT FORCE(X) = -1.187797	
DRIFT FORCE(Y) = 3.0306649E-06	
DRIFT MOMENT(Z) = 6.0593794E-07	

NONDIM.DRIFT FORCE(X) = -3.291001
NONDIM.DRIFT FORCE(Y) = 8.3969917E-06
DRIFT FORCE(X) = -2328082.
DRIFT FORCE(Y) = 5.940103

PERIOD = 27.10773
HEADING = 180.0000

A(11) = 0.6201231	A(33) = 5.1602822E-02
A(55) = 2.156558	A(66) = 0.8688176
B(11) = 1.722938	B(33) = -0.8090822
B(55) = -0.7562411	B(66) = 7.9631351E-02
SURGE MOTION = 1.021045	PHASE = 66.04991
HEAVE MOTION = 0.487154	PHASE = -57.95239
PITCH MOTION = 0.4827384	PHASE = -67.56287
SURGE EX.FORCE = 1.599567	PHASE = -65.76749
HEAVE EX.FORCE = 3.497462	PHASE = -36.57304

PITCH EX.FORCE = 2.150258 PHASE = -59.36693
 DRIFT FORCE(X) = -0.8198050
 DRIFT FORCE(Y) = 2.3704747E-06
 DRIFT MOMENT(Z) = 1.6914228E-06

 NONDIM.DRIFT FORCE(X) = -2.271415
 NONDIM.DRIFT FORCE(Y) = 6.5678182E-06
 DRIFT FORCE(X) = -1606818.
 DRIFT FORCE(Y) = 4.646131

PERIOD = 27.52836
 HEADING = 180.0000

A(11) = 1.100476 A(33) = -0.6978253
 A(55) = 1.631363 A(66) = 0.8579154
 B(11) = 1.297312 B(33) = 1.329930
 B(55) = -0.5732459 B(66) = 7.2665028E-02
 SURGE MOTION = 1.471505 PHASE = 87.89336
 HEAVE MOTION = 0.6203058 PHASE = -46.53110
 PITCH MOTION = 0.6079775 PHASE = -80.44890
 SURGE EX.FORCE = 1.378362 PHASE = -56.52956
 HEAVE EX.FORCE = 4.911064 PHASE = -16.61108
 PITCH EX.FORCE = 2.445283 PHASE = -77.06796
 DRIFT FORCE(X) = 5.2996572E-02
 DRIFT FORCE(Y) = -1.3831197E-08
 DRIFT MOMENT(Z) = 5.6305834E-07

 NONDIM.DRIFT FORCE(X) = 0.1468364
 NONDIM.DRIFT FORCE(Y) = -3.8321769E-08
 DRIFT FORCE(X) = 103873.3
 DRIFT FORCE(Y) = -2.7109146E-02

PERIOD = 27.73975
 HEADING = 180.0000

A(11) = 1.188429 A(33) = -0.5260917
 A(55) = 1.489406 A(66) = 0.8527726
 B(11) = 1.048208 B(33) = 2.223159
 B(55) = -0.3988609 B(66) = 6.9484539E-02
 SURGE MOTION = 1.574234 PHASE = 95.99165
 HEAVE MOTION = 0.6613620 PHASE = -40.98555
 PITCH MOTION = 0.6692080 PHASE = -81.25737
 SURGE EX.FORCE = 1.254201 PHASE = -54.38551
 HEAVE EX.FORCE = 5.319924 PHASE = -8.910408
 PITCH EX.FORCE = 2.698105 PHASE = -80.54503
 DRIFT FORCE(X) = 0.2309085
 DRIFT FORCE(Y) = -8.7154172E-07
 DRIFT MOMENT(Z) = -1.9270342E-07

 NONDIM.DRIFT FORCE(X) = 0.6397728
 NONDIM.DRIFT FORCE(Y) = -2.4147600E-06
 DRIFT FORCE(X) = 452580.8
 DRIFT FORCE(Y) = -1.708222

PERIOD = 28.16478
 HEADING = 180.0000

A(11) = 1.182285 A(33) = 0.2085297
 A(55) = 1.305164 A(66) = 0.8427998
 B(11) = 0.6589920 B(33) = 3.336414
 B(55) = -8.6192511E-02 B(66) = 6.3585751E-02
 SURGE MOTION = 1.638209 PHASE = 107.3401
 HEAVE MOTION = 0.7083383 PHASE = -32.12775
 PITCH MOTION = 0.7465847 PHASE = -79.81175
 SURGE EX.FORCE = 1.052454 PHASE = -54.26161
 HEAVE EX.FORCE = 5.759504 PHASE = 2.111839
 PITCH EX.FORCE = 3.104453 PHASE = -82.36244
 DRIFT FORCE(X) = 0.2300374
 DRIFT FORCE(Y) = -8.3667646E-07
 DRIFT MOMENT(Z) = -1.3243248E-06

 NONDIM.DRIFT FORCE(X) = 0.6373592
 NONDIM.DRIFT FORCE(Y) = -2.3181597E-06
 DRIFT FORCE(X) = 450873.3
 DRIFT FORCE(Y) = -1.639886

PERIOD = 28.70066
 HEADING = 180.0000

A(11) = 1.063126 A(33) = 1.124389
 A(55) = 1.434289 A(66) = 0.8313558
 B(11) = 0.3809553 B(33) = 3.883319
 B(55) = 0.1566763 B(66) = 5.7095718E-02
 SURGE MOTION = 1.609999 PHASE = 115.2526
 HEAVE MOTION = 0.7358965 PHASE = -24.77085
 PITCH MOTION = 0.7832537 PHASE = -77.52126
 SURGE EX.FORCE = 0.9015694 PHASE = -58.25960
 HEAVE EX.FORCE = 5.985287 PHASE = 10.05864
 PITCH EX.FORCE = 3.392599 PHASE = -82.16647
 DRIFT FORCE(X) = 9.0601675E-02
 DRIFT FORCE(Y) = -3.9383150E-07
 DRIFT MOMENT(Z) = -1.3683347E-06

 NONDIM.DRIFT FORCE(X) = 0.2510279
 NONDIM.DRIFT FORCE(Y) = -1.0911796E-06
 DRIFT FORCE(X) = 177579.3
 DRIFT FORCE(Y) = -0.7719097

PERIOD = 29.24207
 HEADING = 180.0000

A(11) = 0.9421501 A(33) = 1.817028
 A(55) = 1.512595 A(66) = 0.8206640
 B(11) = 0.2359848 B(33) = 4.024405
 B(55) = 0.2830066 B(66) = 5.1369470E-02
 SURGE MOTION = 1.555735 PHASE = 119.3112
 HEAVE MOTION = 0.7522381 PHASE = -19.97897
 PITCH MOTION = 0.7888267 PHASE = -76.00623
 SURGE EX.FORCE = 0.8230895 PHASE = -63.34042
 HEAVE EX.FORCE = 6.103336 PHASE = 14.39177
 PITCH EX.FORCE = 3.537306 PHASE = -81.92569
 DRIFT FORCE(X) = -1.5565186E-03
 DRIFT FORCE(Y) = -1.2938006E-07
 DRIFT MOMENT(Z) = -1.5175974E-06

NONDIM.DRIFT FORCE(X) = -4.3126093E-03
 NONDIM.DRIFT FORCE(Y) = -3.5847029E-07
 DRIFT FORCE(X) = -3050.776
 DRIFT FORCE(Y) = -0.2535849

PERIOD = 30.34333
 HEADING = 180.0000

A(11) = 0.7684965 A(33) = 2.703772
 A(55) = 1.651726 A(66) = 0.8015384
 B(11) = 0.1091132 B(33) = 3.942914
 B(55) = 0.3721719 B(66) = 4.1833557E-02
 SURGE MOTION = 1.462135 PHASE = 122.1273
 HEAVE MOTION = 0.7772608 PHASE = -14.31600
 PITCH MOTION = 0.7676228 PHASE = -74.72955
 SURGE EX.FORCE = 0.7588099 PHASE = -71.84511
 HEAVE EX.FORCE = 6.292231 PHASE = 17.97323
 PITCH EX.FORCE = 3.639745 PHASE = -82.37506
 DRIFT FORCE(X) = -6.8652436E-02
 DRIFT FORCE(Y) = 1.2460151E-07
 DRIFT MOMENT(Z) = -9.7919803E-07

 NONDIM.DRIFT FORCE(X) = -0.1902137
 NONDIM.DRIFT FORCE(Y) = 3.4523049E-07
 DRIFT FORCE(X) = -134558.8
 DRIFT FORCE(Y) = 0.2442190

PERIOD = 30.90411
 HEADING = 180.0000

A(11) = 0.7086224 A(33) = 3.001352
 A(55) = 1.704812 A(66) = 0.7928462
 B(11) = 7.9429023E-02 B(33) = 3.852900
 B(55) = 0.3802421 B(66) = 3.7824165E-02
 SURGE MOTION = 1.427968 PHASE = 122.2878
 HEAVE MOTION = 0.7886963 PHASE = -12.51565
 PITCH MOTION = 0.7515257 PHASE = -74.57765
 SURGE EX.FORCE = 0.7442636 PHASE = -75.03093
 HEAVE EX.FORCE = 6.390761 PHASE = 18.53978
 PITCH EX.FORCE = 3.648444 PHASE = -82.91093
 DRIFT FORCE(X) = -7.7003114E-02
 DRIFT FORCE(Y) = 1.5606898E-07
 DRIFT MOMENT(Z) = -9.5850589E-07

 NONDIM.DRIFT FORCE(X) = -0.2133507
 NONDIM.DRIFT FORCE(Y) = 4.3241664E-07
 DRIFT FORCE(X) = -150926.1
 DRIFT FORCE(Y) = 0.3058952

PERIOD = 32.04819
 HEADING = 180.0000

A(11) = 0.6220578 A(33) = 3.444352
 A(55) = 1.784179 A(66) = 0.7769696
 B(11) = 4.6159085E-02 B(33) = 3.660193
 B(55) = 0.3673845 B(66) = 3.1016050E-02
 SURGE MOTION = 1.379750 PHASE = 121.5456

HEAVE MOTION = 0.8103246 PHASE = -9.977066
 PITCH MOTION = 0.7167014 PHASE = -74.73541
 SURGE EX.FORCE = 0.7253001 PHASE = -79.88075
 HEAVE EX.FORCE = 6.601376 PHASE = 18.57285
 PITCH EX.FORCE = 3.627239 PHASE = -84.27519
 DRIFT FORCE(X) = -7.7546034E-02
 DRIFT FORCE(Y) = 1.7816780E-07
 DRIFT MOMENT(Z) = -8.1580168E-07

 NONDIM.DRIFT FORCE(X) = -0.2148605
 NONDIM.DRIFT FORCE(Y) = 4.9364530E-07
 DRIFT FORCE(X) = -151994.1
 DRIFT FORCE(Y) = 0.3492089

PERIOD = 32.63234
 HEADING = 180.0000

A(11) = 0.5901325 A(33) = 3.616407
 A(55) = 1.813407 A(66) = 0.7697201
 B(11) = 3.6412328E-02 B(33) = 3.565932
 B(55) = 0.3537261 B(66) = 2.8125452E-02
 SURGE MOTION = 1.363367 PHASE = 120.8947
 HEAVE MOTION = 0.8204814 PHASE = -9.050644
 PITCH MOTION = 0.6990978 PHASE = -74.94415
 SURGE EX.FORCE = 0.7175267 PHASE = -81.77094
 HEAVE EX.FORCE = 6.711522 PHASE = 18.27949
 PITCH EX.FORCE = 3.604810 PHASE = -85.03099
 DRIFT FORCE(X) = -7.4537806E-02
 DRIFT FORCE(Y) = 1.7258093E-07
 DRIFT MOMENT(Z) = -7.5108477E-07

 NONDIM.DRIFT FORCE(X) = -0.2065201
 NONDIM.DRIFT FORCE(Y) = 4.7816593E-07
 DRIFT FORCE(X) = -146094.1
 DRIFT FORCE(Y) = 0.3382586

PERIOD = 33.22512
 HEADING = 180.0000

A(11) = 0.5632117 A(33) = 3.767319
 A(55) = 1.837530 A(66) = 0.7628774
 B(11) = 2.9180052E-02 B(33) = 3.475045
 B(55) = 0.3379664 B(66) = 2.5524773E-02
 SURGE MOTION = 1.350372 PHASE = 120.1388
 HEAVE MOTION = 0.8301599 PHASE = -8.270882
 PITCH MOTION = 0.6817353 PHASE = -75.19827
 SURGE EX.FORCE = 0.7099004 PHASE = -83.42531
 HEAVE EX.FORCE = 6.823321 PHASE = 17.87849
 PITCH EX.FORCE = 3.577482 PHASE = -85.80290
 DRIFT FORCE(X) = -7.0767097E-02
 DRIFT FORCE(Y) = 1.6923470E-07
 DRIFT MOMENT(Z) = -6.4887053E-07

 NONDIM.DRIFT FORCE(X) = -0.1960727
 NONDIM.DRIFT FORCE(Y) = 4.6889457E-07
 DRIFT FORCE(X) = -138703.5
 DRIFT FORCE(Y) = 0.3317000

PERIOD = 34.43806
HEADING = 180.0000

A(11) = 0.5207458 A(33) = 4.021955
A(55) = 1.873198 A(66) = 0.7503566
B(11) = 1.9428670E-02 B(33) = 3.303639
B(55) = 0.3037479 B(66) = 2.1076541E-02
SURGE MOTION = 1.332985 PHASE = 118.4607
HEAVE MOTION = 0.8480464 PHASE = -7.038033
PITCH MOTION = 0.6480946 PHASE = -75.78218
SURGE EX.FORCE = 0.6942537 PHASE = -86.20634
HEAVE EX.FORCE = 7.049265 PHASE = 16.88271
PITCH EX.FORCE = 3.512018 PHASE = -87.35855
DRIFT FORCE(X) = -6.2529884E-02
DRIFT FORCE(Y) = 1.5289093E-07
DRIFT MOMENT(Z) = -5.2768371E-07

NONDIM.DRIFT FORCE(X) = -0.1732501
NONDIM.DRIFT FORCE(Y) = 4.2361128E-07
DRIFT FORCE(X) = -122558.6
DRIFT FORCE(Y) = 0.2996662

APPENDIX H

MAIN SUBROUTINES IN PROGRAM DPORT2.FOR

Brief Description of Main Subroutines
in
Program DPORT
(in order of occurrence and with pertinent equations
referenced from the text)

CHART computes the characteristics of the floating body

- coordinates of the centroids of the panels
- normals
- panel surface area
- restoring coefficient
- volume
- x-coordinate of center of buoyancy
- wetted surface area
- water plane area

(reads input file and calls subroutine VDOT)

PRNT1 prints to a file the data of the characteristics of
the floating body

LINK1 computes elements of the Green's function matrix
(calls ROOTK, VSUB, GS2, GI2)

PHI78 calculates the PHI7, symmetric part, and PHI8, the
anti-symmetric part

GINVER computes inverse of matrix DG and source Q
(calls INV)

POTEN computes the potential
(calls MPRD)
equation 4.23

AMASS computes added mass and damping coefficients
equations 4.19 and 4.20

EXFOR computes the exciting force
equation 4.21

AMPL computes the response amplitude
(calls INV)
equation 4.22

QTOTAL calculates the total Q for drifting force
equation 4.33

DRIFT calculates drifting force
(calls SIR)
equations 4.36 and 4.37

GI2 calculates Green's function by integral form
(calls DG16)

GS2 calculates Green's function by series form

MPRD computes $R=AxB$ where $A(N \times M)$, $B(M \times L)$



